

AIRPORT
COOPERATIVE
RESEARCH
PROGRAM

ACRP

Web-Only Document 43:

Improving AEDT Modeling for Aircraft Noise Reflection and Diffraction from Terrain and Manmade Structures

J. Micah Downing
Matthew F. Calton
Blue Ridge Research and Consulting, LLC
Asheville, NC

Juliet A. Page
Volpe, The National Transportation Systems Center
Cambridge, MA

Judith L. Rochat
Cross-Spectrum Acoustics Inc.
Pasadena, CA

Contractor's Final Report for ACRP 02-79
Submitted August 2019

The National Academies of
SCIENCES • ENGINEERING • MEDICINE



TRANSPORTATION RESEARCH BOARD

ACRP

Web-Only Document 43:

Improving AEDT Modeling for Aircraft Noise Reflection and Diffraction from Terrain and Manmade Structures

J. Micah Downing
Matthew F. Calton
Blue Ridge Research & Consulting, LLC
Asheville, NC

Judith L. Rochat
Cross-Spectrum Associates Inc.
Pasadena, CA

Juliet A. Page
Volpe, The National Transportation
Systems Center
Cambridge, MA

Contractor's Final Report for ACRP Project 02-79
Submitted August 2019

ACKNOWLEDGMENT

This work was sponsored by the Federal Aviation Administration (FAA). It was conducted through the Airport Cooperative Research Program (ACRP), which is administered by the Transportation Research Board (TRB) of the National Academies of Sciences, Engineering, and Medicine.

COPYRIGHT INFORMATION

Authors herein are responsible for the authenticity of their materials and for obtaining written permissions from publishers or persons who own the copyright to any previously published or copyrighted material used herein.

Cooperative Research Programs (CRP) grants permission to reproduce material in this publication for classroom and not-for-profit purposes. Permission is given with the understanding that none of the material will be used to imply TRB, AASHTO, FAA, FHWA, FMCSA, FRA, FTA, Office of the Assistant Secretary for Research and Technology, PHMSA, or TDC endorsement of a particular product, method, or practice. It is expected that those reproducing the material in this document for educational and not-for-profit uses will give appropriate acknowledgment of the source of any reprinted or reproduced material. For other uses of the material, request permission from CRP.

DISCLAIMER

The opinions and conclusions expressed or implied in this report are those of the researchers who performed the research. They are not necessarily those of the Transportation Research Board; the National Academies of Sciences, Engineering, and Medicine; or the program sponsors.

The information contained in this document was taken directly from the submission of the author(s). This material has not been edited by TRB.

The National Academies of
SCIENCES • ENGINEERING • MEDICINE



TRANSPORTATION RESEARCH BOARD

The National Academies of **SCIENCES • ENGINEERING • MEDICINE**

The **National Academy of Sciences** was established in 1863 by an Act of Congress, signed by President Lincoln, as a private, non-governmental institution to advise the nation on issues related to science and technology. Members are elected by their peers for outstanding contributions to research. Dr. Marcia McNutt is president.

The **National Academy of Engineering** was established in 1964 under the charter of the National Academy of Sciences to bring the practices of engineering to advising the nation. Members are elected by their peers for extraordinary contributions to engineering. Dr. John L. Anderson is president.

The **National Academy of Medicine** (formerly the Institute of Medicine) was established in 1970 under the charter of the National Academy of Sciences to advise the nation on medical and health issues. Members are elected by their peers for distinguished contributions to medicine and health. Dr. Victor J. Dzau is president.

The three Academies work together as the **National Academies of Sciences, Engineering, and Medicine** to provide independent, objective analysis and advice to the nation and conduct other activities to solve complex problems and inform public policy decisions. The National Academies also encourage education and research, recognize outstanding contributions to knowledge, and increase public understanding in matters of science, engineering, and medicine.

Learn more about the National Academies of Sciences, Engineering, and Medicine at www.national-academies.org.

The **Transportation Research Board** is one of seven major programs of the National Academies of Sciences, Engineering, and Medicine. The mission of the Transportation Research Board is to provide leadership in transportation improvements and innovation through trusted, timely, impartial, and evidence-based information exchange, research, and advice regarding all modes of transportation. The Board's varied activities annually engage about 8,000 engineers, scientists, and other transportation researchers and practitioners from the public and private sectors and academia, all of whom contribute their expertise in the public interest. The program is supported by state transportation departments, federal agencies including the component administrations of the U.S. Department of Transportation, and other organizations and individuals interested in the development of transportation.

Learn more about the Transportation Research Board at www.TRB.org.

COOPERATIVE RESEARCH PROGRAMS

CRP STAFF FOR ACRP WEB-ONLY DOCUMENT 43

Christopher J. Hedges, *Director, Cooperative Research Programs*
Lori L. Sundstrom, *Deputy Director, Cooperative Research Programs*
Marci A. Greenberger, *Manager, Airport Cooperative Research Program*
Joseph D. Navarrete, *Senior Program Officer*
Hana Vagnerova, *Senior Program Assistant*
Eileen P. Delaney, *Director of Publications*
Natalie Barnes, *Associate Director of Publications*
Jennifer J. Weeks, *Publishing Projects Manager*

ACRP PROJECT 02-79 PANEL

Field of Environment

Sandra J. Lancaster, *Dallas Fort Worth International Airport, DFW Airport, TX (Chair)*
Ataa Aly, *San Diego County Regional Airport Authority, San Diego, CA*
Justin W. Cook, *HMMH, Anaheim, CA*
Kai Ming Li, *Purdue University, West Lafayette, IN*
Dana M. Nelson, *Metropolitan Airports Commission, Minneapolis, MN*
Dharma R. Thapa, *Ricondo & Associates, Inc., Chicago, IL*
James B. Byers, III, *FAA Liaison*
Bill He, *FAA Liaison*
Christine Gerencher, *TRB Liaison*

AUTHOR ACKNOWLEDGMENTS

The research reported herein was performed under ACRP Project 02-79 by Blue Ridge Research and Consulting, LLC (BRRC) in Asheville, NC with support from Volpe, The National Transportation Systems Center in Cambridge, MA, and Cross-Spectrum Acoustics in Pasadena, CA.

Dr. Micah Downing, Chief Scientist at BRRC, was the Principal Investigator. The other authors of this report are Matt Calton, Engineer at BRRC, Juliet Page, Physical Scientist at Volpe, and Dr. Judith Rochat, Principal Associate at Cross-Spectrum Acoustics. The airport measurements were performed in cooperation with Dan Yeung, Kathryn Pantoja, and Joanne Choi from the Los Angeles World Airport (LAWA) Noise Management office at Los Angeles International Airport, and Ron Reeves and Ryan McMullan from the Airport Noise and Environmental Affairs office at Long Beach Airport.

Contents

Summary	1
1 Background.....	5
2 Research Approach	8
3 Findings and Application	10
3.1 Evaluated Models.....	10
3.1.1 Terrain Effects Modeling.....	10
3.1.2 Barrier Effects Modeling	12
3.1.3 Manmade Structures	12
3.2 Comparison with Data	13
3.2.1 Computational Benchmarking Dataset.....	14
3.2.2 Comparison with Empirical Datasets	21
3.2.3 Airport Noise Measurements.....	35
3.3 Blended Method	56
3.3.1 Selected Models.....	56
3.3.2 Computational Flow for Effects of Terrain and Manmade Structures.....	57
3.3.3 Region of Application	60
3.3.4 Outside of Region.....	65
3.3.5 Blended Method Summary	66
3.3.6 AEDT Integration	66
4 Conclusions and Suggested Research	71
5 References.....	74

List of Figures

Figure 1-1. Conceptual effects of terrain on aircraft noise propagation	6
Figure 1-2. Conceptual effects of manmade structure on aircraft noise propagation	6
Figure 2-1. Proposed blended model development process	8
Figure 3-1. AAM terrain categories for topographic attenuation calculation (Bradley et al. 2016).....	11
Figure 3-2. TNM terrain variation with a barrier showing multiple diffraction points.....	12
Figure 3-3. Calculation of warning siren coverage in an urban setting	13
Figure 3-4. Example of the benchmarking computational case geometry.....	14
Figure 3-5. Comparison of different models dB Gain results as a function of receiver distance for a line source at various heights: (a) 1.5 m, (b) 12.5 m, (c) 50 m, (d) 100 m, (e) 400 m, and (f) 800 m at a distance of 400 m away from a 64 x 16 x 64 m (H x D x W) building	17
Figure 3-6. Effect of source distance for (a) 1.5 m high and (b) 400 m high line source from the facade of a 64 x 16 x 64 m (H x W x D) building calculated by TNM 3.0	18
Figure 3-7. Effect of source height for lines sources at distances for (a) 25 m and (b) 2000 m for 64 x 32 x 64 m (H x W x D) building calculated by CadnaA ISO 9613-2	19
Figure 3-8. Effect of building width for a line source at distances of 100 m and height of 12.5 m for (a) small building (8 x 8 m (H x D)) and (b) large building (64 x 64 m (H x D)), calculated by TNM 3.0.....	20
Figure 3-9. Urban high-density setting from the NYC helicopter measurements	22
Figure 3-10. Overview of the Narvik measurement area and layout	24
Figure 3-11. A-weighted time history comparison for the Narvik noise monitoring sites for Operation A06	26
Figure 3-12. Site 12CA showing microphones behind a highway noise barrier for the TNM validation measurements.....	27
Figure 3-13. Site 12CA, measured, TNM-predicted, and ISO-predicted reduction in noise from reference	29
Figure 3-14. Site 12CA, TNM-predicted and ISO-predicted barrier insertion loss (comparing sound levels with and without barrier)	30
Figure 3-15. Site 14CA, measured, TNM-predicted, and ISO-predicted reduction in noise from reference	30
Figure 3-16. Site 14CA, TNM-predicted and ISO-predicted barrier insertion loss (comparing sound levels with and without barrier)	31
Figure 3-17. Diagram from NCHRP study “Field evaluation of reflected noise from a single noise barrier”	32
Figure 3-18. Site SR-71, NCHRP 25-44 Study; top: cross section with barrier, bottom: cross section without barrier	33
Figure 3-19. Site SR-71, NCHRP 25-44 Study, 9:49 time block; 3 sets of comparisons: from left to right, receiver between highway and barrier, opposite side receiver close to road, opposite side receiver far from road.....	34
Figure 3-20. Site SR-71, NCHRP 25-44 Study, 12:45 time block; 3 sets of comparisons: from left to right, receiver between highway and barrier, opposite side receiver close to road, opposite side receiver far from road.....	34
Figure 3-21. Instrumentation deployed at measurement sites. Left: sound level meter system, right: meteorological system and sound recorder system	36
Figure 3-22. Measurement locations during measurement campaign at Los Angeles International Airport	38

Figure 3-23. El Segundo neighborhood measurements; top: microphone locations labeled A00 – A09, middle: view toward south runways from position A05, bottom: view away from south runways from position A01..... 40

Figure 3-24. Kittyhawk Ave neighborhood measurements; top: microphone locations labeled B00 – B03, middle: view toward flight path from position B02, bottom: view away from flight path from position B02..... 42

Figure 3-25. Playa Del Oro neighborhood measurements; top: microphone locations labeled E00 – E06, middle: view toward N runways from position E02, bottom: view away from N runways from position E02 44

Figure 3-26. Measurement locations during measurement campaign at Long Beach Airport 45

Figure 3-27. LGB measurements; top/middle: view toward and away from runway from position G09, bottom: in front and behind end-of-runway berm (from G01 and G02, respectively)..... 47

Figure 3-28. Processed LiDAR data for El Segundo; buildings are displayed in orange, terrain in brown.. 49

Figure 3-29. 3D visualization of process LiDAR data..... 50

Figure 3-30. Digitized SoundPLAN model of LGB; building footprints and elevation obtained via satellite imagery and Google Earth 3D buildings 51

Figure 3-31. Digitized SoundPLAN model of Kittyhawk; building footprints & elevations obtained via LiDAR 51

Figure 3-32. Results at LGB computed using existing AEDT calculations. 58

Figure 3-33. Calculated GL_{BM} factors associated with manmade structures for an arrival at LGB. 58

Figure 3-34. Blended noise estimate with the existing AEDT aircraft noise and the acoustic effect from manmade structures. 59

Figure 3-35. Comparison of altitude profiles for arrivals and departures 61

Figure 3-36. TNM insertion loss for a ground-based (0 m AGL) noise source at an offset distance of 2,000 m 62

Figure 3-37. TNM insertion loss for a 100 m AGL noise source at an offset distance of 2,000 m 63

Figure 3-38. TNM reflection gain for a ground-based noise source at an offset distance of 2,000 m 64

Figure 3-39. Illustration of regions of application and transition for the blended method building effects 65

Figure 3-40. AAM geometric terrain models (Bradley et al. 2016)..... 67

Figure D-1. Conceptual schematic of segmentation and manmade structures 111

Figure D-2. AEDT schematic for a departure at LGB relative to a community receiver location 111

Figure D-3. Uncertainty introduced in noise fraction calculations due to reduced segment length 112

Figure D-4. Results at LGB computed using existing AEDT calculations 113

Figure D-5. Acoustic effect associated with manmade structures at LGB according to ISO 9613-2 114

Figure D-6. Combination of existing AEDT calculations and acoustic effect from manmade structures . 114

List of Tables

Table 3-1. Summary of preliminary measured acoustic datasets.....	21
Table 3-2. NYC Urban Helicopter: measured and modeled data comparisons for level flight.....	23
Table 3-3. NYC Urban Helicopter: measured and modeled data comparisons for departure flight	23
Table 3-4. Comparison of measured and modeled results for Narvik, Norway Terrain Measurements	24
Table 3-5. TNM Validation sites and attributes	28
Table 3-6. LAX, El Segundo neighborhood measurement positions and site descriptions	39
Table 3-7. LAX, Kittyhawk Ave neighborhood measurement positions and site descriptions	41
Table 3-8. LAX, Playa Del Oro neighborhood measurement positions and site descriptions	43
Table 3-9. LGB measurement positions and site descriptions.....	46
Table 3-10. Distribution of individual measured events.....	53
Table 3-11. Comparison of overall pooled events	54
Table 3-12. SEL grouped results by operational type compared to overall results	55
Table 3-13. SEL grouped results by manmade structural effect (re: TNM) compared to overall results ...	55
Table 3-14. SEL combined grouping results	56
Table 3-15. Example of manmade structural effect calculation values for Site G11 at LGB	60
Table C-1-1. LAX, Hotel district measurement positions and site descriptions.....	102
Table C-1-2. LAX, LAWA administration building area measurement positions and site descriptions	106

Summary

This research project has focused on improving AEDT modeling for aircraft noise reflection and diffraction from terrain and manmade structures.

The objectives of this research were the following:

1. Develop and evaluate noise propagation models that account for these effects.
2. Recommend methods for inclusion into the AEDT integrated noise modeling framework.
3. Provide updated AEDT user guidance on the influence terrain and manmade structures have on aircraft noise.

The integration of these effects into AEDT has involved several steps. First, existing models were identified for application within AEDT. Second, the candidate models were evaluated based on comparisons with computational, empirical, and measured datasets. These comparisons allow the development of a blended method to address the complex objectives for AEDT. The final step involved the refinement of a blended method for the integration into AEDT to model the desired effects of terrain and manmade structures.

The candidate models included the following:

- Advanced Acoustic Model (AAM) – inclusion of diffraction from terrain on a one-third octave band (OTOB) basis in a simulation-based computational method (Bradley et al. 2016).
- NoiseMap7 – inclusion of terrain diffraction and ground impedance variation effects on ground and airborne aircraft noise in an integrated computational method (Czech and Plotkin 1998).
- Traffic Noise Model (TNM) 3.0 – inclusion of diffraction from terrain and barriers, and reflections from barriers on roadway noise (FHWA 2017).
- ISO 9613-2 – general method for effects of barriers, reflections, and manmade structures.
- NORD2000 – published algorithms for diffraction from terrain and barriers (Plovsing 1994).
- National Cooperative Highway Research Program (NCHRP) Screening Tool – a simple method to estimate the reflection of traffic noise from a roadside barrier (Bowlby et al. 2015).

Along with preliminary comparisons with computational benchmarking and historic empirical datasets, high-fidelity measurements were obtained with this project at Los Angeles International Airport (LAX) and Long Beach Airport (LGB). The comparisons with this new dataset allowed the refinement of the blend method and the computational approach for integration into AEDT's Aircraft Acoustics Module.

The candidate models were observed to predict similar acoustic effects for reflections and shielding. Overall, the effects of manmade structures are localized to the general area of the buildings, but within these areas the effects can be noticeable. The majority of the models showed reflection gains of up to 3 dB near a building façade, decreasing rapidly with distance from the façade. The magnitude of shielding effects can be greater and diminish less rapidly than reflection effects as a function of distance behind the building.

The results from the benchmarking analysis were used to estimate expected shielding, diffraction, and reflection effects for similar geometries around airports. The estimates were also used to inform measurement site selection and receiver positions during the measurement campaign. The comparison with existing empirical datasets demonstrated the natural separation in the modeling of effects of terrain and manmade structures as well as the blended computational approach. The aircraft noise measurements obtained at LAX and LGB captured the effects of acoustic shielding, diffraction, and reflection for various geometries and building parameters for numerous aircraft events. These measured data facilitated the evaluation and selection of the recommended models and guided the development of the blended method.

The recommended algorithms for the blended method approach for AEDT are the following:

- **Terrain effects:** utilize the terrain attenuation routines from AAM, which has shown reliability for propagation/diffraction over complicated terrain for time histories and event sound levels with elevated sources; and
- **Manmade structural effects:** utilize the reflection and insertion loss routines from TNM v3.0, which handles the modeling of reflection gains and shielding losses from buildings and barriers in complex environments.

The computational flow of the blended method approach involves two computational modes. First, the effects of terrain can be modeled throughout the calculation area. The inclusion of terrain effects will only involve modifications to algorithms within the Acoustic Module, and no changes are required for the user interface. Second, the effect of manmade structures only needs to be applied in a region where flight operations are at low altitudes or on the ground-based on the computational benchmarking and empirical analyses. Within this region, the gain/loss factors of the blended method (GL_{BM}) for structures can be calculated separately from the aircraft noise, and then they can be combined with AEDT calculations for a final noise exposure estimate. This computational mode will require the development of a new module within the Acoustic Module for the independent calculation of spectral gain/loss factors from buildings. This independent calculation will only have to be accomplished once as long as the surrounding manmade structures remain unchanged. In addition, the user interface will require a new screen to enter (or import) building data and to confirm the region of application for these calculations.

In addition, the NCHRP Barrier Reflections Screening Tool can be used to screen for potential reflection effects outside of the AEDT. This tool has been modified for application to aircraft noise and can be used now to estimate reflection effects while the blended method recommendations are being incorporated into AEDT.

Suggested Future Research:

- Simple Reflection Tool
- Taxi Noise Modeling
- Ground Run-up Enclosures
- Urban Canyon Effects
- Blended Method Verification and Validation

Simple Reflection Tool: The updated NCHRP Barrier Reflections Screening Tool has been modified for airport planners to screen for potential reflection effects outside of the FAA AEDT. This tool has been modified for application to aircraft noise and can be used immediately to estimate reflection effects while the blended method recommendations are being incorporated into AEDT.

Taxi Noise Modeling: AEDT 3 does have the ability to model taxi operations in a limited fashion. The ACRP 02-27 project developed improved taxi noise-power-distance (NPD), spectral class and directivity data for AEDT and incorporation of improved taxi noise modeling is currently on the FAA roadmap for AEDT 4 (Page 2009; Page 2010; Page Hobbs 2012; Page 2013; Page 2014). The insertion losses from terrain and manmade structures is independent of the source noise level, so these future taxi improvements to AEDT will be compatible with the terrain and manmade structure recommendations made under this ACRP project.

Moreover, taxi operations were captured as part of the measurements at LGB. It is suggested that that data be used to test the use of TNM algorithms for calculating the gain/loss factors for these ground operations. Based on the test site layout, the reflection effect should be easily assessed. The shielding effect is more complicated due to nearby structures, and as such, additional data may be required to further test this effect. It is expected, however, that both reflection and shielding effects due to the nearby buildings can be properly calculated, since the ground operations are similar to TNM's intended purpose of calculating such effects for surface transportation.

Ground Run-up Enclosures: In addition to the tested application of TNM for the effects of buildings around airports, it may also be possible to apply the same algorithms to capture the noise-reducing effects of ground run-up enclosures. The modeling approach of the blended method can be combined with the ACRP 02-27 taxi noise project to model the stationary noise from a ground run-up enclosure. However, since these enclosures vary in configurations and sound absorption characteristics, it is recommended that the effect of these enclosures be evaluated by comparing the blended method results to data measured in the vicinity of enclosures. These comparisons will evaluate the validity of the blend method to these enclosures as well as refine the blended method for this application.

Urban Canyon Effects: Initial examination of TNM- and ISO 9613-2-calculated gain/loss factors for a complex urban environment (in this case, the hotel district at LAX), showed that both models were not properly capturing related complex reflections. TNM 3.0 is designed to account for only one reflecting surface, a highway noise barrier, so it has no secondary or higher order reflections, and results from multiple building reflecting surfaces is limited (even with just single reflections). To improve TNM results in an urban environment, additional orders of reflection would need to be added, as well as the ability to incorporate effects from more surfaces than it currently allows. Without these modifications to the TNM reflection algorithms, the proposed method for applying reflection effects is applicable to many standard applications, but it is limited in application to complex building environments with multiple rows of high-rise buildings, which result in the urban canyon effect. However, algorithms for handling the shielding effects for complex urban environments are already implemented in TNM.

Blended Method Verification and Validation: Finally, the data measured as part of this project can be used to validate the results of the blended method when it has been integrated into AEDT. The complete measured airport noise dataset is archived for this potential application. The dataset includes the noise data (raw and analyzed), operational data, observed field notes, weather, terrain and building data, and AEDT modeling data. This archive will be held by the Volpe Center.

1 Background

The Federal Aviation Administration, Office of Environment and Energy (FAA-AEE) developed AEDT to evaluate aircraft noise, emissions, and fuel burn for airport environmental studies. This model has replaced the legacy noise model, the Integrated Noise Model (INM) (Dinges 2007), and the emission model, Emissions and Dispersion Modeling System. The noise modeling capabilities incorporated in FAA's AEDT have been extensively developed over several decades through INM. The robustness of the AEDT approach has proven to provide accurate estimates of noise generated in the communities surrounding airports.

Through the years, additional features of aircraft noise propagation have been added to the AEDT model as technical refinements have been developed and computational power has increased. Some of the additions include acoustic impedance adjustments, noise from thrust reversers, and supplemental metrics (Boeker 2008). AEDT includes the ability to model simple blocked line-of-sight and supplemental metrics, including the calculation of audibility and time above to support the US National Park Service (NPS) modeling needs. Recent research and refinements are looking at improving the noise modeling capabilities of AEDT in the areas of helicopter modeling (TRB 2016; Page 2015), variations in ground impedance (Hobbs 2017), enhanced modeling of flight profiles (Dinges 2017), higher fidelity propagation models (Rosenbaum 2012), and taxi operations (Page 2009; Page 2010; Page Hobbs 2012; Page 2013; Page 2014). When implemented, each of these capabilities will enable AEDT's aircraft noise predictions to become more refined. Additional enhancements to AEDT include the incorporation of high-fidelity weather and terrain databases for the air quality models, which can facilitate the expansion of the Acoustic Module to incorporate methods for acoustic modeling impacts of terrain and manmade structures.

Barriers, berms, buildings, and natural terrain may affect the propagation of aircraft noise by shielding or reflecting sound energy. If terrain and manmade structures obstruct the line-of-sight between the source and the receiver, then sound energy will be attenuated at the receiver. This attenuation increases with the terrain and structures' size and proximity to either the source or the receiver. If gaps exist in the terrain or structures, then the potential benefits of acoustical shielding will be substantially reduced. Even when the line-of-sight is not obstructed, terrain can reflect the sound and create multiple pathways affecting the sound arriving at the receiver. When a reflection occurs, a receiver can be exposed to more sound energy. If the terrain or structures provide vertical or near-vertical surfaces, and the source and receiver are on the same side, then the received sound exposure is increased due to the reflected sound energy. Variations in terrain and manmade structures can have other secondary effects, but these are the primary drivers.

Figure 1-1 illustrates these concepts for terrain effects on sound propagation, and Figure 1-2 illustrates the effects of manmade structures on sound propagation. The sound from the aircraft has a direct path to the person on the right side of each diagram. For the case shown in Figure 1-1, the person may receive a small amount of additional sound energy from scattered reflections. However, the person near manmade structures will receive stronger reflections since the structures provide hard vertical surfaces that reflect the sound. In both cases, the direct sound is blocked for the person on the left, since the sound must travel over the obstruction (hill or structures) to the person. The greater the change in direction of

the sound path at the top of the obstruction, the greater the reduction in sound. The change in direction can be increased by increasing the height of the obstruction or moving the source or receiver closer to the obstruction. This shielding effect will be strongest for the terrain since terrain features generally have fewer gaps than those found between typical manmade structures. Both acoustic reflection and shielding effects are most prominent for sound sources on or near the ground. If the aircraft in Figure 1-1 or Figure 1-2 were to climb upward, sound from the aircraft would have a direct path to both people on the ground with minimal reflection and shielding, which would result in similar sound exposures for each receiver.

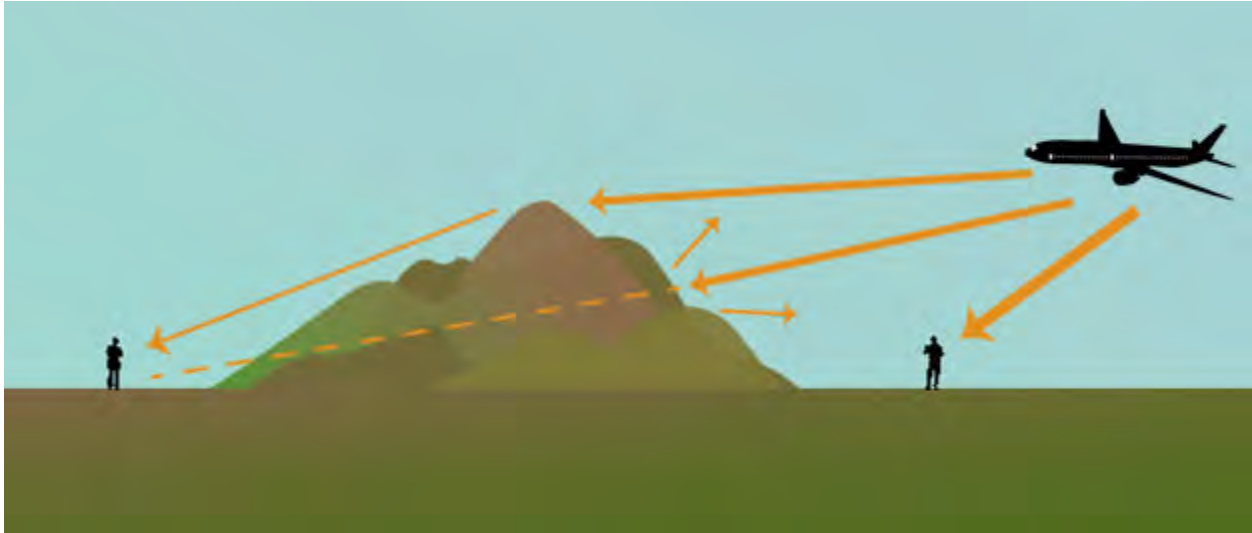


Figure 1-1. Conceptual effects of terrain on aircraft noise propagation



Figure 1-2. Conceptual effects of manmade structure on aircraft noise propagation

It is important to note that AEDT includes a line-of-sight adjustment that only accounts for thin barrier insertion loss with diffraction occurring at a single point at the top of a barrier or terrain feature. Diffraction is the interference of sound waves, bending around an obstruction or changing characteristics

due to other features in a propagation path, e.g. ground type changes and barriers. This adjustment does not include multiple diffraction points along the propagation path nor any reflections (FAA 2016).

The objectives of this research were the following:

1. Develop and evaluate noise propagation methods that account for aircraft noise reflection and diffraction from terrain and manmade structures. These methods shall account for both ground and airborne aircraft operations.
2. Recommend methods for inclusion into the AEDT integrated noise modeling framework. These recommendations address both the physics and the software integration process and the expected influence these new methods have on AEDT's data input requirements, computational load, and resulting uncertainty.
3. Provide updated AEDT user guidance on the influence terrain and manmade structures have on aircraft noise and the applications these new methods have for airport noise analyses.

2 Research Approach

The project objectives were met through a series of reviews, evaluations, and comparisons. A high-level overview of the project is provided in Figure 2-1.

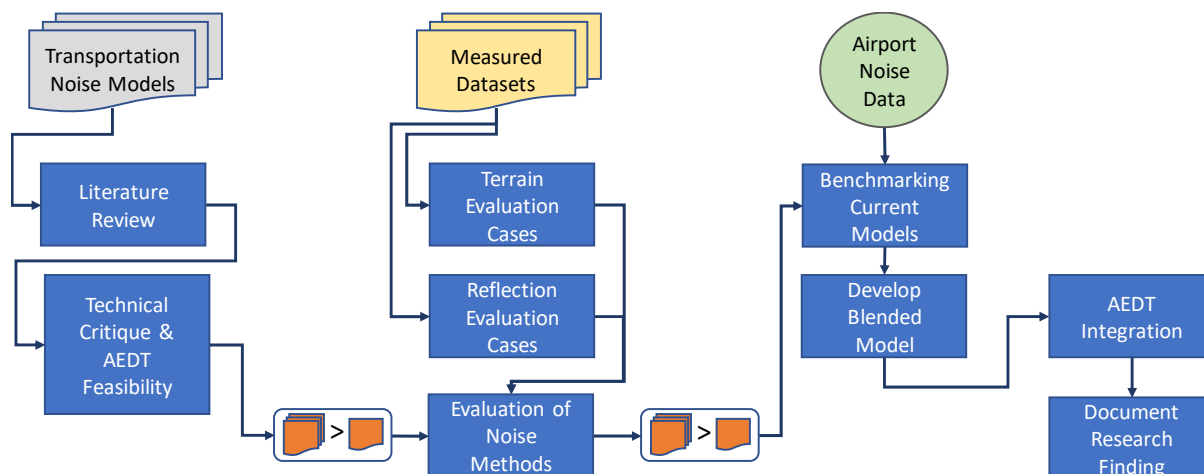


Figure 2-1. Proposed blended model development process

As a first step, a comprehensive review of current models was conducted to select those that showed potential in addressing the objectives. The selected models included both simplistic and high-fidelity models currently used for environmental noise modeling. Each model was evaluated for its potential to accurately predict aircraft noise in the presence of terrain and manmade structures, as well as its integration potential into AEDT. Furthermore, each method was critiqued according to the following considerations:

- Integrated modeling with segments,
- Ground and airborne sources,
- OTOB source data,
- Publicly available input data,
- Computational requirements, and
- Level of validation.

This review and selection resulted in the following models being carried forward for evaluation and comparison with computational and measured datasets:

- AAM – inclusion of diffraction from terrain on an OTOB basis in a simulation-based computational method.
- NoiseMap7 – inclusion of terrain diffraction and ground impedance variation effects on ground and airborne aircraft noise in an integrated computational method.
- TNM 3.0 – inclusion of diffraction from terrain and barriers, and reflections from barriers on roadway noise.
- ISO 9613-2 – general method for effects of barriers, reflections, and manmade structures.

- NORD2000 – published algorithms for diffraction from terrain and barriers.
- NCHRP Screening Tool – a simple method to estimate the reflection of traffic noise from a roadside barrier.

The next step identified the conditions of applicability for each of the models under consideration to facilitate the development of a blended method. Selected models were evaluated in two ways. First, the benchmarking cases were utilized to examine trends and differences in the prediction methods. Second, the methods' predictions were compared to empirical datasets including four historical acoustic datasets and two new acoustic datasets gathered in 2018 at LAX and LGB. The various models' predictions were also compared by isolating the reflection and shielding effects. The effects were isolated by examining the differences in predictions with and without the effect implemented. This isolation also provided the best approach for developing recommendations for implementing the effect of manmade structures to the overall prediction of aircraft noise.

For integration into AEDT, the effects of terrain and manmade structures are handled differently. The terrain effects algorithms can be directly integrated into the noise exposure computational flow within AEDT by utilizing the line-of-sight blockage algorithms within AEDT's Aircraft Acoustics Module. For the manmade structural effects, the reflection and shielding from structures are calculated separately for each modeled operation and then added to the noise prediction.

3 Findings and Application

This section provides the description of this project's findings in the development of the blended method as well as the recommended application of the blended method within AEDT. Section 3.1 describes the models that were reviewed and evaluated for consideration. Section 3.2 discusses the comparisons of the model calculations with computational benchmarking, historical and measured datasets. And, Section 3.3 identifies the selected models for inclusion into the blended method and the recommend computational approach and integration into AEDT's Aircraft Acoustic Module.

3.1 Evaluated Models

The first step involved the basic evaluation of the selected models. Summaries of all reviewed models are provided in Appendix A, which provides individual overviews for each considered model/method. For each model/method, the following information was reviewed:

- Model overview (main purpose, source type, calculation method, method summary),
- Noise source (data source, spectra, directivity, additional comments),
- Propagation algorithm (atmospheric absorption, atmospheric refraction, ground impedance, terrain, barriers, manmade structures, reflections),
- Source code (access, language, whether or not it has been acquired).

For the blended method, both open source and restricted codes were considered. The proprietary codes generally allow for higher complexity in representing the environment and propagation conditions. The team used these more complex models, such as CadnaA and SoundPLAN with NORD2000 and ISO 9613-2 method implementations, for computational benchmarking of the other models as well as the developed blended method. The subsections below review the relevant effects and the application of the various models.

3.1.1 Terrain Effects Modeling

Current transportation models include simple terrain effects such as the blocked line-of-sight effect, from the simple calculations in SAE-AIR-6501 to more complex calculations as in NoiseMap, TNM, NMSim, and AAM. Both ISO 9613-2 and SAE-AIR-6501 use a basic formulation based on the path length difference to calculate the attenuation when the line-of-sight is blocked and only include the diffraction occurring at the top of the barrier or terrain feature.

The physics in AAM's methodology is based on Rasmussen (1985). Rasmussen's theoretical model for the calculation of sound propagation over varying terrain is based on the Geometrical Theory of Diffraction (GTD), which was originally introduced by Keller (1962). The computational methodology for ground reflection and attenuation over areas where topographic features are significant is twofold. First, the effect of terrain and receiver altitude relative to vehicle location (slant range) are computed for both direct and blocked line-of-sight. Second, the effects of terrain and ground cover on ground reflection and attenuation due to the multiple ray paths are computed with Rasmussen's algorithms (1985). These algorithms account for shielding (modeled as wedges) and structures (modeled as thin screens), multiple forward ground reflections in valleys, and the effects of ground impedance.

Rasmussen, by hypothesis, developed a technique for predicting diffracted waves, as determined by local geometry between the source and receiver. A series of approximate solutions (based upon the assumption that the distances are long with respect to the wavelength) are categorized and implemented for several geometric configurations. AAM contains the extensions of the GTD to finite impedance terrain, by means of physical formulae. The sound field at a receiver point can be described as the sum of direct, reflected, and diffracted waves. The model performs a geometric “slice” through the three-dimensional terrain from the source to the receiver location and using a numerical fitting technique, classifies the principal features into five geometric models. These models allow for variable ground impedance across five different terrain categories: Flat, Uphill (Valley), Downhill, Thin Screen, and Wedge with one or two flats as shown in Figure 3-1. AAM’s topography algorithms do not include backward reflections of the propagated sound.

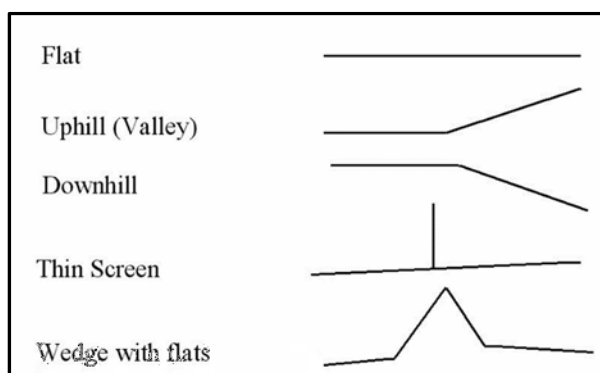


Figure 3-1. AAM terrain categories for topographic attenuation calculation (Bradley et al. 2016)

The topography algorithms in NoiseMap are limited to A-weighted sound level and only include the Flat, Valley and Wedge terrain cuts. However, NoiseMap is an INM, and its implementation fits within the AEDT computational assumption. Thus, following this construct, the improved physics of the AAM algorithms can be implemented in AEDT using the NoiseMap integral implementation.

The effects of terrain and ground cover in FHWA TNM are included with a combination of shielding and ground effects calculations, leading to an adjustment to the source noise based on user-specified terrain. TNM allows for input of terrain lines that define the elevation of the ground between the sound source and receiver (as shown in Figure 3-2). The model also allows for user-defined ground type, where selection of pre-defined types with associated effective flow resistivity values or user-defined values are used in ground impedance and ground reflection calculations. TNM accounts for any terrain protruding into the sound propagation path, using diffraction equations to determine the amount of sound that bends over or around the top of the ground protrusion. TNM accounts for propagation over the ground by applying reflection equations that account for the user-specified ground type(s) and diffraction at points where two ground types meet. The intended use of the model is for highway traffic noise predictions, and the model shows good agreement with measured data out to approximately 150 m (Rochat 2004). Beyond that distance, TNM has proven to partially over-predict ground effects. Suggested improvements to TNM to increase accuracy out to much farther distances were documented at the completion of TNM version 2.5; since farther distances are not typically of concern in highway noise studies, these improvements

were never implemented. These suggested improvements to TNM can be applied to the calculations for the blended method implementation for AEDT.

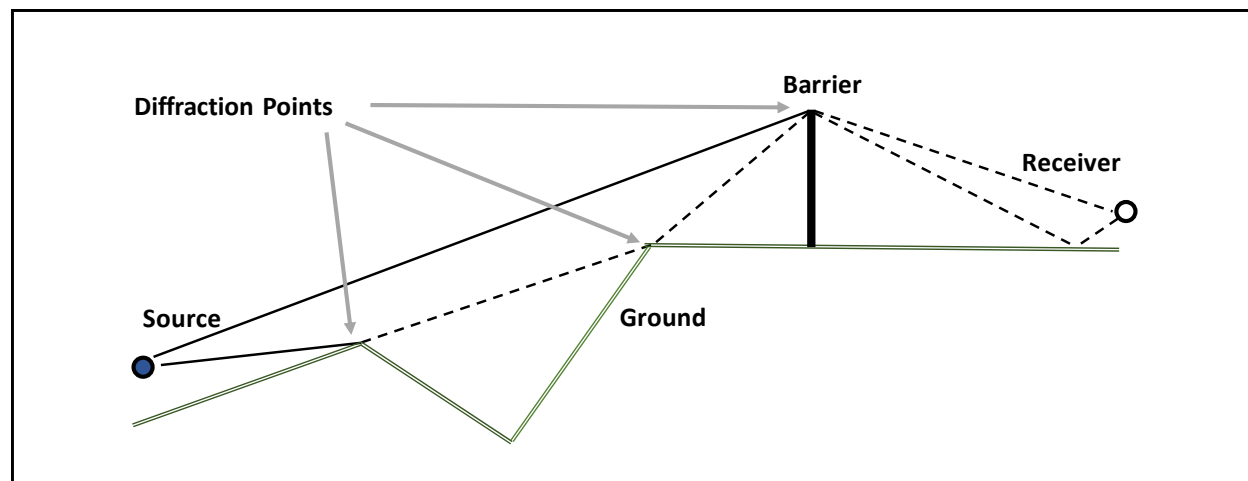


Figure 3-2. TNM terrain variation with a barrier showing multiple diffraction points

3.1.2 Barrier Effects Modeling

ISO 9613-2 provides simple equations for the calculation of insertion loss from barriers for single and double diffraction and finite barrier width. TNM includes noise barriers (walls and berms) as input objects, where height and length (and slope for berms) are user-defined. The length can be defined in segments, and each segment can have multiple heights to help users with noise abatement design. For sound propagation, diffraction and sound absorption calculations are applied. The shielding effect can include single and multiple diffractions, accounting for more than one barrier. The TNM Validation Study (Rochat 2004) shows that predictions for distances out to 94 m (308 ft.) behind barriers (the farthest distance studied) matched well with measured sound levels. Parallel barrier effects are calculated in a separate ray tracing module of TNM. For TNM version 3.0, barrier reflections (where noise reflects off the barrier surface and back across the highway) are included in the calculations. The NCHRP Barrier Reflections Screening Tool provides an efficient estimate for the regions where reflections from barriers can elevate the noise levels. These three methods were evaluated for the calculation of insert loss and reflections from barriers within the blended method.

3.1.3 Manmade Structures

The weaker feature of the reviewed models is the direct inclusion of manmade structural effects. In addition to a structure's barrier effect as described above, manmade structures in aggregate, are less uniform than a roadside barrier and can generate multiple reflections and canyon effects. TNM 3.0, which includes reflection from barriers, can also be applied to building reflection. Building façades, which may reflect noise, can be modeled as short length barriers within TNM. TNM translates the geometry to create image sources that account for the interaction with all of a site features, and then it combines the direct and reflected sounds at a receiver to determine the resultant sound level.

ISO 9613-2 provides a simple calculation of reflection effects by using image sources and reflection coefficients for various reflection surfaces. CadnaA and SoundPLAN provide estimates for an urban environment that include multiple reflection paths. For example, Figure 3-3 shows the results of SoundPLAN's calculation for a warning siren's coverage within an urban setting. Regions of shielding can easily be observed, and smaller regions enhanced by building reflections can be found, as well. Our team used these standard higher fidelity noise models to evaluate the application of ISO 9613-2.



Figure 3-3. Calculation of warning siren coverage in an urban setting

3.2 Comparison with Data

Selected models were evaluated by comparing predictions to the computational benchmarking cases, previously measured acoustic datasets (empirical data), and new empirical data obtained at LAX and LGB for aircraft operations. For the evaluation, the effects of reflection and shielding were isolated by examining the difference in calculation with and without the effect implemented within each model. The following sections summarize the results of the comparisons for each dataset.

3.2.1 Computational Benchmarking Dataset

CadnaA and SoundPLAN were used along with AAM, NCHRP Screening Tool, and TNM to assess the direct effect of shielding and reflection from manmade structures on aircraft noise propagation for simple computational cases. These cases included an array of simple building layouts for the initial comparative benchmarking cases to evaluate the effect of manmade structures in terms of distance and incident angle. This type of examination provided a focus of propagation effects both in terms of physical trends in the effects of structure but also the efficiency of the selected models to perform the calculations. The evaluation involved both point and line source, but the results for the line sources were used for the evaluation since they were more applicable to aircraft noise modeling.

The cases consist of simple geometries with a line source at various offset distances and altitudes, a building of varying heights, widths, and depths, and multiple receivers both on the source side and behind the building. Figure 3-4 provides a partial view of the benchmarking case. The line sources are placed at offset distances from 25 to 2,000 m (82 to 6,562 ft) from the building façade and at altitudes from 1.5 to 800 m (5 to 2,625 ft). The line sources were parallel to the building façade and extended 2,800 m (9,187 ft) in both directions at a constant height above the ground. Receiver points in front of the building span 1 to 2,048 m (3 to 6,719 ft) at doubled distances. Ten receivers were located behind the building from 12.5 to 2,000 m (41 to 6,562 ft) from the building façade. Sound power for each source is defined as 100 dB re 1 pW in each octave or OTOB. Also, the ground was modeled as acoustically soft. Building widths had the strongest factor and were set at 8, 16, 32, and 64 m (26, 52, 105, and 210 ft). The heights and depths were set to 8 and 64 m (26 and 210 ft) since they had a secondary effect. These simple geometries allowed an evaluation of the regions of influence for areas with reflection gains and shielding losses.

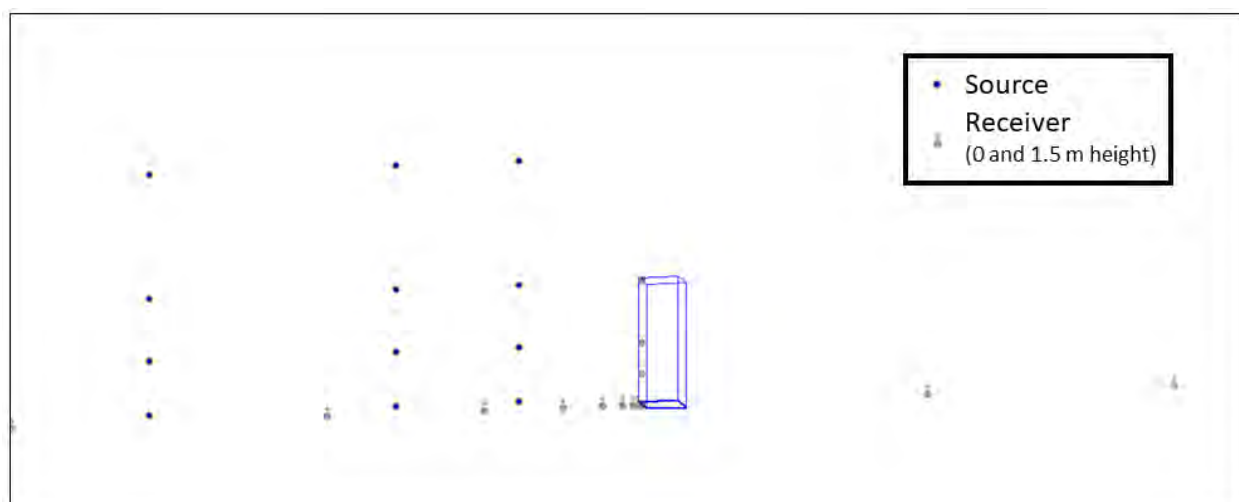


Figure 3-4. Example of the benchmarking computational case geometry

The benchmarking cases provided the basis for a series of graphics, which isolate the various parameters that influence the regions of reflections and shielding. All of the series include calculations from AAM, ISO 9613-2 (as implemented in both CadnaA and SoundPLAN), NORD2000, NCHRP Screening Tool, and TNM. The following representative examples provide an overview of the findings from the benchmarking comparisons. These representative results focus on the region near the building façade and not on the

entire computational space. In these plots the source is to the left with the building façade located at $X = 0$. In addition, two dashed lines are shown for ± 0.25 dB to provide a visual reference for when the effects are considered marginal. These comparisons help to show trends in the dependencies of the reflection gains and shielding losses.

3.2.1.1 Comparison of Models

The initial comparison shows the overall differences among the models. For this comparison, six plots are provided in Figure 3-5 to demonstrate how the models compare with variations in source height. The modeled building dimensions are 64 x 16 x 64 m (210 x 52 x 210 ft) (Height (H) x Depth (D) x Width (W)), and the line source is offset 400 m (1,312 ft) from the building front façade. Overall, the models provide similar trends for both the reflections (except for AAM, which has no reflections) and shielding (except for NCHRP which has no shielding). NCHRP predicts larger reflection gains over a significantly longer distance. For source heights 50 m (164 ft) and below, AAM predicts the largest shielding followed by TNM. For higher source heights, AAM predicts minimal shielding, while the others show decreasing shielding losses.

3.2.1.2 Effect of Source Distance from the Building

The second comparison highlights the effect of source offset distance from the building on the calculated results. Figure 3-6 provides two representative results for two line sources with altitudes of 1.5 m (5 ft) and 400 m (1,312 ft) as calculated by TNM. The sources were modeled at offset distances of 25, 100, 400, and 2000 m (82, 328, 1,312, and 6,562 ft). The reflection effects are 3 dB at the façade for all source distances and for both altitudes, but quickly decrease to less than 1 dB within a distance of 50 m (164 ft). As increasing source distance provides a slight increase in the extent of the reflection region since the path length difference decreases, which enhances the contribution of the reflected sound. For shielding losses for the low altitude result (Figure 3-6 (a)), no significant dependence on source distance is observed and the maximum loss ranges from 2.5 to 4.5 dB at the façade and quickly decreases below 1 dB within 50 m (164 ft). For the higher altitude result (Figure 3-6 (b)), shielding loss increases with increasing distance because the slant angle is shallower, effectively increasing the line-of-sight blockage.

3.2.1.3 Effect of Source Height

The third comparison demonstrates the effect of source height (altitude) on the calculation of reflection gains and shielding losses. Figure 3-7 shows the results for a building that is 64 x 32 x 64 m (210 x 105 x 210 ft) (H x D x W) for source distances of 25 m (82 ft) and 2000 m (6,562 ft). Again, these results were calculated with CadnaA ISO 9613-2 method. For the closer source, the results are more diverse than the more distance source because the higher source heights do not have their line-of-sight blocked by the building for points behind the building. The reflection gains are 2 to 2.5 dB at the façade, and they decrease rapidly. At a source height of 50 m (164 ft), the reflection effect is the greatest, but it diminishes to negligible levels for source altitudes 400 m (1,312 ft) and above. For the more distant source, the line-of-sight is always blocked so the reflection gains and shielding losses are not dependent on source height. The reflection gain is above 1 dB within 50 m (164 ft); the shielding loss is greater than 1 dB within 50 m (164 ft).

3.2.1.4 Effect of Building Width

The final comparison shows the effect of building width on the reflection gain and shielding loss. Figure 3-8 provides two examples for a source at 400 m (1,312 ft) away from the façade and at 12.5 m (41 ft) height

for a small (8 x 8 m (26 x 26 ft) (H x D)) and a large (64 x 64 m (210 x 210 ft) (H x D)) building. This comparison utilizes the results from TNM 3.0. As expected, the reflection gains and shielding losses increase with width for both of these cases. The reflection gains are 3 dB at the façade and increase their extent with increasing building width. The influence is stronger on the shielding losses. The losses are greater than 5 dB for the wider building, and they fall below 1 dB at 150 m (492 ft) for the largest building. The other building dimensions have little influence on the result.

3.2.1.5 Computational Benchmarking Summary

The results of the benchmarking highlight two major trends for the models and effects. First, the models provide fairly similar results for both reflection gains and shielding losses, except where a model does not capture an effect. Second, the regions of influence for both building reflections and shielding are localized to within 300 m (984 ft) to the building façades for low altitude sources (<152 m (500 ft)). For higher altitude sources the regions of reflections and shielding is greatly reduced as expected.

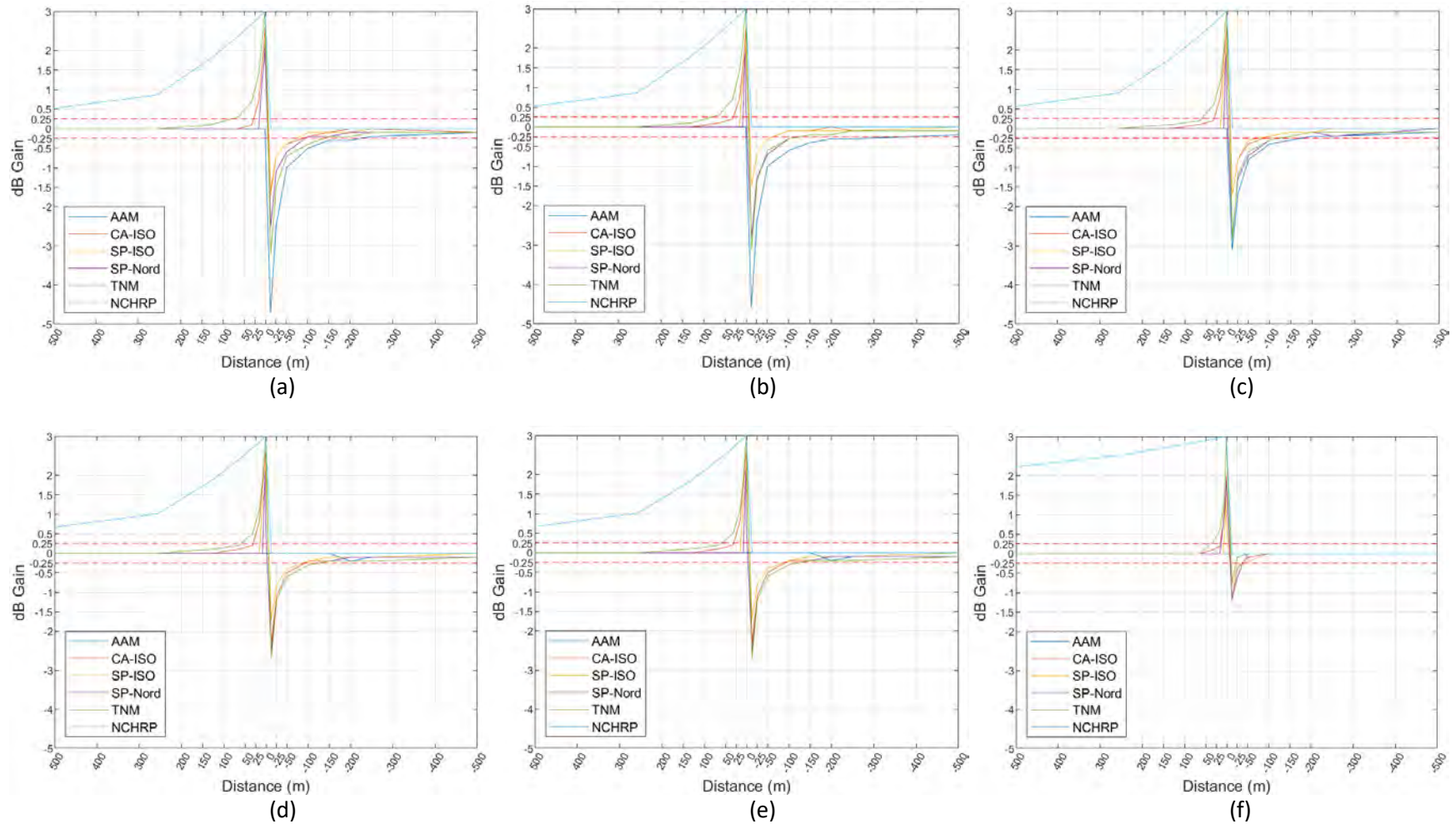


Figure 3-5. Comparison of different models dB Gain results as a function of receiver distance for a line source at various heights: (a) 1.5 m, (b) 12.5 m, (c) 50 m, (d) 100 m, (e) 400 m, and (f) 800 m at a distance of 400 m away from a 64 x 16 x 64 m (H x D x W) building

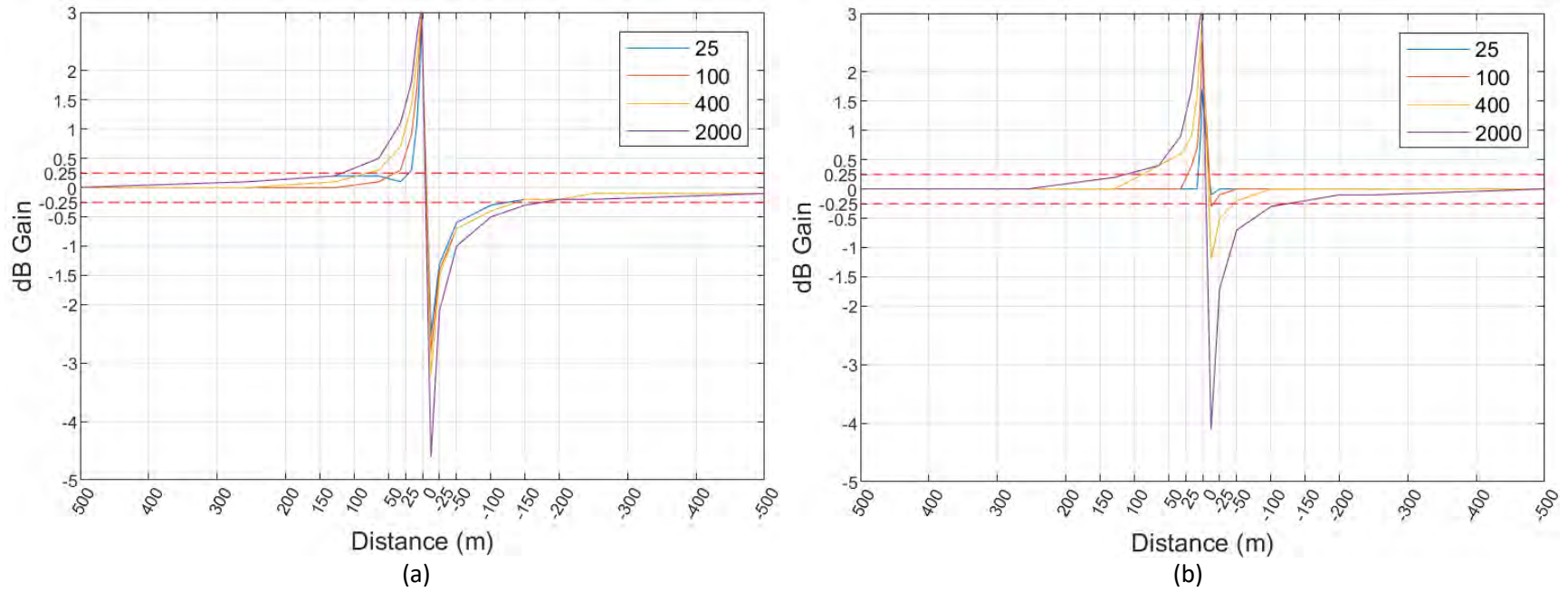


Figure 3-6. Effect of source distance for (a) 1.5 m high and (b) 400 m high line source from the façade of a 64 x 16 x 64 m (H x W x D) building calculated by TNM 3.0

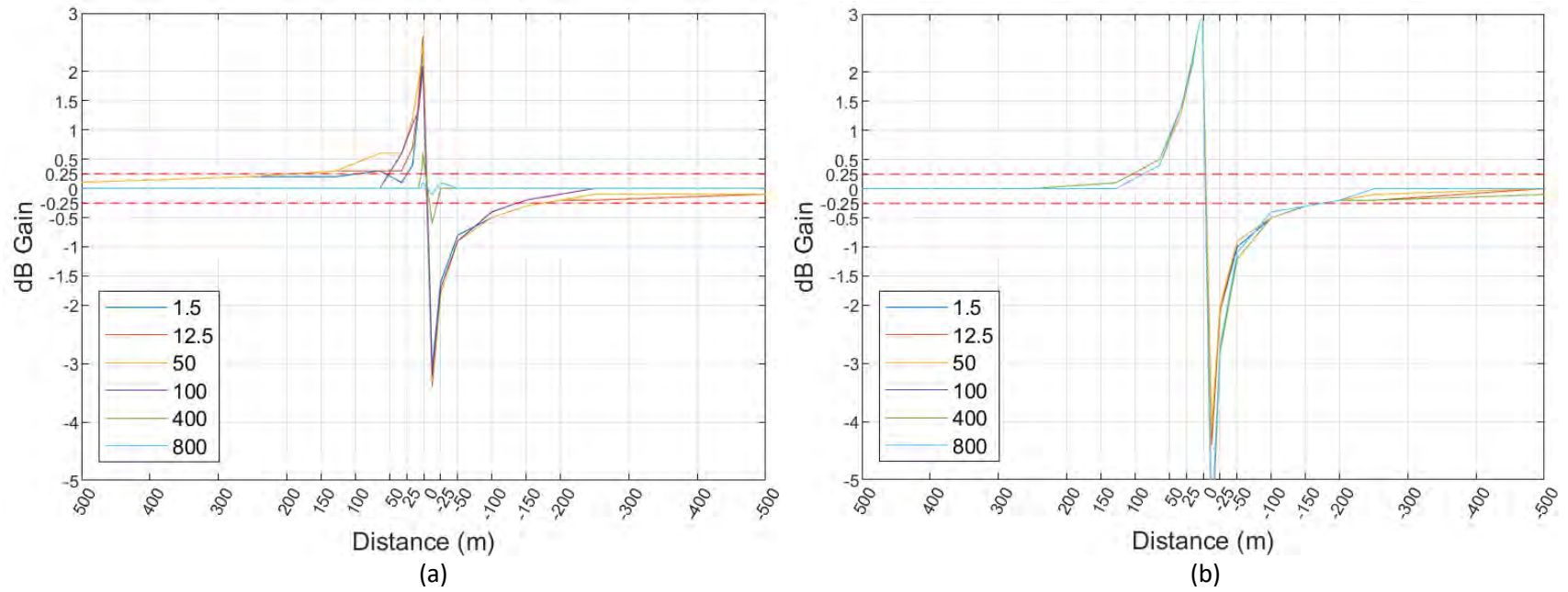


Figure 3-7. Effect of source height for lines sources at distances for (a) 25 m and (b) 2000 m for 64 x 32 x 64 m (H x W x D) building calculated by CadnaA ISO 9613-2

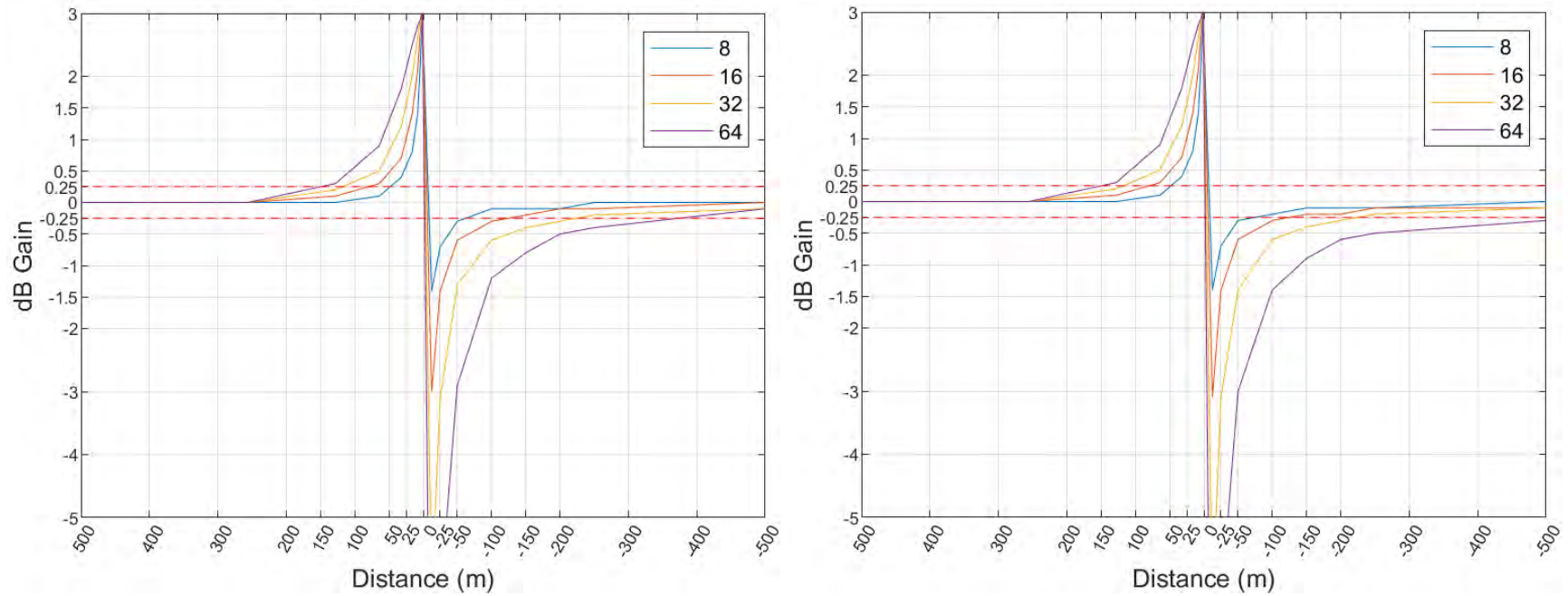


Figure 3-8. Effect of building width for a line source at distances of 100 m and height of 12.5 m for (a) small building (8 x 8 m (H x D)) and (b) large building (64 x 64 m (H x D)), calculated by TNM 3.0

3.2.2 Comparison with Empirical Datasets

Acoustic data from previously collected field measurements were used to compare the prediction from the selected models. The empirical data used for this project are from two aircraft noise measurements and two highway noise measurements. The aircraft noise studies are the New York City (NYC) Urban Helicopter Study and the Narvik NoiseMap Terrain Study. The two highway studies are the TNM Validation Study and the NCHRP Barrier Reflections Study. Table 3-1 provides a summary of these empirical datasets. The comparative analyses for each model are in the form of either direct comparison with measured values or as a relative gain/loss compared to with and without the feature. The relative comparison construct is useful to minimize errors from uncertainty in the reference source noise for given measured dataset or model. For some of the datasets, only a limited number of microphones and/or operational conditions were obtained for empirical comparisons.

Table 3-1. Summary of preliminary measured acoustic datasets

Dataset	Effect Included	Purpose of Study	General Site Setup	Sound Source	Other Site Features	Number of Measurement Positions	Data
NYC Urban Helicopter Study (FAA 2004)	Propagation in urban setting	Validation of noise modeling from heliport	Nearby heliport and propagation to high-rise balcony and other sites	Helicopters	Propagation over water	1 outdoor, 1 indoor	Overall A-wt Sound Levels
Narvik NoiseMap Terrain (Lee et al. 1996)	Natural topography, shielding, diffraction	Validation of propagation over natural terrain	Military aircraft takeoff / landing and flight over natural fjords with extreme Terrain	Military aircraft (F-16C)	Moving source, TO and LA and in flight	8 measurement sites at various distances and terrain heights	OTOB time histories, terrain elevations, aircraft trajectory
TNM Validation (Rochat and Fleming 2002, 2004)	Shielding/ diffraction	Assess the accuracy of TNM predictions including barriers	Microphones placed in line perpendicular to highway	Highway traffic	Mostly flat, hard and soft ground	Typically, 1.4 and 4.6 m above ground at two distances from barrier/berm	5-minute L_{Aeq} , OTOB; 3-6 hours of data per site
NCHRP Barrier Reflections (Bowlby et al. 2015)	Reflection	Determine the effect of highway noise barrier reflections	Microphones placed on opposite side of highway from a noise barrier wall and at an equivalent site with no wall	Highway traffic	Mostly flat, hard and soft ground	Typically, 6, 3 at each site (with and without wall): reference above wall or between wall and highway and two on opposite side of road	1-minute L_{Aeq} , OTOB; 4-5 hours of data per site

A few of the model comparisons were removed because a model's assumed physics does not include the physical phenomena included in the measured data. For example, the AAM does not include reflections,

so the comparison with the barrier reflection measured data was removed since it would not provide any additional insight.

3.2.2.1 NYC Urban Helicopter Results

The Volpe National Transportation Systems Center Acoustics Facility (Volpe Center) conducted helicopter noise field measurements in the greater NYC area to support FAA analysis of helicopter noise impacts (FAA 2004). The area was chosen for the collection of operational helicopter noise data because NYC consisted of an urban environment with significant helicopter operations. Of interest to our project, data were collected near one of the downtown heliports, adjacent to the Wall Street financial district (see Figure 3-9). For this high-density area, at least two measurement locations were obtained along with observation of helicopter operations.



Figure 3-9. Urban high-density setting from the NYC helicopter measurements

For this comparison, AAM provided direct comparisons for both the level and departure flights that were measured at this location. The AAM calculations include the barrier insertion loss of the building, but they do not include any reflections. For TNM, relative comparisons of the predicted sound levels (with and without reflections) were used since exact reference helicopter noise data are not available within TNM. For ISO 9613-2 (as implemented in SoundPlan), relative comparisons (with and without reflections) were computed for the level flight only. Table 3-2 shows the results for level flight, and Table 3-3 shows results for a departure flight. For level flight, the measured value is an average of ten events; the data for the departure flight represents just one event.

Results indicate that AAM is underpredicting by 1.8 to 3.3 dB; these underpredictions are expected since AAM does not account for reflections, and the measurement position is very close to the building façade. TNM and the NCHRP Barrier Reflections Screening Tool each indicate that about 3 dB should be added for the reflection effect, which, when applied to the AAM results, produces predicted sound levels within about 1 dB of the measured sound levels. ISO 9613-2 results indicate 2.5 dB should be added for the reflection effect for the level flight case, which, when applied to the AAM results, also produces predicted sound levels within about 1 dB of the measured sound level. Overall, TNM provides the best reflection effect results, although the other models show similar results.

Table 3-2. NYC Urban Helicopter: measured and modeled data comparisons for level flight

Data source	Reflection effect (dB)	Sound in front of building (dBA)	Delta (modeled minus measured, dB)
Measured	Unknown	77.3	NA
AAM	NA	74.0	-3.3
TNM 3.0	3.4	77.4 [†]	0.1
NCHRP Screening Tool	3.0	77.0 [†]	-0.3
ISO-9613 (as implemented in SoundPlan)	2.5	76.5 [†]	-0.8

Notes: (†) Calculated by adding reflection effect to AAM predicted sound in front of the building (which does not include the reflection effect)

Table 3-3. NYC Urban Helicopter: measured and modeled data comparisons for departure flight

Data source	Reflection effect (dB)	Sound in front of building (dBA)	Delta (modeled minus measured, dB)
Measured	Unknown	92.0	NA
AAM	NA	90.2	-1.8
TNM 3.0	2.8	93.0 [*]	1.0
NCHRP Screening Tool	3.0	93.2 [*]	1.2

Notes: (*) Calculated by adding reflection effect to AAM predicted sound in front of the building (which does not include the reflection effect).

3.2.2.2 Narvik Results

The North Atlantic Treaty Organization (NATO) countries under the NATO Current Challenges for a Modern Society (CCMS) conducted an aircraft noise measurement program at Narvik, Norway to measure the effects of topography (variations in both elevation and surface type) from aircraft flight operations. (Lee et al. 1996) The measurements involved several low approaches of an F-16C with eight measurement locations (Figure 3-10). The propagation conditions involved variations in ground cover and ground elevation between the source and receiver. The propagation distances are considered relatively long-

range (>300 m) for aircraft noise. The acoustic data have been analyzed and reduced to time-synchronized OTOB spectral time histories. In addition, the actual trajectories for each low approach were obtained as well. The present evaluation focused on one flight that has been used for AAM and NMSim algorithm update verifications.

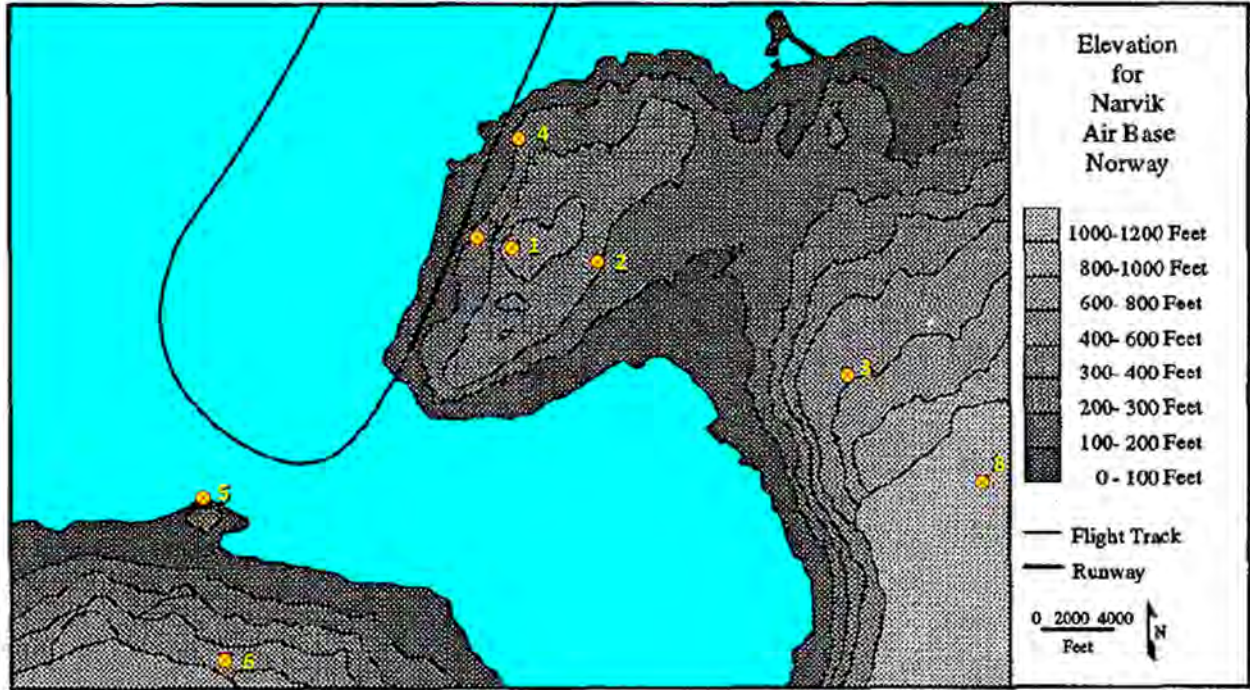


Figure 3-10. Overview of the Narvik measurement area and layout

This test case consists of a low power approach with a military (full power without the use of afterburner) departure. Calculations were performed with AAM Acoustic data collected by six sound level meters are used for the comparison. The original plan was to include data from eight sound level meters, but after reviewing the archive of field measurements and observer logs, two sites were removed from the comparisons. One site was next to the runway (Site 7), which provides little propagation effects, and the modeled results are extremely sensitive to timing and precision of engine thrust changes. Another site (Site 2) was removed due to complications with the measurement location: the observer notes included the following statement, “behind a concrete roof”. Additionally, the resolution of the exact locations for the sound level meters utilized in the comparison was found to be less than expected, particularly for Site 2. For the archived dataset, several coordinates were listed, so the uncertainty in the locations vary from 9 to 31 m (30 to 100 ft).

The comparative results are provided in Table 3-4 where delta values are presented as AAM calculations minus measured values for each metric.

Table 3-4. Comparison of measured and modeled results for Narvik, Norway Terrain Measurements

Site ID	Measured (dBA)	AAM (dBA)
---------	----------------	-----------

	L_{Amax}	SEL	L_{Amax}	SEL	ΔL_{Amax}	ΔSEL
1	107.7	115.7	103.2	108.6	-4.5	-7.1
3	83.8	93.9	88.9	94.9	5.1	0.9
4	94.8	103.9	97.8	102.0	3.0	-1.9
5	103.3	113.5	103.4	111.3	0.1	-2.3
6	100.9	109.1	95.7	103.5	-5.2	-5.6
8	83.3	93.0	86.1	93.2	2.8	0.2
Averages					0.2	-2.6

A comparison of the measured and predicted time histories shows better correlation than the integrated metrics suggest. Comparisons were made to understand the propagation results and better interpret the physics. These time history comparisons are shown in Figure 3-11 for the eight noise monitoring locations and include the measurement data (“Meas”-orange) and AAM results (AAM-light blue).

Some key points the Narvik dataset illustrates when examining the AAM results include:

- Mixed propagation over ground and over water can result in distinct local peaks in the time history which may not strongly affect the L_{Amax} as it is often determined from the point of closest approach. The sound exposure level (SEL) calculations are within 10 dBA of the maximum, but multiple peaks are pronounced in the time history calculations. INMs could have difficulty capturing such details when considering supplemental metrics like time above and time audible.
- AAM algorithms tend to underpredict sound levels for propagation over terrain after long-distance propagation over water. This trend is also observed when examining the AAM time history for the later part of the time history (after 30 s) for Sites 2, 3 and 5 when the aircraft has turned and is heading northbound.
- Even though it was dropped from the benchmark, Site 2, which had shielding from a building, illustrates qualitatively the shielding effect after the 18 s mark when the aircraft was crossing the runway at low altitude.
- For elevated sites with direct line-of-sight (Sites 1 and 6), AAM is underpredicting L_{Amax} and SEL values. This could be due to source spectral directivity and aircraft trajectory, thrust and orientation uncertainty.
- For a site that has direct line of site and is close to the water with propagation over the water (Site 5), AAM is somewhat underpredicting SEL but predicting L_{Amax} well. L_{Amax} appears to occur at the closest point of approach, where the propagation distance is the shortest. These observations indicate that AAM is predicting the levels well when the propagation distance over water is short and not as well when the distance is longer.
- For a site that is likely shielded at and near the closest point of approach (Site 3), AAM is over-predicting L_{Amax} but predicting SEL well. This result indicates that the shielding/diffraction effects may not be performing as desired at the closest point of approach.



Figure 3-11. A-weighted time history comparison for the Narvik noise monitoring sites for Operation A06

- For a site that has complicated terrain over a long distance and likely some diffraction, particularly at the path to the closest point of approach (Site 8), AAM is over-predicting L_{AMax} but predicting SEL well. Again, this observation indicates that the diffraction effects at the closest point of approach may not be modeled as desired, but the overall exposure estimate is promising for this dataset.
- Aircraft source directivity effects are important and are likely inaccurate as can be seen by comparing the first portions of the time histories approaching the initial maximum values (Site 4). The modeled rise in the sound level is much steeper than the more gradual measured increase in the sound level. This inaccuracy is due to the omission of supersonic exhaust forward-flight effects (Michalke and Michel, 1979, and Reichman et al, 2018) in the original 3D source model.

3.2.2.3 TNM Validation Results

The FHWA TNM Validation Study (Rochat and Fleming 2002, 2004) assessed the accuracy of the model to make recommendations on its use. The study involved highway traffic noise data collection and TNM modeling for the purpose of data comparison. Over 100 hours of highway traffic noise data were collected at seventeen sites across the US. The sites had characteristics of those most commonly modeled by TNM users, where it was relatively simple to isolate individual features in TNM. The sites included: open areas next to the highway with acoustically soft ground (e.g. lawn); open areas with acoustically hard ground (e.g. pavement or water); and areas next to the highway with an open area behind a single noise barrier as shown in Figure 3-12. Instrumentation was deployed at each measurement site for capturing acoustical, meteorological, traffic, and site survey data. Acoustical data were captured at distances ranging from 15 to 388 m (50 to 1,273 ft) from the roadway. For sites with a noise barrier, acoustical data were captured at distances from 15 to 91 m (50 to 300 ft) behind the barrier. The study for which the validation data were collected showed that TNM v2.5 performs very well at both open area and barrier sites, particularly within 152 m (500 ft) of the road (i.e. typical use of TNM); but beyond that distance, for these flat sites with shallow-angle ground reflections, TNM tends to exaggerate ground effects.



Figure 3-12. Site 12CA showing microphones behind a highway noise barrier for the TNM validation measurements

From the TNM validation dataset, two sites were examined to help determine how TNM v3.0 and ISO 9613-2 (as implemented in CadnaA) perform in calculating the effects of diffraction/shielding. The

chosen sites and their attributes are shown in the Table 3-5. For each site, 1-second A-weighted equivalent sound levels (L_{eq}) were measured continuously for four hours. The measurement positions were above the barrier (as a reference for sound levels with minimal barrier influence), and at three distances (two heights each) behind the barrier. For each site, three clean 5-minute data blocks were selected. The traffic data associated with each data block were used as input to the two models, and sound levels were predicted for each data block. For the measured and predicted data, the sound levels were arithmetically averaged for the three data blocks for each site.

Table 3-5. TNM Validation sites and attributes

TNM Validation Sites	Highway	Barrier	Terrain	Microphone Locations xxxd_yyyh [†] (ft)
12CA	8 lanes	12 feet	Mostly flat, behind barrier -6 feet from road elevation	000d_005h (above barrier) 050d_005h, 100d_005h, 200d_005h 050d_015h, 100d_015h, 200d_015h
14CA	8 lanes	16 feet	Mostly flat, behind barrier -2 feet from road elevation	000d_005h (above barrier) 050d_005h, 100d_005h, 150d_005h 050d_015h, 100d_015h, 150d_015h

Notes: (†) Distance in feet where xxx and yyy are distance behind barrier and height above ground, respectively (exception: for the reference microphones, the height above the top of the noise barrier is shown).

The data were examined in two ways: 1) the difference between the reference microphone and each of the other microphones (how much the sound is reduced over distance from the unshielded sound level), and 2) the difference between sound levels with and without the barrier (barrier insertion loss). The first examination was done with the measured and predicted datasets, and the second examination with just the predicted datasets.

Figure 3-13 shows the first examination for Site 12CA. For the low microphone, TNM and ISO show more reduction in sound level from reference compared to the measured data. For the high microphone, TNM matches well with the measured reduction, and ISO shows more reduction than measured. Figure 3-14 shows the second examination for Site 12CA. ISO predicts more insertion loss than TNM, particularly for receivers farther from the barrier.

Figure 3-15 shows the first examination for Site 14CA. For the low microphone, TNM and ISO both show more reduction in sound level from reference compared to the measured data close to the barrier and

are matching measured reduction well farther from the barrier. For the high microphone, TNM matches the measured reduction, and ISO matches only farther from the barrier. Figure 3-16 shows the second examination for Site 14CA. Only for the lower microphone, TNM is calculating slightly more insertion loss than ISO close to the barrier; the higher microphone results match.

Overall, TNM matches the measured shielding/diffraction effects better than ISO (as implemented in CadnaA).

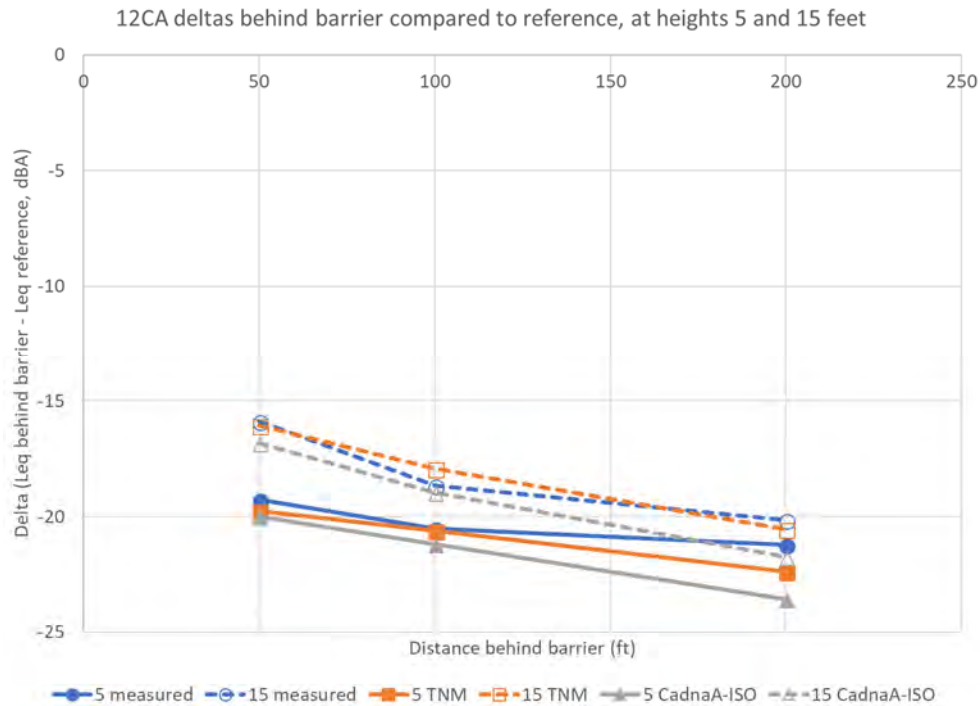


Figure 3-13. Site 12CA, measured, TNM-predicted, and ISO-predicted reduction in noise from reference

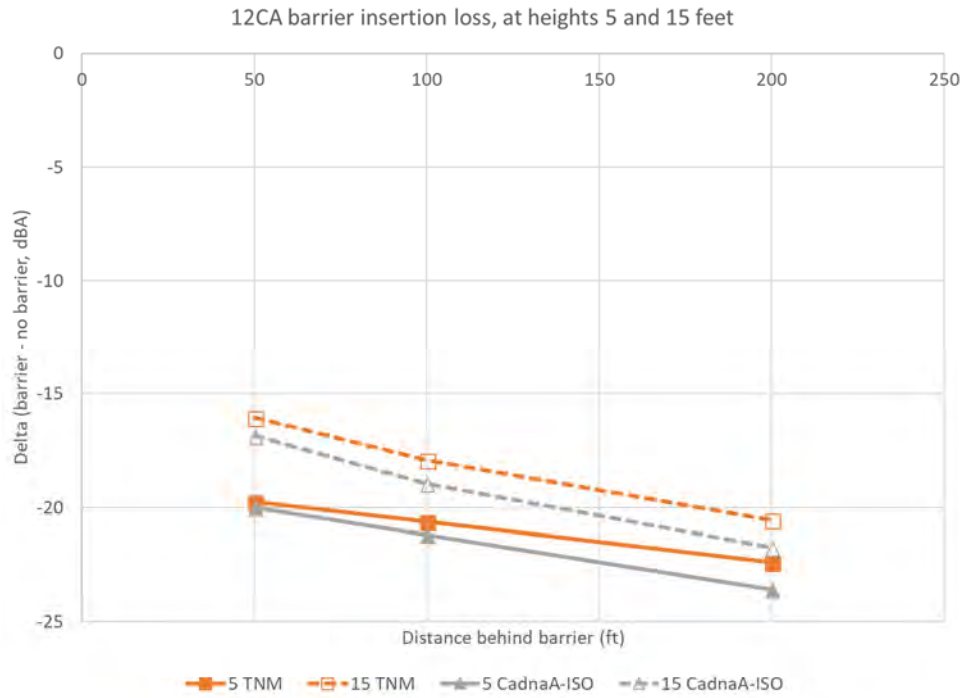


Figure 3-14. Site 12CA, TNM-predicted and ISO-predicted barrier insertion loss (comparing sound levels with and without barrier)

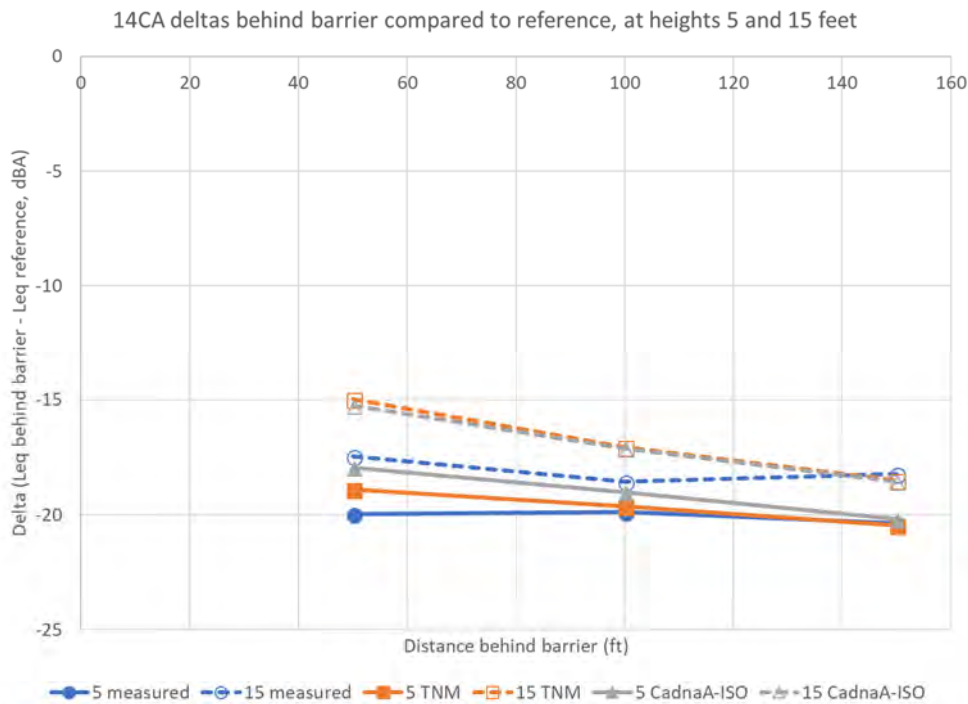


Figure 3-15. Site 14CA, measured, TNM-predicted, and ISO-predicted reduction in noise from reference

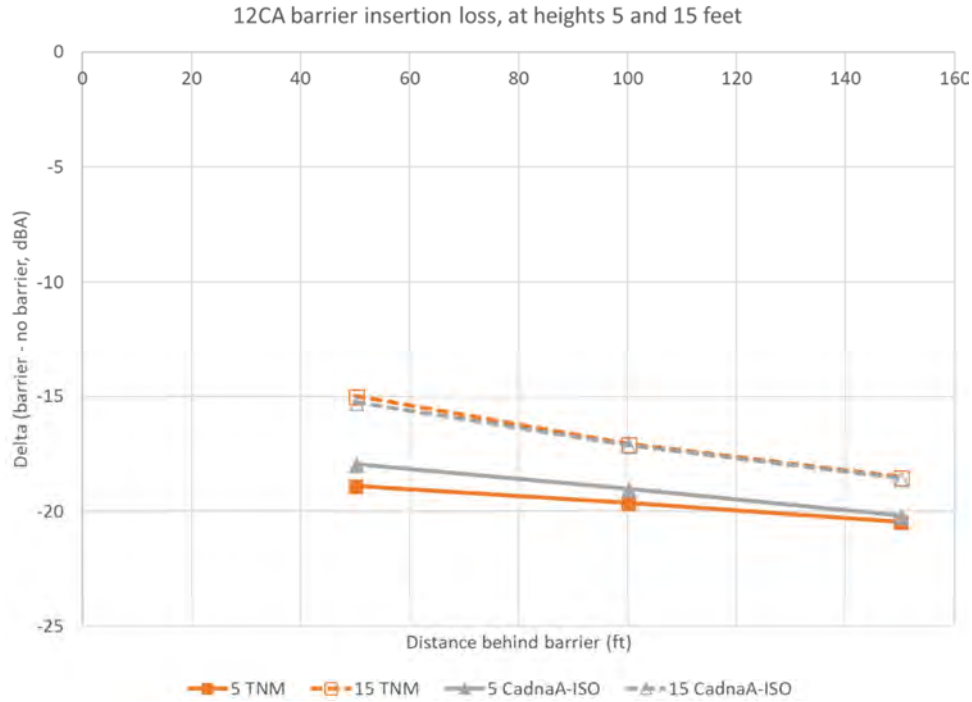


Figure 3-16. Site 14CA, TNM-predicted and ISO-predicted barrier insertion loss (comparing sound levels with and without barrier)

3.2.2.4 NCHRP Highway Results

The NCHRP study “Field Evaluation of Reflected Noise from a Single Noise Barrier” was conducted to determine changes in sound levels and characteristics caused by sound reflections off of a barrier on the opposite side of a highway (Bowlby et al. 2015). The analysis was done using measurements at multiple sites with reflective or absorptive noise barriers and adjacent equivalent sites without a barrier as highlighted in Figure 3-17. Three microphones were placed at each site (barrier site and no-barrier site), with one of them being a reference microphone on the barrier side of the road, and two being on the opposite side of the road, at two distances or two heights (see Figure 3-14). Four to five hours of acoustical, meteorological, and traffic data were collected at each site. Distances out to 122 m (400 ft) from the road were examined. The study for which the data were collected showed increases in noise on the opposite side of the road due to the barrier’s presence. Near the road (within 33 m (100 ft)), sound levels increased up to about 2 dB overall, with larger increases seen in some OTOB frequencies. Farther from the road (122 m (400 ft)), sound levels increased up to 4 dB overall. Through spectrogram analysis, it was determined that the highest sound levels for each event increased in magnitude and extended in time due to the barrier, and that increases at harmonically-related frequencies were likely changing the character of the sound.

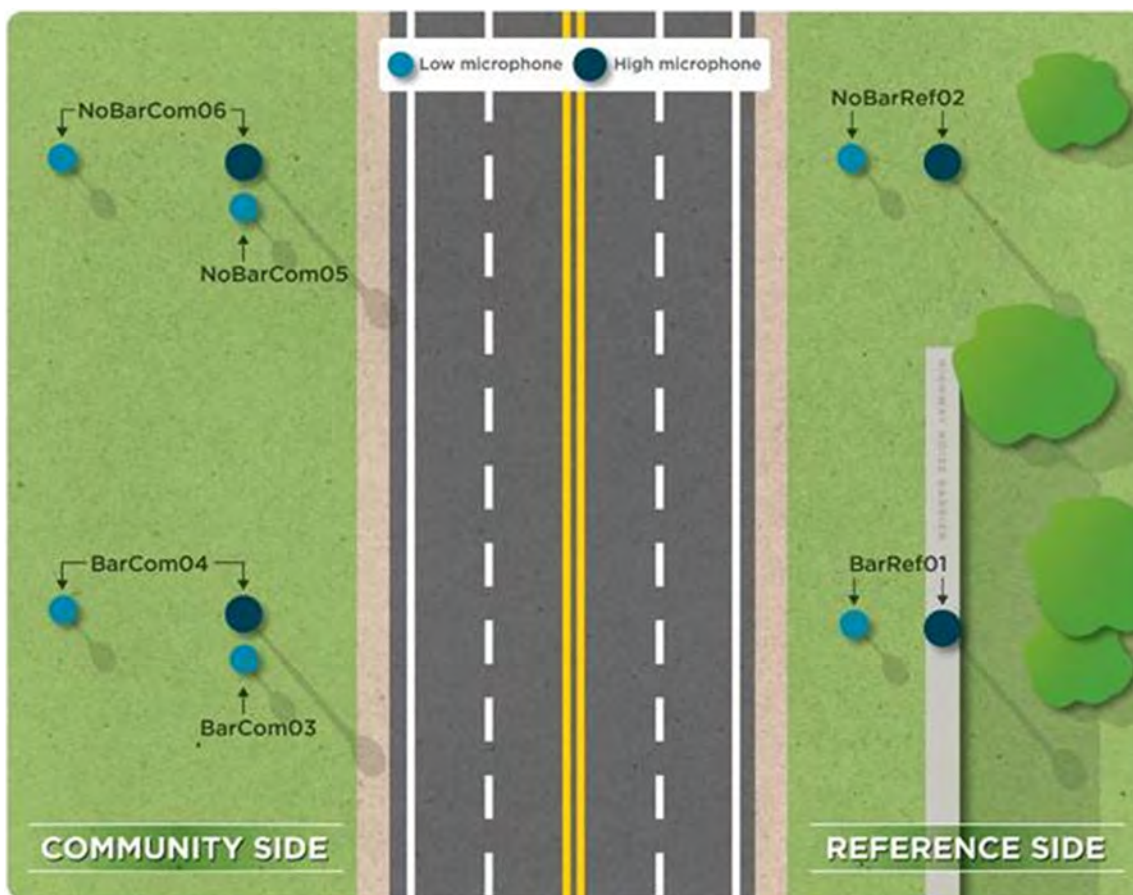


Figure 3-17. Diagram from NCHRP study “Field evaluation of reflected noise from a single noise barrier”

From this dataset, Site SR-71 in Chino Hills, CA was used to compare reflection effects for the following receiver locations: between the highway and barrier, on the side opposite the barrier and close to the road [7.6 m (25 ft)], and on the side opposite the barrier far from the road [122 m, (400 ft)]. The measured data were collected at fairly equivalent sites with and without the highway noise barrier present. Differences in the terrain for the far distance receivers were present, and these differences were determined to affect frequencies below 500 Hz. Figure 3-18 shows the cross sections for the barrier site and no-barrier site. Two time-blocks of data (A-weighted L_{eq}) were used in this analysis, four minutes from 9:49-9:53 and five minutes from 12:45-12:50. During these data blocks, traffic was free-flowing. Actual traffic data were logged and included in the predictions.

Direct comparisons were made with the measured data for TNM 3.0, NCHRP barrier method, and ISO 9613-2 method (as implemented in CadnaA), since reference highway source noise data are available for these methods. Simplified cross sections were modeled to eliminate complications with the terrain. Figure 3-19 and Figure 3-20 show the reflection effects for the three different receiver locations as measured and predicted with the different methods for the 9:49 time block and 12:45 time block, respectively. The following is observed based on receiver location:

- Receiver between the road and barrier: the measured reflection effect is less than 1 dBA; predicted values for TNM and ISO are approximately 1.5 dBA and for the NCHRP barrier method about 2 dBA. All methods are over-predicting within 7.3 m (24 ft) of the reflecting surface.
- Receiver on the opposite side of the road from barrier and near highway: the measured reflection effect is insignificant; predicted values for TNM and ISO are also insignificant and about 1 dBA for the NCHRP barrier method. The NCHRP barrier method is slightly over-predicting the effect.
- Receiver on the opposite side of the road from barrier and far from highway: the measured reflection effect is in the 2-3 dBA range; predicted with TNM it is about 1 dBA, with ISO it is insignificant, and with the NCHRP barrier method it is about 2 dBA. TNM and ISO are underpredicting the reflection effect, more so for ISO. It would need to be investigated further to understand why TNM and ISO are underpredicting the reflection effect at the farther distance for this particular case. Since TNM is predicting the reflection effect well for farther distances in aircraft scenarios/geometries, the slight underprediction in effect for the roadway geometry may not be an issue.
- For the farthest distance, likely more typical of aircraft operation geometries than the other positions, the NCHRP Barrier Reflections Screening Tool best matches the measured increase in sound due to barrier reflections.

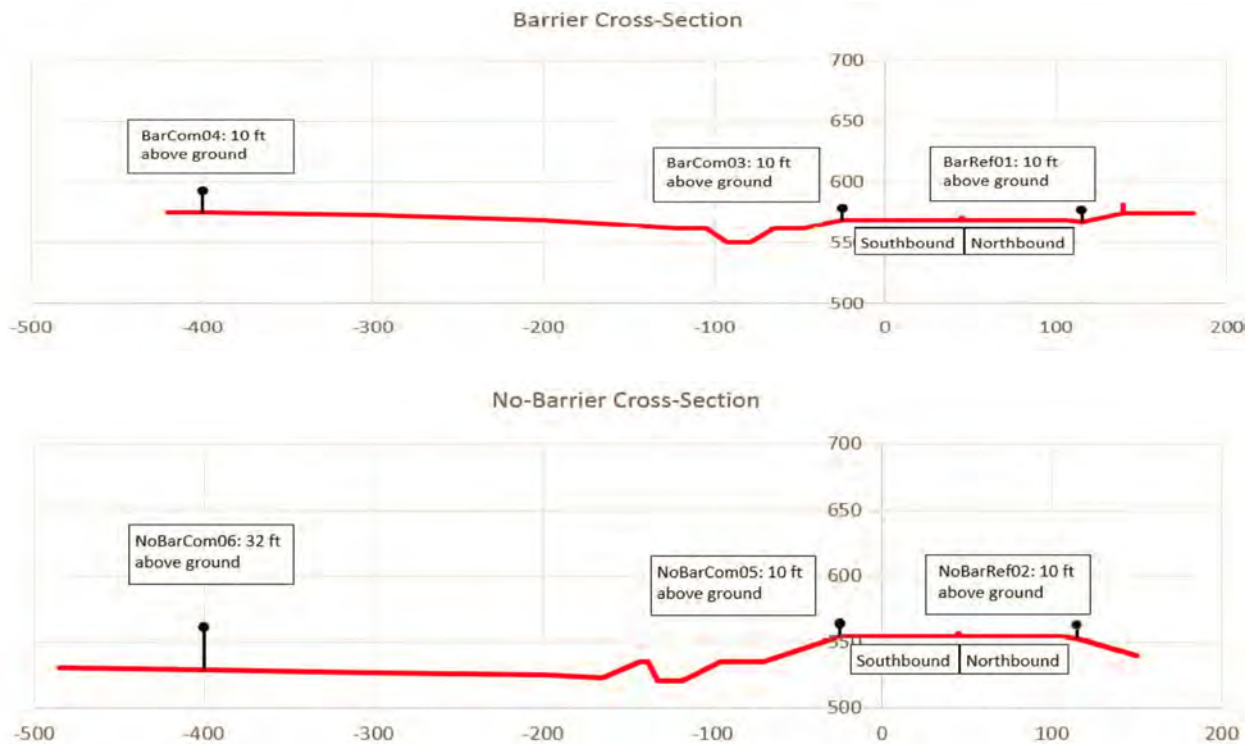


Figure 3-18. Site SR-71, NCHRP 25-44 Study; top: cross section with barrier, bottom: cross section without barrier

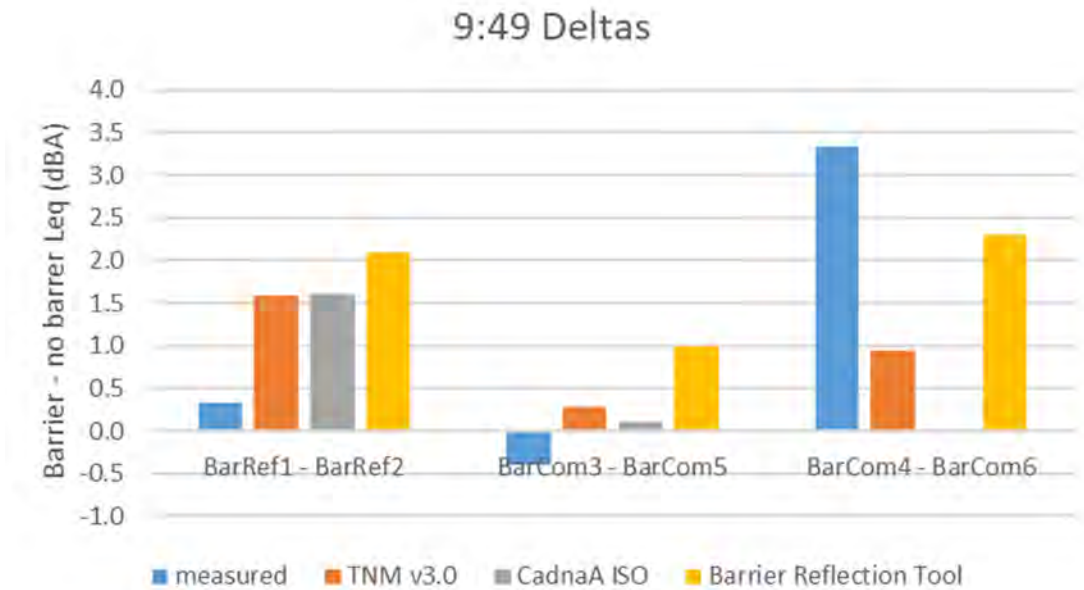


Figure 3-19. Site SR-71, NCHRP 25-44 Study, 9:49 time block; 3 sets of comparisons: from left to right, receiver between highway and barrier, opposite side receiver close to road, opposite side receiver far from road

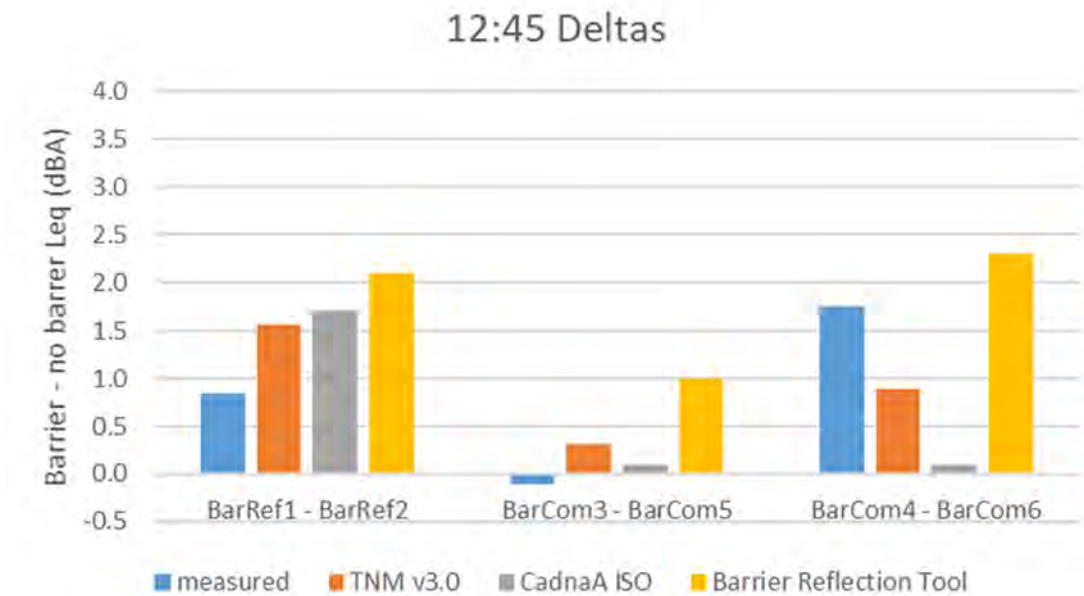


Figure 3-20. Site SR-71, NCHRP 25-44 Study, 12:45 time block; 3 sets of comparisons: from left to right, receiver between highway and barrier, opposite side receiver close to road, opposite side receiver far from road

3.2.2.5 Summary of Empirical Comparison Results

Focusing mainly on two effects, reflections and shielding/diffraction, a review of the results for each empirical dataset indicate the following:

- For reflections, the NYC Helicopter and NCHRP barrier datasets show that TNM and the NCHRP Screening Tool are performing well with this effect, and ISO 9613-2 is slightly underpredicting the reflection effects.
- For shielding/diffraction, the TNM validation and Narvik datasets show the following:
 - An elevated source and propagation over complicated terrain, particularly with some shielding, can result in over-predictions for the maximum sound level for AAM. This observation may indicate that not enough sound is being diffracted over terrain features at the closest point of approach, although this overprediction may be somewhat complicated by ground cover effects.
 - An elevated source and propagation over complicated terrain can result in good predictions for SEL for AAM. AAM is doing a good job predicting time histories.
 - For a single wall barrier out to about 60 m (200 ft) behind the barrier, TNM and ISO 9613-2 perform well at predicting shielding/diffraction effects for 5-minute average sound levels (TNM slightly better).

3.2.3 Airport Noise Measurements

For the purpose of further evaluating a blended method and its components, our team collected aircraft noise from actual flight operations at two commercial airports: Los Angeles International Airport (LAX) and the Long Beach Airport (LGB). The measurements occurred from 2 to 8 May 2018. These airports each have robust noise monitoring systems. These systems provide both noise data and aircraft telemetry required for the accurate assessment of airport noise prediction methods. The selected locations for aircraft noise data collection included shielding or reflections from manmade structures or terrain. For this analysis, our team focused on noise data from selected types of flight operations. The data are grouped by aircraft type from a selected runway and airline. Since the goal is improving propagation modeling (not source modeling), the focus on selected operations helped to reduce the scatter caused by variations in aircraft type and aircrew procedures.

3.2.3.1 Data Collection Procedure and Instrumentation

For each measurement location (described in the next section), several hours of data were collected, enough to capture an adequate number of acceptable aircraft events. The adequate number of events and acceptability were based on having at least twenty events for a specific aircraft type (e.g., A321) performing the same operation (e.g., departure from the same runway) at approximately the same altitude for the closest point of approach, and the data were not influenced by other noise sources (e.g., loud car driving by microphone). For each of the measurement locations, noise measurements were conducted during the morning hours. This period was selected to minimize background noise levels as well minimize atmospheric effects of wind and turbulence on the aircraft noise propagation.

Our team deployed Larson Davis 831 and LxT Sound Level Meters (SLM). The SLM setup included an omni-directional, random incidence microphone, environmental pre-amplifier, windscreen, mounting tripod, securable environmental case, and eight D-cell batteries. The microphones were typically placed at a height of 1.5 m (5 ft) above the ground, oriented vertically. The SLMs were set to collect metrics such as 1-second L_{Aeq} and OTOB spectral data.

For each aircraft event, the following data were captured:

- Sound levels: 1-second A-weighted equivalent sound levels (L_{Aeq}) and maximum sound levels (L_{Amax}), fast response, OTOB. This was accomplished using Larson Davis LxT and 831 class 1 SLM deployed at all positions. The SLM captured data continuously during the measurement period. An example system is shown in Figure 3-21. These data are supplemented with data captured using B&K class 1 SLM as part of the airport noise monitoring systems deployed at various positions around the airports.
- Sound recorder: Audio recordings for aircraft events. This was accomplished using a Surface Pro system triggered for each potentially viable aircraft event, deployed at one position for each general measurement location. These data were captured to supplement the sound levels, if needed for event assessment. The microphones for the system can be seen in Figure 3-21.



Figure 3-21. Instrumentation deployed at measurement sites. Left: sound level meter system, right: meteorological system and sound recorder system

- Meteorological data: 1-second air temperature, wind speed/direction, relative humidity, air pressure. This was accomplished using a HOBO weather system, deployed at one position for each general measurement location, capturing data continuously during the measurement period. The meteorological data are used to ensure wind speeds did not exceed 5 m/s during aircraft events (speed at which there is the potential for wind-generated microphone noise), to help understand received sound levels, and to use in modeling, if/when appropriate. System shown in Figure 3-21.

- Observer log: Observers were located at several positions throughout the general measurement area. Observers logged aircraft event times and information (e.g., arrival, runway, etc.), as well as times and descriptions of extraneous sounds that could potentially influence the aircraft noise data.
- Flight operations data: For each airport noise monitoring location, flight operations data were provided by the airports. Data include aircraft type and airline, operation type, distances, and elevations. Additionally, LAX and LGB have provided their real time operational inputs for AEDT. These operational inputs greater diminish the uncertainty in the modeling of the actual flights.

3.2.3.2 Los Angeles International Airport (LAX)

Three general measurement locations in and around LAX are used for the comparative analysis. These locations provide several individual measurement sites with reflections and shielding from both residential and multistory buildings. These are indicated in Figure 3-22 and include the following:

- El Segundo neighborhood,
- Kittyhawk Ave (Westchester) neighborhood, and
- Playa Del Oro (Westchester) neighborhood.

Additional information on these measurement locations are included in Appendix B.

In addition to these locations, data were collected at a hotel district and at the LAWA administrative building as indicated in Figure 3-22. These locations had complex reflections as well as higher levels of interference from outside noise sources and concurrent aircraft operations, which increased the uncertainty of the measured levels. Descriptions of these two locations are provided in Appendix C.

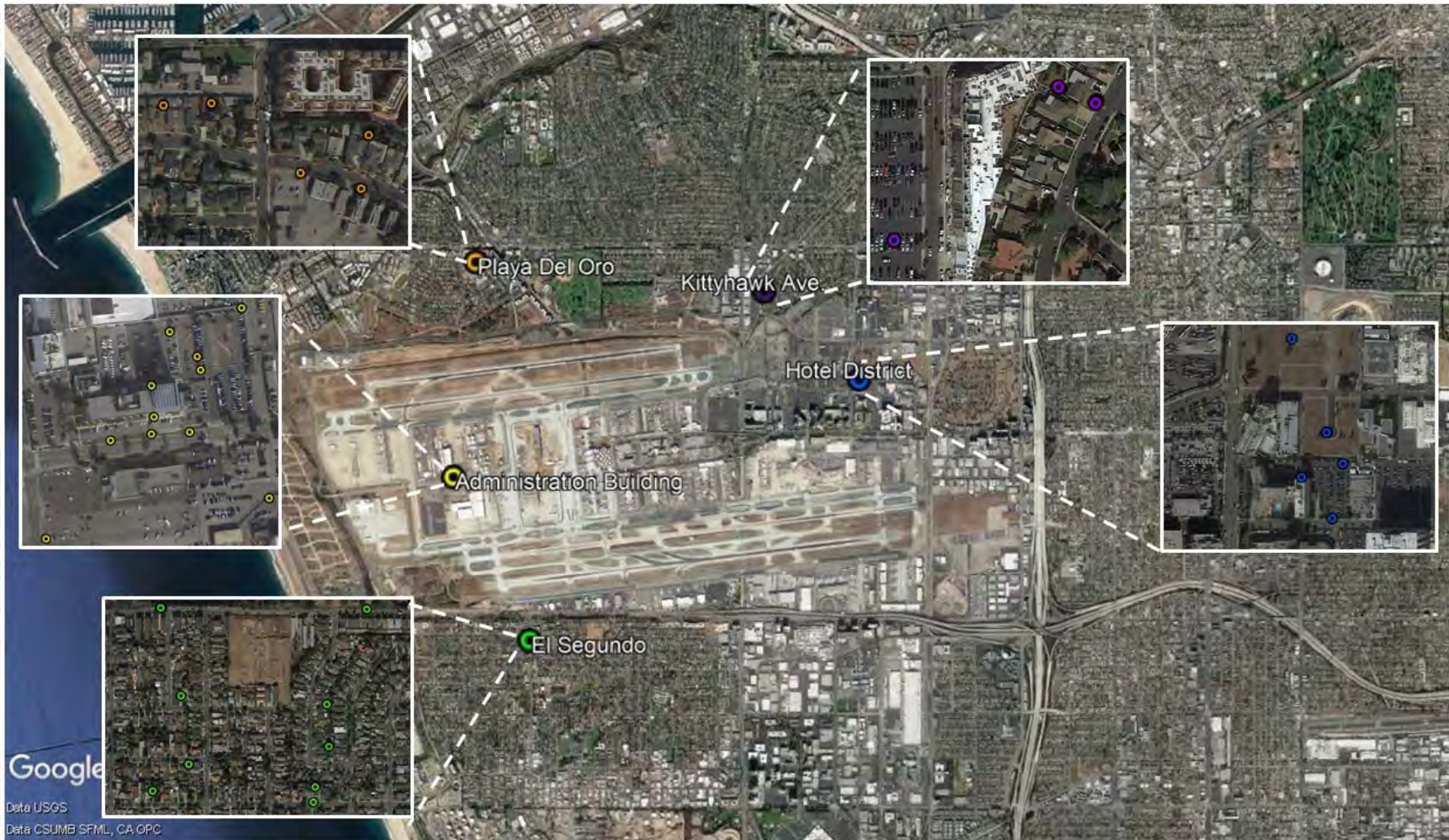


Figure 3-22. Measurement locations during measurement campaign at Los Angeles International Airport

3.2.3.3 El Segundo Neighborhood

Table 3-6 lists each of the positions at which sound was measured and associated site attributes. Figure 3-23 shows the positions on an aerial map and photographs of the neighborhood from the A05 position looking toward the airport and of the apartments across the street from A01. Appendix B provides photographs for each of the measurement positions.

The operations utilized for this comparison were Runway 25L departures of an Airbus A321 aircraft. The filtering of data to remove events with interference yielded 19 departures. These departure events did have variation in climb-out rates and rotation points. For the model comparison, two profiles were utilized from the LAX INM database. One profile related to a low climb-out rate, and the other a medium rate.

Table 3-6. LAX, El Segundo neighborhood measurement positions and site descriptions

Position	Site	Potential Effects	
		Diffraction/Shielding	Reflection Effect
A01	Sidewalk, top of slope	Possibly airport structures only for ground operations; direct line-of-sight for departures on runway 25L	2-story apartments
A02	Backyard of home	Surrounding homes/terrain	Surrounding homes
A03	Backyard of home	Surrounding homes/terrain	Surrounding homes
A04	Front yard of home	Adjacent home, far homes/terrain	Homes across street
A05	Backyard of home	Elevated with minimal shielding; direct line-of-sight for departures after rotation. For ground and low altitude shielding possible from far homes/terrain	House wall and adjacent homes
A06/A00	Sidewalk, top of slope	None	2-3-story apartments
A07	Side of home	Surrounding homes/terrain	Surrounding homes
A08	Backyard of home	Surrounding homes/terrain	Surrounding homes
A09	Backyard of home	Surrounding homes/terrain	Surrounding homes



Figure 3-23. El Segundo neighborhood measurements; top: microphone locations labeled A00 – A09, middle: view toward south runways from position A05, bottom: view away from south runways from position A01

3.2.3.4 Kittyhawk Ave Neighborhood

Table 3-7 lists each of the positions at which sound was measured and associated site attributes. Figure 3-24 shows the positions on an aerial map and photographs of the neighborhood from the B02 position looking toward and away from the flight path. Appendix B provides photographs for each of the measurement positions.

The operations utilized for this comparison were arrivals to Runway 24R of a Southwest Boeing 737 aircraft. The filtering of data to remove events with interference yielded 14 arrivals. These arrival events were very consistent so only one arrival profile was utilized for the model comparison.

Table 3-7. LAX, Kittyhawk Ave neighborhood measurement positions and site descriptions

Position	Site	Potential Effects	
		Diffraction/Shielding	Reflection Effect
B01	Backyard of home	Adjacent home and surrounding homes	Adjacent 5-story apartments
B02/B00	Front yard of home	Surrounding homes	Adjacent home, surrounding homes, nearby 5-story apartments
B03	Parking lot	Nearby 5-story apartments and commercial structures	Nearby commercial structures, nearby 5-story apartments

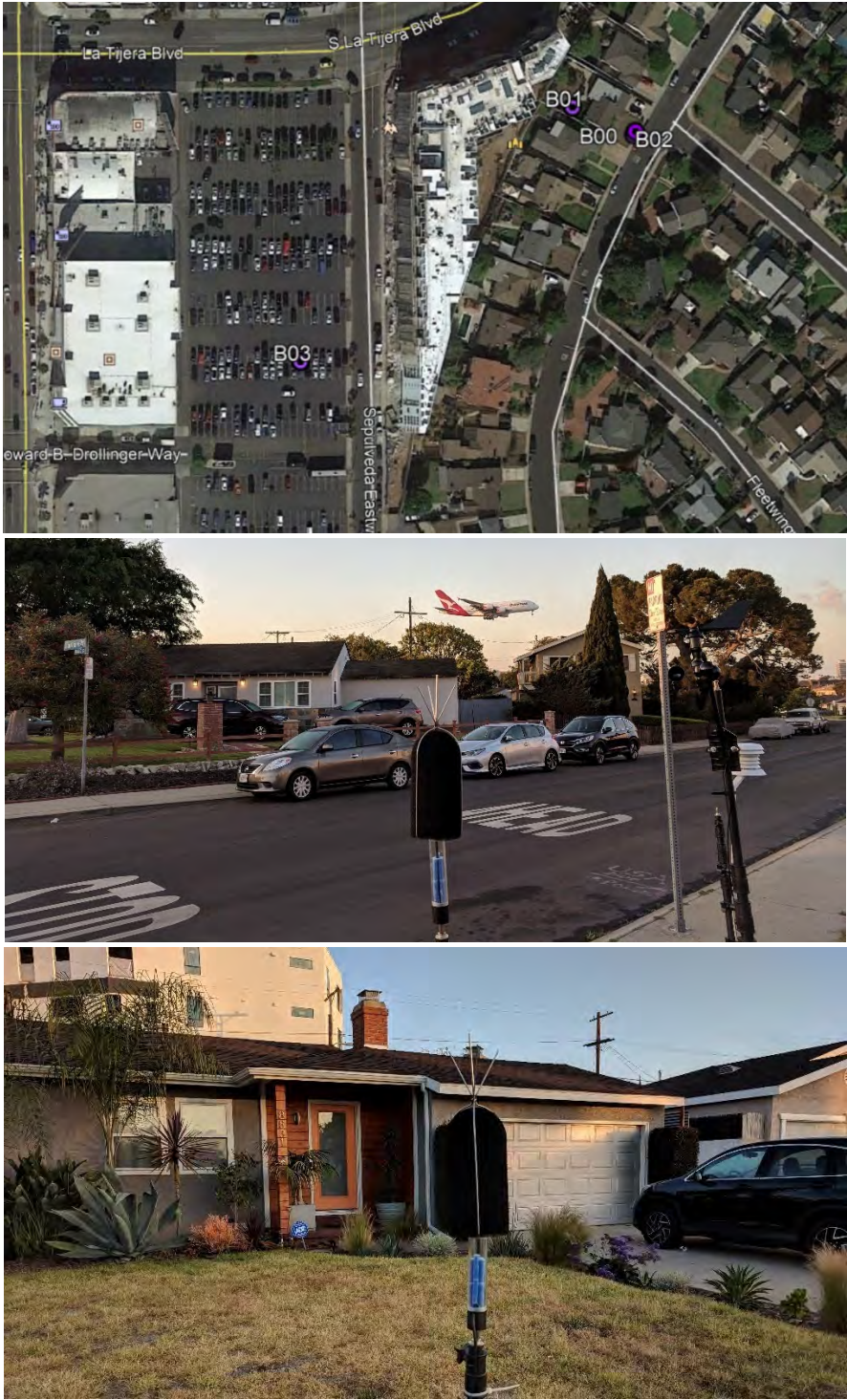


Figure 3-24. Kittyhawk Ave neighborhood measurements; top: microphone locations labeled B00 – B03, middle: view toward flight path from position B02, bottom: view away from flight path from position B02

3.2.3.5 Playa Del Oro Neighborhood

Table 3-8 lists each of the positions at which sound was measured and associated site attributes. Figure 3-25 shows the positions on an aerial map and photographs looking toward and away from the airport from position E02. Appendix B provides photographs for each of the measurement positions.

At this location the primary aircraft noise was departures from 24L, but a few reverse thrusts on runway 24R were measured as well. The operations utilized for this comparison were departures of a Southwest Boeing 737 aircraft. The filtering of data to remove events with interference yielded 10 departures. These departure events were consistent so only one departure profile was utilized for the model comparison.

Table 3-8. LAX, Playa Del Oro neighborhood measurement positions and site descriptions

Position	Site	Potential Effects	
		Diffraction/Shielding	Reflection Effect
E01	[canceled]		
E02	Sidewalk	Possibly from school buildings and homes for low altitude	4-story apartments and homes across street
E03	Backyard of home	Adjacent home	Adjacent 4-story apartments
E04	Sidewalk	School buildings	4-story apartments and homes across street
E05	Backyard of home	Adjacent home	Possibly from surrounding homes, side of 4-story apartments
E06	Backyard of home	Adjacent home	From backyard fence and possibly from surrounding homes

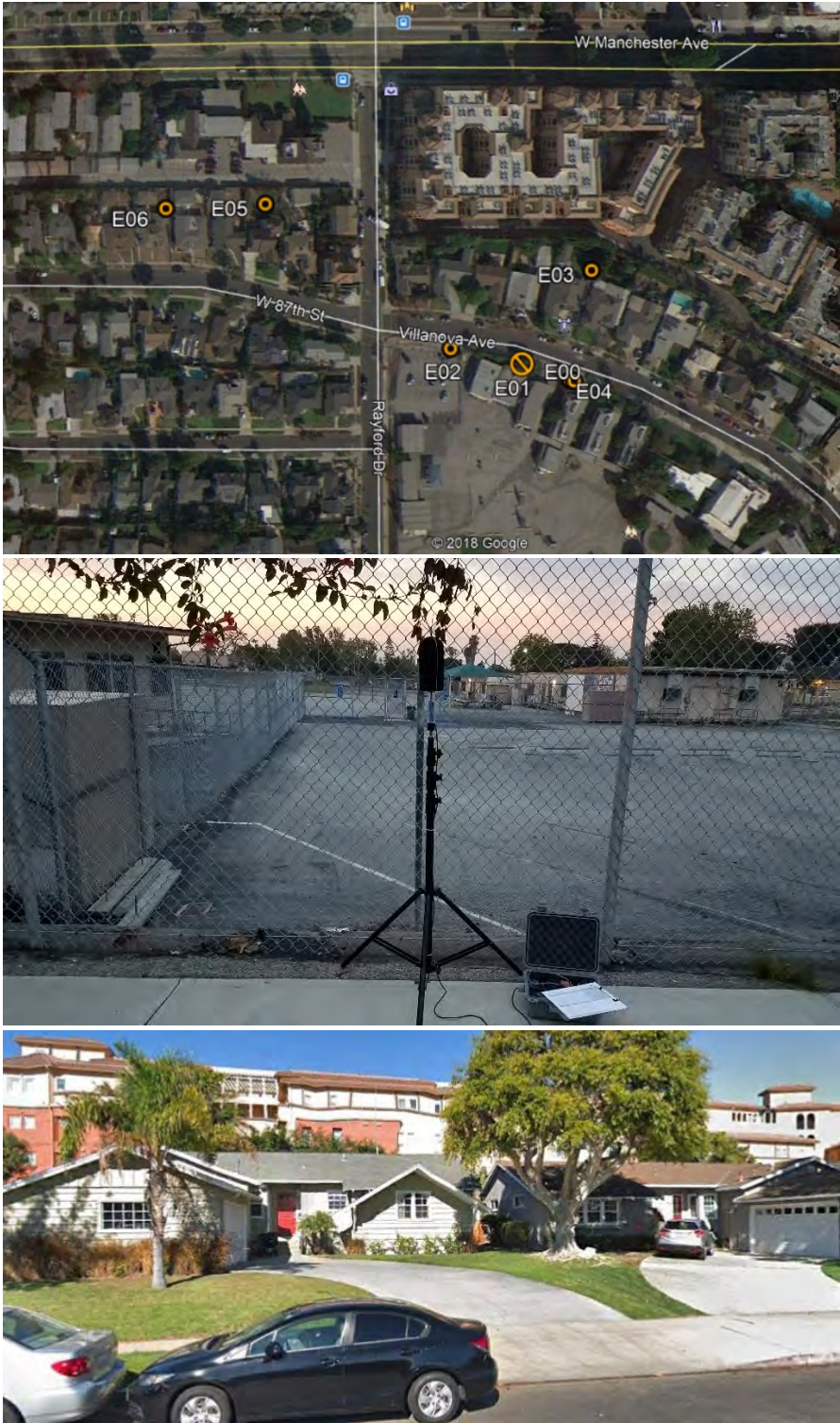


Figure 3-25. Playa Del Oro neighborhood measurements; top: microphone locations labeled E00 – E06, middle: view toward N runways from position E02, bottom: view away from N runways from position E02

For our analysis of the measured data the operational data were filtered to the selection of the following events for each location:

- **El Segundo:** 20 departures of various airlines of Airbus A321 aircraft from runway 25L.
- **Kittyhawk:** 20 arrivals of Southwest Airline Boeing B737-700 to runway 24R.
- **Playa Del Oro:** 23 departures of Southwest Airline Boeing B737-700 from runway 24L and some reverse thrust on arrivals to runway 24R.

Data collected at the hotel district and LAWA administrative building as well as the additional events (more than 100 events at each location) provide additional data to verify the implemented blended method.

3.2.3.6 Long Beach Airport (LGB)

The measurement locations for LGB are indicated in Figure 3-26. Noise measurements were conducted during the morning hours for two days since fewer commercial operations occur at LGB.

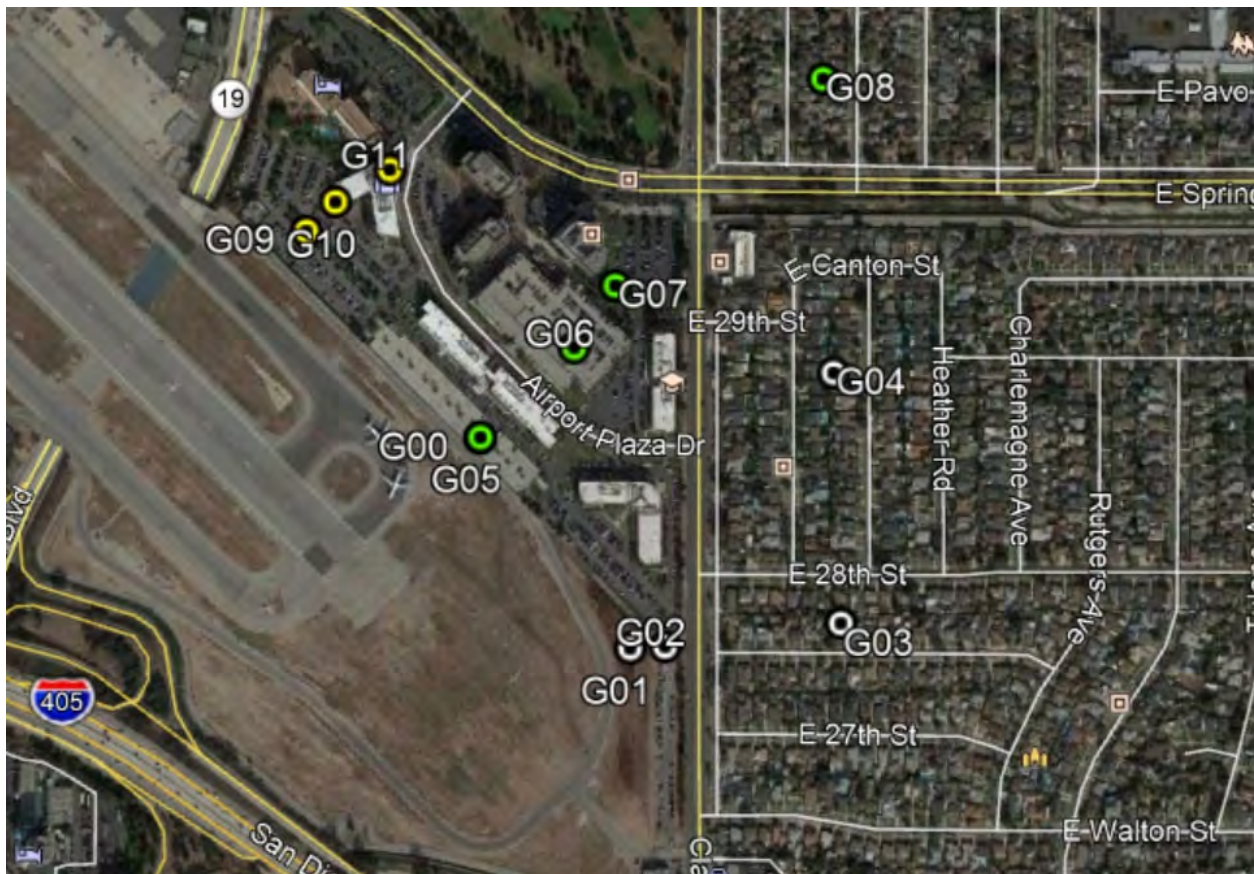


Figure 3-26. Measurement locations during measurement campaign at Long Beach Airport

The data were analyzed to identify and remove events with interference. From the original data, 16 arrivals and 14 departures of Jet Blue Airbus A320 aircraft were selected at LGB. The arrival events provided elevated sources, and the departure events provided ground-based sources. This difference arises from the displaced landing threshold at LGB for runway 30. For modeling, only one profile was required for both the arrival and the departure.

Table 3-9 lists each of the positions at which sound was measured and associated site attributes. Figure 3-27 shows photographs looking toward and away from the airport from position G09; it also shows in front and behind the end-of-runway berm from positions G01 and G02. Appendix B provides photographs for each of the measurement positions.

The data were analyzed to identify and remove events with interference. From the original data, 16 arrivals and 14 departures of Jet Blue Airbus A320 aircraft were selected at LGB. The arrival events provided elevated sources, and the departure events provided ground-based sources. This difference arises from the displaced landing threshold at LGB for runway 30. For modeling, only one profile was required for both the arrival and the departure.

Table 3-9. LGB measurement positions and site descriptions

Position	Site	Potential Effects	
		Diffraction/Shielding	Reflection Effect
G01	Front of runway berm	Berm	None
G02	Behind runway berm	Berm	Possibly 2-story building
G03	Backyard	Surrounding homes	Surrounding homes
G04	Backyard	Surrounding homes	Surrounding homes
G05	Top deck parking lot	Parking deck wall (ground ops only)	4-story building
G06	Top deck far parking lot	Possibly 4-story building (ground ops only)	7-story building
G07	Shielded far parking lot	4-story parking structure	7-story building
G08	Backyard	Surrounding homes	Surrounding homes
G09	Parking lot	None	3-4-story buildings
G10	Parking lot near building	None	3-4-story buildings
G11	Parking lot behind building	4-story building	8-story building

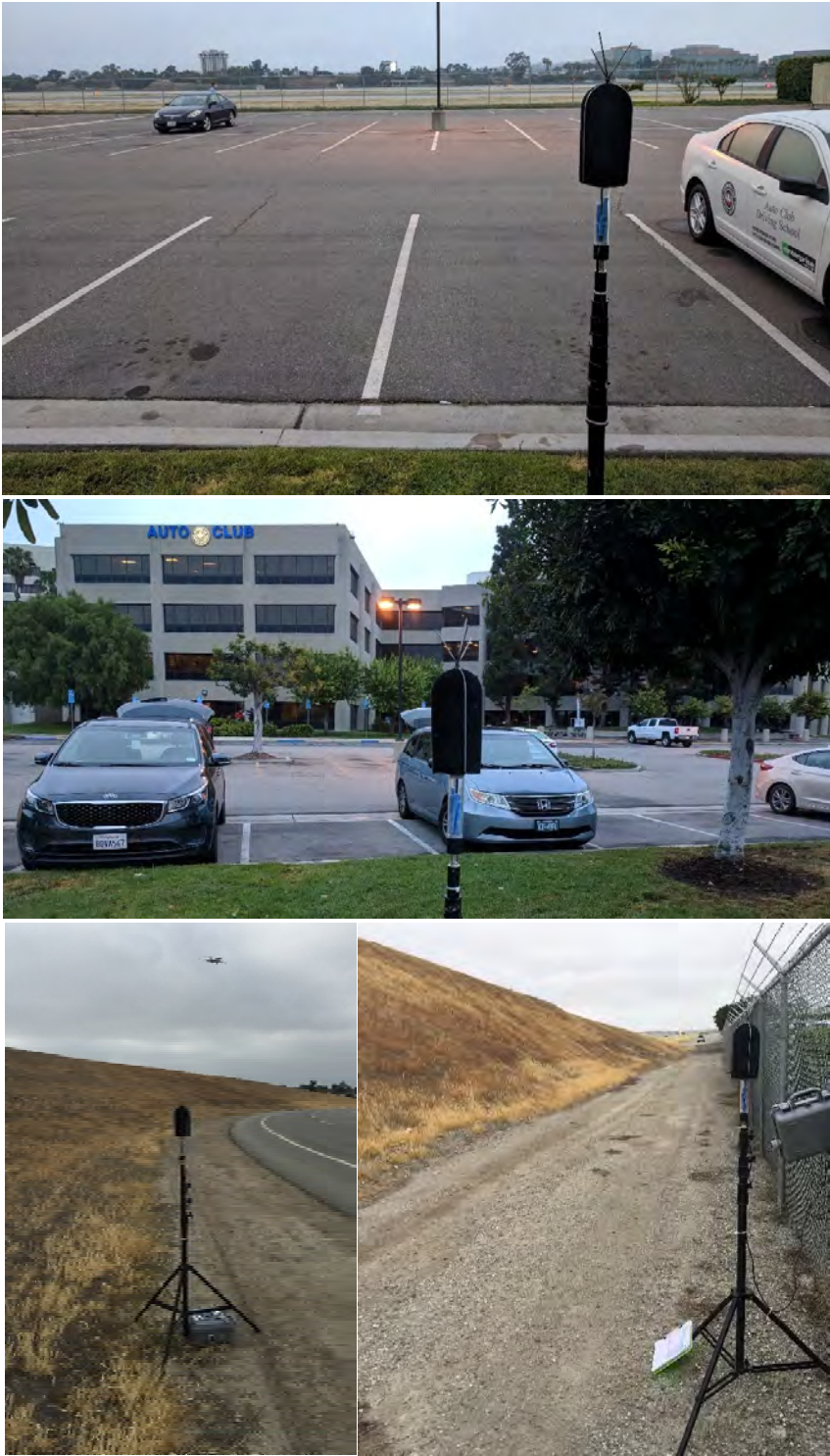


Figure 3-27. LGB measurements; top/middle: view toward and away from runway from position G09, bottom: in front and behind end-of-runway berm (from G01 and G02, respectively)

3.2.3.7 Observations from Airport Measurements

During the measurements, our team observed several interesting acoustic phenomena. At the neighborhood of El Segundo, departing aircraft could be acoustically tracked although the aircraft could not be seen. This observation probably arises from the reflection and scattering from the houses. At Playa del Oro neighborhood, in the backyard (Site E03) the reflections from the multistory apartment building resulted in hearing two distinct aircraft flyovers. One from the actual aircraft and one from the reflected image in the direction of the multistory building. The owner of this residence noted that the noise levels had significantly increased with the recent construction of the apartment building.

For the hotel district sites, the multiple reflections provided some interesting acoustical observations as well. As the aircraft approached the sites, the aircraft could be heard without being seen. However, unlike the observation in the neighborhoods, the aircraft could not be tracked visually or aurally. This observation means that the direct sound propagation path was blocked, but multiple reflected paths were heard. These observations were for the initial and final portions of the time history, but they did not occur at the point of closest approach. An initial examination of TNM and ISO 9613-2 calculated gain/loss factors for the hotel district showed that both models were not properly capturing related complex reflections, which was present in the measured data. TNM 3.0 is designed to account for only one reflecting surface, a highway noise barrier, so it has no secondary or higher order reflections, and its results for multiple building reflecting surfaces is limited (even with just single reflections). Even with this limitation, TNM did match the trends at some of the sites. However, ISO 9613-2, which allows multiple reflections, calculated losses at all of the sites. Nevertheless, these complex reflection effects were localized.

3.2.3.8 Results from Airport Measurements

The evaluation of the blended method involves comparison of averaged measured sound level values with AEDT predicted noise levels along with building reflection gains and shielding loss values. The gain/loss values were calculated by TNM and ISO 9613-2, and gains only by the NCHRP Screening Tool.

3.2.3.8.1 Modeling Analysis Procedure for Structural Effects Evaluation

To compare the performance of each model, digital terrain and building models of each measurement site were created for AEDT, ISO 9613-2, and TNM. All modeling included precise receiver and source locations per on-site observations and RealContours flight tracks.

All receiver locations and flight profiles were modeled using the sound propagation algorithms currently present in AEDT. Although several flight profiles showed discrepancies between on-site observations and as-flown trajectories – particularly for departure climb angles – all analysis used the available flight profiles for consistency.

SoundPLAN 7.4 was used to implement ISO 9613-2 for all measurement locations. All modeling parameters used in the benchmarking and evaluation of transportation noise methods were carried over to the blended method evaluation described in Section 3.2.1.

Terrain elevation data were obtained from the publicly accessible United States Geological Survey (USGS) database via the National Map web portal. Where few large structures populated the measurement area,

such as Long Beach, building footprints were manually defined in SoundPLAN. Corresponding elevations were obtained through Google Earth’s 3D building layer. Measurement sites with more complex building layouts, such as El Segundo, Kittyhawk, and Playa del Oro, were defined using publicly available Light Detection and Ranging (LiDAR) data. Raw LiDAR point clouds are available via USGS’ National Map for select areas in the United States, including Los Angeles County. After extensive processing, building footprints and heights were extracted for modeling in SoundPLAN. The underlying terrain elevation data were also obtained from the LiDAR point cloud. Figure 3-28 shows an example of building footprints in El Segundo obtained through processed LiDAR data, while Figure 3-29 shows a 3D visualization.



Figure 3-28. Processed LiDAR data for El Segundo; buildings are displayed in orange, terrain in brown

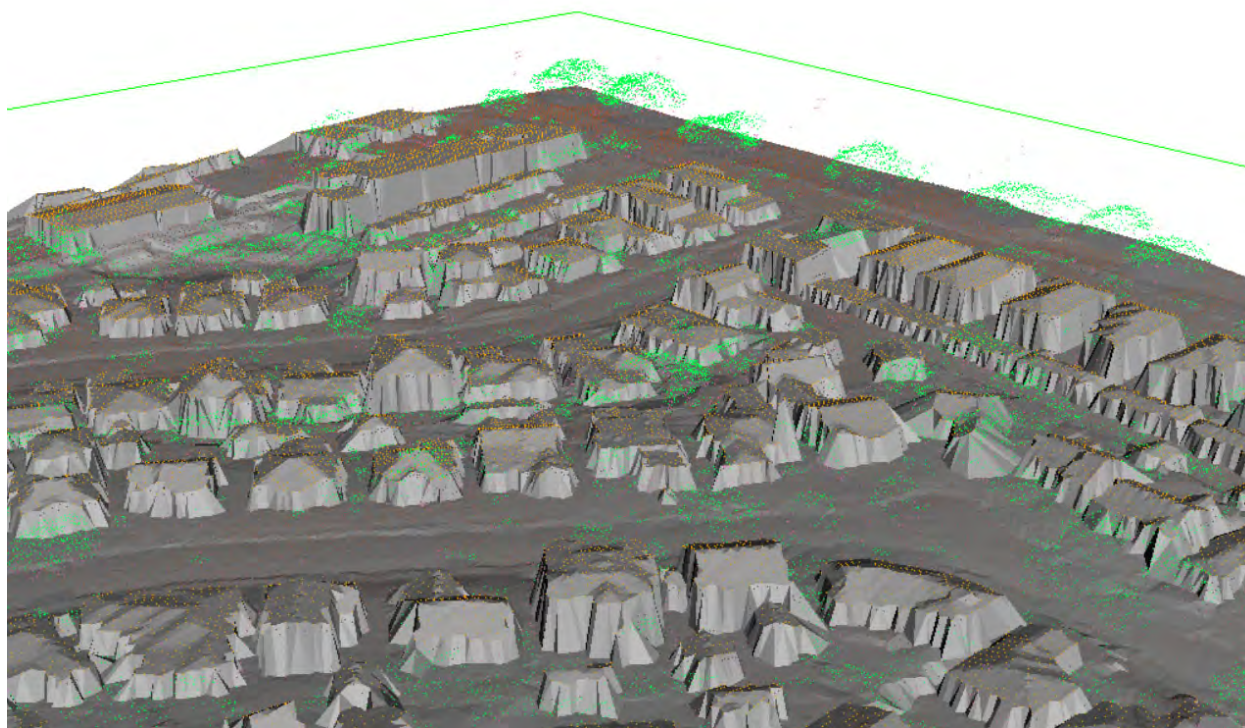


Figure 3-29. 3D visualization of process LiDAR data

Figure 3-30 and Figure 3-31 show representative examples of digitized buildings throughout two measurement areas in SoundPLAN with underlying satellite imagery for reference.

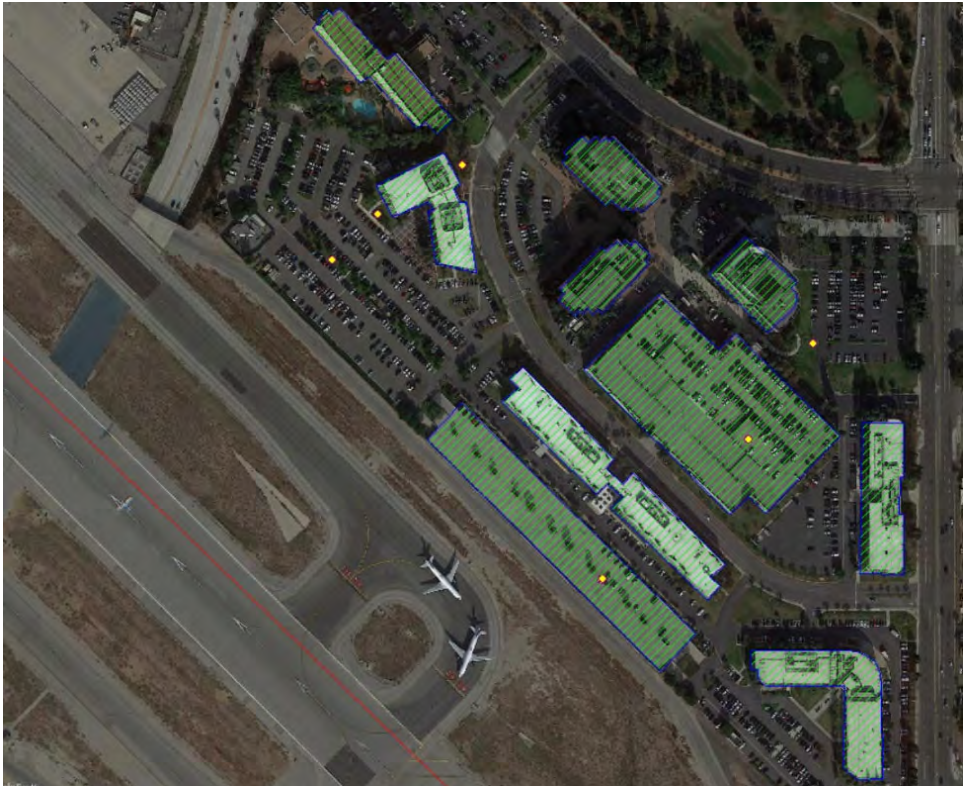


Figure 3-30. Digitized SoundPLAN model of LGB; building footprints and elevation obtained via satellite imagery and Google Earth 3D buildings



Figure 3-31. Digitized SoundPLAN model of Kittyhawk; building footprints & elevations obtained via LiDAR

TNM models were created using identical flight profiles, but terrain and building definitions differed from SoundPLAN. Terrain data and building locations were obtained through Google Earth for all sites. Also, TNM allows for two types of building structures: building rows and reflective barriers. Users can specify the location and building density of long rows of buildings, such as single-story dwellings. The building row objects and barrier objects are used to calculate shielding losses for acoustic propagation. The barrier objects are used for shielding when a receiver is in close proximity to a building and is, at that specific location, dominantly shielded by that building. The reflective barrier object can be used to simulate the façade and sides of a building and compute reflection effects. All measurement areas were defined in TNM using a mix of building rows and reflective barriers to recreate the structural environment around each receiver.

Finally, the geometries for each receiver were defined using the NCHRP Barrier Reflections Screening Tool. As this tool is not a full simulation model, the appropriate distances were specified for each measurement site in relation to the closest reflective surface.

Once the terrain and building models were developed for each tool, calculations were made with and without building data included. From these calculations, the structural gain/loss factors (GL_{BM}) from each model were determined at each measurement site and for each modeled operation. GL_{BM} values were calculated by TNM and ISO 9613-2, and only gains by the NCHRP Screening Tool as described above.

3.2.3.8.2 Overall Building Effects Results Comparison

The evaluation of the blended method involves comparison of averaged measured sound level values with AEDT predicted noise levels along with structural GL_{BM} values. These comparison data are pooled together to evaluate the overall effectiveness of the models and the blended method approach. The first comparison involves all of the data points with no grouping of the data. The next comparisons are made from groupings of the data points. The groupings are based on aircraft operation type and manmade structural effects as well as combined. Operation type is split between departures and arrivals. The manmade structures effect is divided among shielded, no effect, and reflected areas. The structure effect grouping was determined by model calculations of TNM and ISO, since their calculations are based on the actual geometry of the noise propagation. The results between TNM and ISO grouping are very similar so only the grouping by TNM is presented in this evaluation.

For our dataset, 566 individual measured SEL events are utilized. The distribution of these events is listed in Table 3-10. These individual events were averaged for each unique aircraft operation measured at each measurement location. Some of the events were removed because of interference from other noise sources. The averaging produced 46 comparison events. These events are pooled together and used for comparisons with TNM, ISO 9613-2 and NCHRP Screening Tool. For the grouped arrival comparisons, five (5) events are used for shielded sites; nine (9) events are used for reflection sites; and two (2) events were in a “no effect” site. For the grouped departure comparisons, thirteen (13) events occur within shielded areas, and seventeen (17) events occur within reflection areas. Estimated shielding loss ranges from -0.1 to -15.0 dBA. For estimated reflection gains, the range is 0.1 to 2.7 dBA.

Table 3-10. Distribution of individual measured events

Site Name	Number of Flights	Number of Sites	Number of Individual Recordings Removed	Total Measured Data Points
LGB	30	11	32	298
El Segundo	20	9	4	176
Kittyhawk	14	3	0	42
Playa del Oro	10	5	0	50

For the comparison, the difference between the AEDT predicted levels (P_{AEDT}) and measured values (M_{SEL}) are compared to the estimated GL_{BM} values from TNM and ISO 9613-2. For the NCHRP Screening Tool, comparisons are only done for the reflected area points. The difference between AEDT predicted and measured data is calculated by subtracting the predicted values from the measured ones. When this difference is negative, shielding loss is indicated, and when it is positive, reflection gain is indicated. This trend matches the calculated GL_{BM} values from the models. The comparison is accomplished by subtracting the measured difference for the GL_{BM} values and this value is referred to as the “offset” (Off_{BM}). This comparison process is represented in the following equation:

$$Off_{BM} = GL_{BM} - (M_{SEL} - P_{AEDT})$$

Thus, the ideal result would produce an Off_{BM} value equaling 0, which means the calculated GL_{BM} values match the measured difference at a given location and event. Positive values of the offset indicate overprediction of a particular model, and negative values indicate underprediction.

Table 3-11 provides the overall pooled group of comparison points, which are specific to the modeled scenarios at LAX and LGB for the measured locations. This table provides the following information: Event ID, operation type, area type (shielded or reflected), mean of the measured SEL along with its standard deviation, the AEDT predicted SEL, the difference between measured and predicted SEL, the predicted structural gain/loss for TNM and ISO 9613-2 along with the resulting offset. The results for NCHRP Screening Tool are not included in this table since its results are only valid for reflecting conditions. Table 3-11 provides the average and standard deviations of the differences and offsets at the bottom of the table. These values reveal that both methods provide improvement to the prediction of the received noise. The measured difference shows an underprediction of 1.9 dBA. TNM shows overprediction of 0.9 dBA, and ISO 9613-2 provides only a 0.1 dBA overprediction. In terms of variation, TNM reduced the variability by 0.9 dBA, while ISO 9613-2 reduces it by 0.4 dBA. For all events averaged together, ISO 9613-2 provides slightly better results, however, TNM provides slightly greater reduction in variability.

Table 3-11. Comparison of overall pooled events

Event ID	Op Type	Area Type	Mean Measured SEL (dBA)	Standard Deviation (dBA)	AEDT With Terrain SEL (dBA)	Measured - AEDT	Structural Gain/Loss TNM	Offset TNM	Structural Gain/Loss ISO 9613-2	Offset ISO 9613-2
AL1	D	R	90.3	2.1	86.6	3.7	1.2	-2.6	0.0	-3.7
AL2	D	S	82.0	3.6	83.5	-1.5	-0.4	1.1	-0.3	1.2
AL3	D	S	78.4	3.1	81.9	-3.5	-0.2	3.3	-0.3	3.2
AL4	D	S	82.1	1.9	80.7	1.4	-0.6	-2.0	-4.6	-6.0
AL5	D	R	84.8	3.7	81.0	3.8	1.2	-2.6	-0.6	-4.4
AL6	D	R	93.9	1.8	91.6	2.3	0.1	-2.2	-0.1	-2.4
AL8	D	R	82.7	3.9	84.0	-1.2	1.4	2.7	0.0	1.2
AL9	D	S	78.4	2.5	83.7	-5.3	-0.3	5.0	-1.1	4.2
AM1	D	R	90.9	6.6	91.7	-0.8	0.2	1.0	0.0	0.8
AM2	D	N	84.1	8.4	88.3	-4.2	0.0	4.2	-0.3	3.9
AM3	D	S	80.3	5.4	86.6	-6.3	-0.5	5.8	-0.3	6.0
AM4	D	S	81.9	3.6	85.1	-3.2	-0.5	2.7	-4.6	-1.4
AM5	D	R	85.9	2.4	85.5	0.4	1.8	1.4	-0.6	-1.0
AM6	D	R	94.4	1.8	93.4	1.0	0.1	-0.9	-0.1	-1.1
AM8	D	R	85.7	5.3	87.4	-1.7	0.9	2.6	0.0	1.7
AM9	D	R	80.2	5.8	86.8	-6.6	0.5	7.1	-1.1	5.5
B1	A	S	76.0	0.7	80.8	-4.8	-2.1	2.6	-0.3	4.5
B2	A	S	82.0	1.1	81.2	0.8	-0.6	-1.4	0.2	-0.6
B3	A	S	84.5	1.1	82.9	1.6	-0.7	-2.3	-1	-2.6
E2	D	R	82.8	2.2	76.8	6.0	1.6	-4.4	1.3	-4.7
E3	D	R	79.2	2.4	76.6	2.7	2.7	0.0	1.2	-1.5
E4	D	R	81.0	2.5	76.9	4.2	1.6	-2.5	0.7	-3.5
E5	D	R	80.4	1.7	76.4	4.0	1.7	-2.2	-1	-5.0
E6	D	S	77.8	2.6	76.5	1.2	-2.8	-4.0	-0.3	-1.5
G1 A	A	R	88.8	0.6	89.1	-0.3	0.2	0.5		
G1 D	D	N	82.5	1.9	86.0	-3.5	-0.02	3.4		
G10 A	A	R	83.5	0.9	81.8	1.8	0.3	-1.5	2.1	0.3
G10 D	D	R	93.0	1.4	92.5	0.5	2.4	1.9	2.7	2.2
G11 A	A	S	81.6	2.5	79.0	2.6	-2.1	-4.7	-5.8	-8.4
G11 D	D	S	83.3	3.5	89.9	-6.6	-11.1	-4.5	-8.8	-2.2
G2 A	A	S	82.8	0.9	87.3	-4.5	-0.1	4.3		
G2 D	D	S	79.9	1.2	87.8	-7.9	-10.1	-2.1		
G3 A	A	R	79.0	1.1	82.1	-3.1	1.2	4.2	-0.1	3.0
G3 D	D	S	72.6	2.2	83.0	-10.3	-2.2	8.1	-1.6	8.7
G4 A	A	R	72.7	0.7	76.0	-3.3	1.1	4.4	-0.5	2.8
G4 D	D	S	70.7	2.5	84.3	-13.5	-3.6	9.9	-2.6	10.9
G5 A	A	R	88.3	2.8	86.1	2.3	0.2	-2.1	0.6	-1.7
G5 D	D	R	95.8	2.1	97.9	-2.1	1.8	3.9	0.6	2.7
G6 A	A	R	83.2	1.1	80.3	2.9	1.0	-1.9	0.1	-2.8
G6 D	D	R	87.3	2.3	91.0	-3.7	0.5	4.2	-4.1	-0.4
G7 A	A	R	77.0	1.1	77.0	0.0	1.3	1.3	-6.3	-6.3
G7 D	D	S	76.6	1.9	87.4	-10.8	-15.0	-4.1	-14.6	-3.8
G8 A	A	R	72.4	1.4	70.1	2.3	1.8	-0.5	-0.8	-3.1
G8 D	D	S	71.7	1.3	80.5	-8.8	-2.3	6.4	-3.2	5.6
G9 A	A	R	84.1	1.2	83.9	0.2	0.3	0.0	1	0.8
G9 D	D	R	92.7	2.1	94.4	-1.7	1.0	2.7	1.2	2.9
Overall Comparison Results					Average	-1.9		0.9		0.1
					St. Deviation	4.8		3.9		4.4

The data are grouped to further evaluate the methods. These grouping results are provided in summaries of averages and standard deviations. Table 3-12 through Table 3-14 provide the results of the grouped data. The results for NCHRP Screening Tool are included in reflected area groups. The operational type grouping results (Table 3-12) shows that TNM estimates are consistent in that for each group TNM overpredicts whereas ISO 9613-2 underpredicts for the arrival group and overpredicts for the departure group. TNM and ISO 9613-2 provide improved estimated levels and reduced variation for the departure group. For the arrival group, TNM is close to both the measured average differences and their standard deviation. On the other hand, ISO 9613-2's results for the arrival group show a worse estimated level and more variation.

Table 3-12. SEL grouped results by operational type compared to overall results

Operation Type	Measured-AEDT		Offset TNM		Offset ISO 9613-2	
	Ave	St Dev	Ave	St Dev	Ave	St Dev
All	-1.9	4.8	0.9	3.9	0.1	4.4
Arrival	-0.1	2.7	0.2	2.8	-1.2	3.8
Departure	-2.3	4.9	1.4	3.9	0.6	4.2

Table 3-13 shows the results for the manmade structural effect based on TNM GL_{BM} values. Again, the TNM estimates are consistent between the groups, and ISO 9613-2 results are opposite. For shielded areas, both models improve the estimated noise levels, but ISO 9613-2 results slightly increase the observed variation. For the reflected areas, TNM results are similar to the measured values. ISO 9613-2 results are 1.2 dBA less than the measured data with similar variation. The results for the NCHRP Screening Tool show about 2 dBA overprediction with a similar variation. Note that only a few sites represented a pure effect (either all shielding or all reflections). Most sites incorporated effects from each, and the dominant effect determined how they were sorted into groups. Although the NCHRP Screening Tool is over-predicting reflections on average, it predicted reflection effects fairly well when shielding effects were minimal. For example, for low departures at LAX El Segundo, for positions A01, A06, and A05, the average measured difference was 3.3 dBA (0.9 variation); when applying the NCHRP results, the average offset was reduced to -0.6 dBA (standard deviation of 0.7 dBA) for point source assumptions and -0.4 dBA (standard deviation of 0.8 dBA) for line source assumptions.

Table 3-13. SEL grouped results by manmade structural effect (re: TNM) compared to overall results

Operation Type	Measured-AEDT		Offset TNM		Offset ISO 9613-2		Offset NCHRP Pt.		Offset NCHRP Line	
	Ave	St Dev	Ave	St Dev	Ave	St Dev	Ave	St Dev	Ave	St Dev
All	-1.9	4.8	0.9	3.9	0.1	4.4				
Shielding	-4.4	4.8	1.3	4.6	1.1	5.3				
Reflection	0.5	2.2	0.6	2.3	-0.7	2.3	1.8	2.2	2.1	2.2

Table 3-14 provides the results for the combined grouping of the comparison events, divided by operational type and manmade structural effect. These comparisons show that in these individual groups, TNM follows the gain/loss trends more consistently among the subgroups compared to ISO 9613-2. TNM maintains similar variability with the measured data based on standard deviation within the subgroups,

whereas ISO 9613-2 mostly increases the variability. The NCHRP Screening Tool results show good agreement for the departure and reflected area subgroup, but it overpredicts for the arrival subgroup; when analysis isolates reflections, the tool provides good estimates of the reflection effect.

Table 3-14. SEL combined grouping results

Op Type	TNM Sorting	Measured-AEDT		Offset TNM		Offset ISO 9613-2		Offset NCHRP Pt.		OffsetNCHRP Line	
		Ave	St Dev	Ave	St Dev	Ave	St Dev	Ave	St Dev	Ave	St Dev
Arrivals	Shielding	-0.9	3.5	-0.3	3.7	-1.8	5.3				
	Reflection	0.3	2.3	0.5	2.4	-0.9	3.2	1.9	2.6	2.2	2.4
Departures	Shielding	-5.8	4.6	2.0	5.0	2.1	5.2				
	Reflection	0.6	3.3	0.6	3.1	-0.6	3.1	0.5	3.4	0.7	3.3

In summary, these comparisons substantiate the selection of TNM to provide the most consistent improvements to the predicted noise levels compared with the measured data. Also, the NCHRP Screening Tool appears to provide good estimates for the isolated reflection effect. The Tool calculations assume there is an effect regardless of other factors such as shielding or interfering surfaces. Thus, there may be circumstances where the estimate is too high, particularly when the prediction location is behind a building or when the source and receiver are not similar in elevation (the reflected sound path for an elevated source may actually point toward the ground, causing interference, rather than fully reaching the receiver).

3.3 Blended Method

3.3.1 Selected Models

The evaluation of the blended method approach to terrain and manmade structures has resulted in the recommendation of algorithms from the following methods for incorporation into AEDT:

- Terrain effects: utilize the routines from the AAM v2.0; and
- Structure effects: utilize the routines from TNM v3.0.

In addition, the NCHRP Barrier Reflections Screening Tool can be used to screen for potential reflection effects outside of the FAA AEDT. This tool has been modified for application to aircraft noise and can be used immediately to estimate reflection effects while the blended method recommendations are being incorporated into AEDT.

The recommendation for terrain effects is based on mature development of terrain effects within NoiseMap and AAM (Lee et al. 1996; Page 2002; Plotkin et al. 1993; Plotkin et al. 2013). The terrain algorithms are well established and can be integrated simply within AEDT's computational structure.

The recommendation for structure effects is based on comparisons of parametric cases in TNM (FHWA 2017) and ISO 9613-2. The results have been verified with measured data at LAX and LGB. These comparisons demonstrate how the application of these effects to AEDT's predictions improves the accuracy of predicted sound levels. Both models utilize a combination of algorithms, including those for shielding (diffraction) and reflections. Both models evaluate the effects of structures over the entire

length of the flight path affecting the sound at a particular point. For the calculation of the structural effects, TNM calculations include the effects of terrain. However, the gain/loss factors are based on the difference in the calculations between with and without the manmade structures while all other modeling parameter (i.e. terrain) remain constant.

3.3.2 Computational Flow for Effects of Terrain and Manmade Structures

For the computational flow within the blended method, the effects of terrain can be modeled throughout the calculation area, but the effect of manmade structures only needs to be applied in a region close to a runway. Within this region, the GL_{BM} factors for structures can be calculated separately from the aircraft noise, and then they can be combined for a final noise exposure estimate.

This recommended approach leverages key results from the models considered in this research to independently calculate regions of influence near manmade structures and terrain features. During the evaluation of the various methods and models in this study, direct calculations of the aircraft noise can be linearly combined with the calculation of various effects such as building reflections to compare with measured field results. Utilizing linear acoustics, the aircraft noise calculations can follow the existing AEDT integrated framework without manmade structures (but with the improved terrain effects algorithms). Then, the acoustic effect of all manmade structures can be calculated for the region of application. The two results can then be combined to produce a final result. This hybrid method has the advantage of using high fidelity prediction methods for nearby buildings to calculate the effects of reflection gains and insertion losses. Effects of manmade structures are considered separately and can be toggled on and off. In addition, this approach reduces overall computational cost as the structural effects can be calculated once and updated only when the physical environment changes.

An example of this process is provided in Figure 3-32 through Figure 3-34. Figure 3-32 provides the SEL footprint of an arrival to LGB focused on our measurement area. Figure 3-33 provides the gain/loss predicted by ISO 9613-2, which is used in this example due to ease of creating grid within SoundPLAN. These two calculations can simply be combined because of linear acoustics to provide an estimate of the SEL with the inclusion of the effects of manmade structures. This process should follow AEDT's steps for the line-of-sight adjustment.

The recommended process for the inclusion of manmade structures is the following:

- Perform an independent calculation of the effect of manmade structures using TNM 3.0 algorithms on a OTOB basis for each unique modeled trajectory (independent of aircraft type).
- Compute aircraft noise on a OTOB basis for each operation using the AEDT noise calculation with the improved AAM terrain effects algorithms.
- On a OTOB basis, combine the independent calculation of the effect of manmade structures with the AEDT noise calculation for each modeled operations.
- The adjusted OTOB is then used to determine the broadband noise level with the reflection gains and shielding losses included.

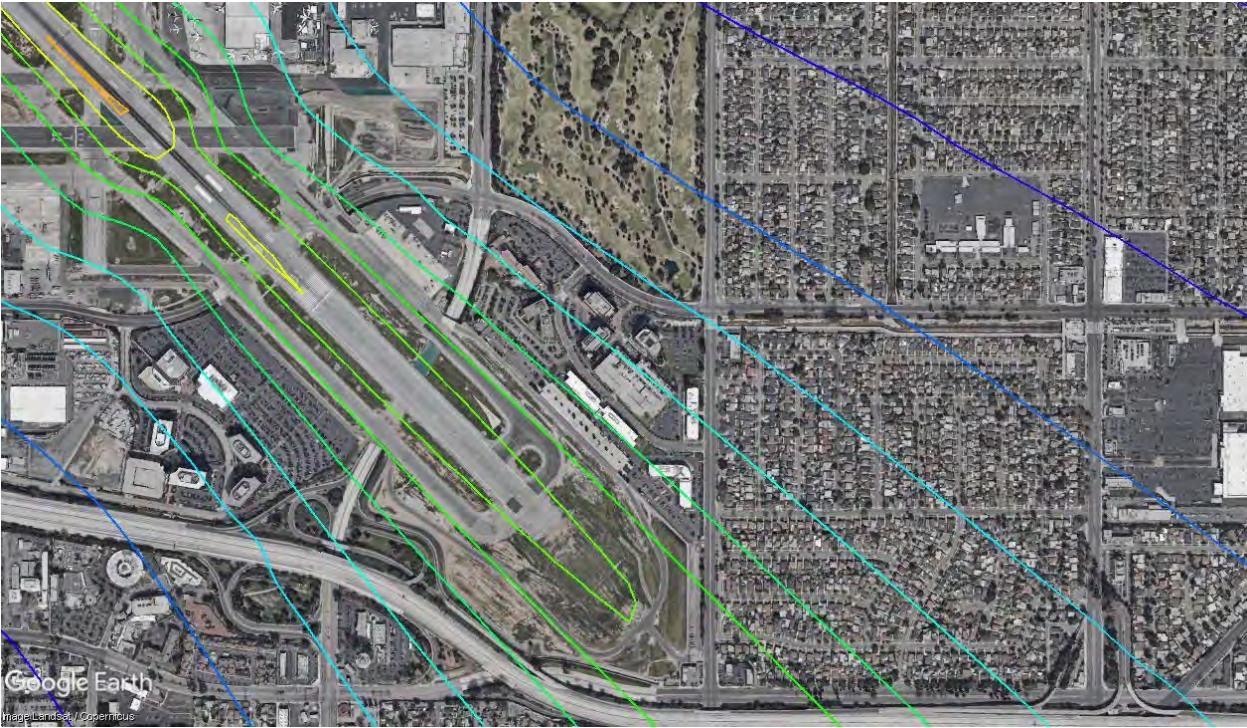


Figure 3-32. Results at LGB computed using existing AEDT calculations



Figure 3-33. Calculated GL_{BM} factors associated with manmade structures for an arrival at LGB

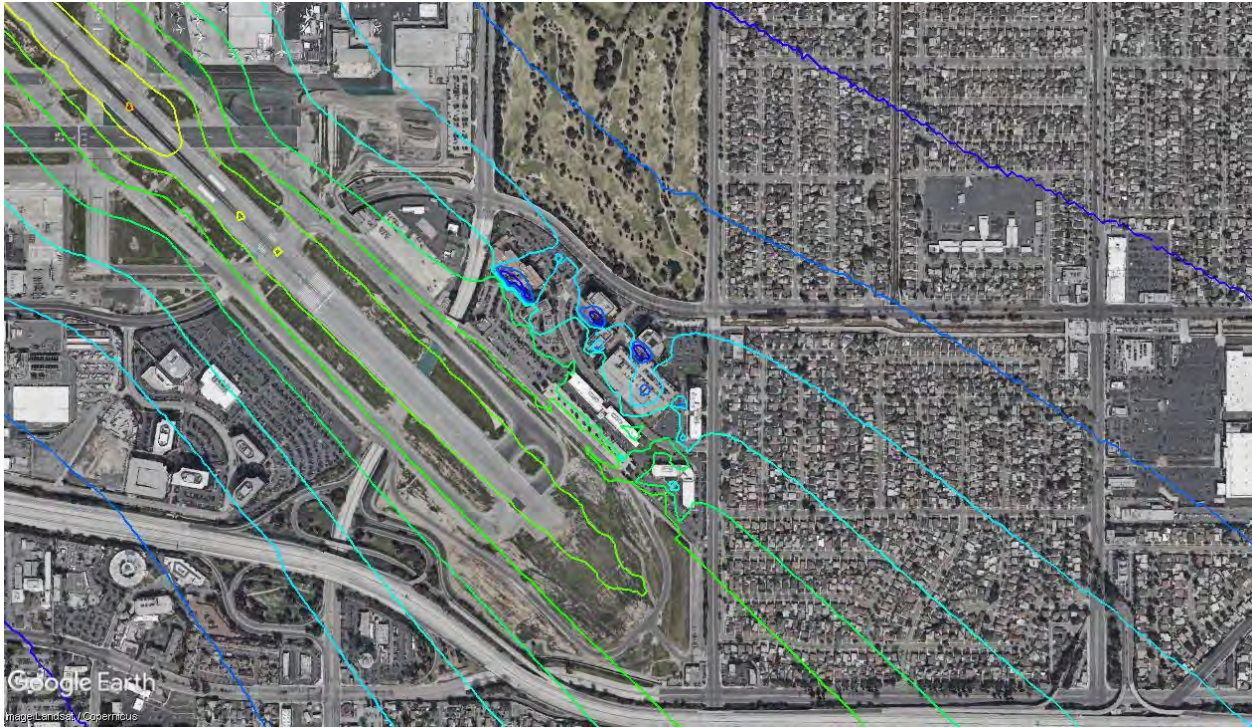


Figure 3-34. Blended noise estimate with the existing AEDT aircraft noise and the acoustic effect from manmade structures

The proposed calculation for the manmade structural effects are provided with the following steps.

1. The calculated $GL_{BM,i}$ factors are provided as a function of OTOB (i denotes an individual OTOB value).
2. The received noise ($RN_{SC,i}$) is calculated by AEDT for a given aircraft/operational spectral class.
3. The $GL_{BM,i}$ factors are added to the received noise to estimate the effective received noise ($RN_{eff,i}$) on an OTOB basis:

$$RN_{eff,i} = RN_{SC,i} + GL_{BM,i}.$$

4. The energy is summed over of the $RN_{eff,i}$ and converted to the adjusted overall noise level by the following equation:

$$ORN_{eff} = 10 \log_{10} \left(\sum_{i=11}^{40} 10^{\frac{RN_{eff,i}}{10}} \right).$$

5. The energy is summed over the $RN_{SC,i}$ and converted to the overall noise level noise level by the following equation:

$$ORN_{SC} = 10 \log_{10} \left(\sum_{i=11}^{40} 10^{\frac{RN_{SC,i}}{10}} \right).$$

6. The last step computes the overall adjustment of the manmade structural effect, GL_{adj} , using the following equation:

$$GL_{adj} = ORN_{eff} + ORN_{SC}.$$

An example of these calculation steps is provided for Site G11 at LGB Airport. For this site, the OTOB $GL_{BM,i}$ values, $RN_{SC,i}$, and $RN_{eff,i}$ are provided in Table 3-15. The effective levels are based on the equation in Step 3. The next step is to calculate the overall noise levels to determine the overall adjustment level for the manmade structural effect. This step is shown in the following equation:

$$-9.4 \text{ dB} = 75.7 \text{ dB} + 85.1 \text{ dB}$$

Table 3-15. Example of manmade structural effect calculation values for Site G11 at LGB

OTOB Frequency (Hz)	50	63	80	100	125	160	200	250	315	400	500	630
GL_{BM} , dB	-4.4	-5.2	-6.1	-7.0	-7.9	-8.7	-9.3	-9.7	-10.2	-10.4	-10.5	-10.7
Received, dB	56.7	66.1	70.1	72.8	76.6	73.0	74.5	77.0	75.3	72.2	72.2	71.2
Effective, dB	52.3	60.9	64.0	65.8	68.7	64.3	65.2	67.3	65.1	61.8	61.7	60.5

OTOB Frequency (Hz)	800	1k	1.25k	1.6k	2k	2.5k	3.15k	4k	5k	6.3k	8k	10k
GL_{BM} , dB	-12.4	-15.1	-10.1	-12.6	-15.6	-19.3	-21.8	-24.7	-26.4	-23.5	-29.0	-33.0
Received, dB	70.2	70.0	69.6	71.1	70.6	67.1	63.4	63.5	58.2	51.2	42.3	37.7
Effective, dB	57.8	54.9	59.5	58.5	55.0	47.8	41.6	38.8	31.8	27.7	13.3	4.7

3.3.3 Region of Application

The final step for the blended method is defining the region of application for the calculation of GL_{BM} factors from manmade structures near an airport or a vertiport. The blended method requires a finite geographic region where the manmade structural GL_{BM} factors are calculated and applied. The effects of structures are a function of their size, as well as their location relative to the airport or heliport flight operations. These manmade structure acoustic effects can be applied to fixed-wing and rotorcraft operations where the aircraft are at low altitudes and close to a runway or heliport. Effects are applied geometrically over this region.

Two approaches to defining the region of application were considered: standard and dynamic. The standard approach uses a simple rectangular area centered on a runway as the region of application. This approach allows simple integration of the method and a standardized approach. However, a single size may not work for all airports because of the actual location of multistory buildings relative to the runways. Nevertheless, a standard size can be defined such that it limits the effects of multistory buildings that lie outside of the application region. Outside of the defined region, building effects may still occur, but their effects are localized and limited.

The dynamic approach considers the layout of buildings near the runway region and determines the appropriate application area. This approach requires a calculation routine to determine the influence of buildings based on their size, geometry, orientation, and distance to the runway. This approach is complex.

A balance between these two approaches to define the region of application is to simply use a rectangular area as the region of influence. With this approach, a standard rectangular size is established as the default, and the rectangular implementation allows for simple adjustments for a given runway and neighboring buildings.

Based on the benchmarking results and the measurement data from LAX and LGB, the effect of manmade structures is localized to the runway or taxiway regions when the aircraft are operating close to the ground. For example, around the neighborhoods of El Segundo and Playa del Oro, the region of concern for residential structures extends to about 1,372 m (4,500 ft) laterally to the runway when the aircraft are below 152 m (500 ft) AGL. For arrivals near residential areas, the region is recommended to extend 2,621 m (8,600 ft) before the runway threshold based on aircraft altitude of 152 m (500 ft) AGL at a 3° glide slope (see Section 3.2.1.3). For departures, the extended distance is dictated by the lowest climb-out rate. Since departing aircraft are at higher altitudes for a given distance from a runway, the arrival extension is longer compared to the departure extension, as demonstrated in Figure 3-35, which shows standard AEDT for arrival and departures at LAX. In this figure, the zero location is the runway threshold. For this comparison, the arrival track crosses the 152 m (500 ft) AGL altitude at 2,621 m (8,600 ft) before the runway threshold, while the departure profile crosses the 152 m (500 ft) altitude close to the runway end. Thus, a departure extension is only apply to airports that typically have departures in a single direction like LAX, and the extension distance based on the point where the lowest climb-out passes through 152 m (500 ft) AGL.

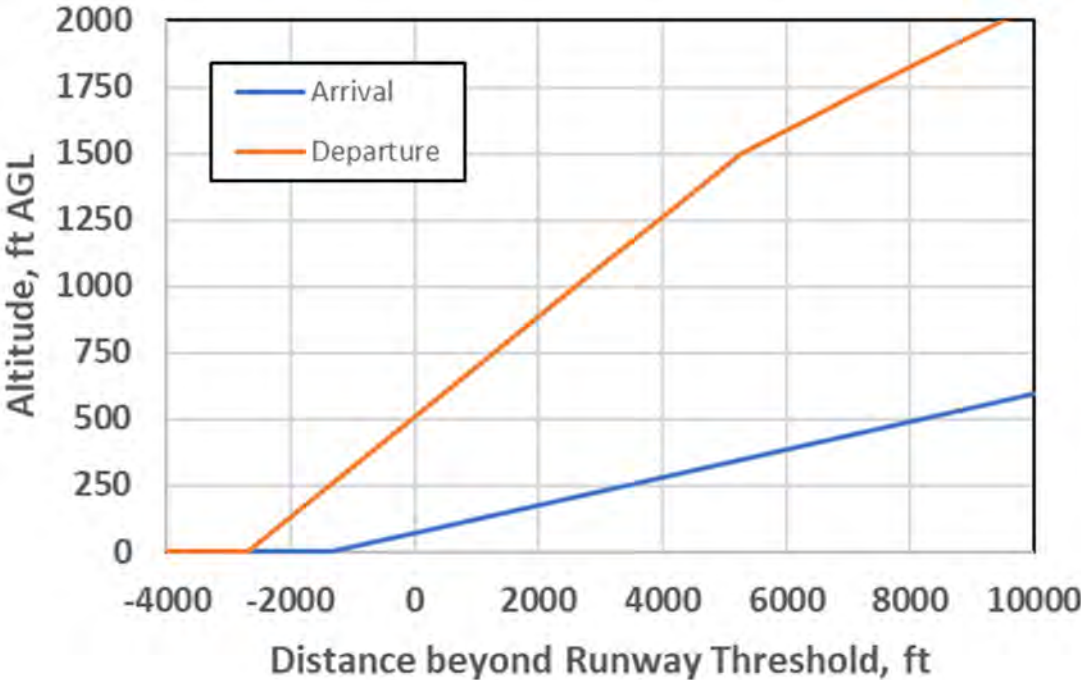


Figure 3-35. Comparison of altitude profiles for arrivals and departures

For commercial structures, the region of influence depends on their exact location relative to the flight tracks. From the benchmarking results, the effect of shielding calculated by TNM is a function of building

dimensions for operations along and close to a runway. A series of figures were developed based on the benchmarking results where the building dimensions are listed as height by width by depth in the legend. For example, “8 x 32 x 10” represents a building that has a height of 8 m (26 ft), a width of 32 m (105 ft), and a depth of 10 m (33 ft). Figure 3-36 provides the results for a ground-based line source at a lateral distance of 2,000 m (6,562 ft). Maximum insertion loss from buildings occurs when the aircraft is on the ground. At a distance of 200 m (762 ft) behind the building, the insertion loss is equal to or less than 0.5 dBA for the representative buildings. Figure 3-37 provides the TNM calculated insertion loss for a line source at 100 m AGL (328 ft AGL) at the same lateral offset distance of 2,000 m (6,562 ft). At this altitude the insertion is less than 0.5 dBA at a distance of 200 m (762 ft) behind the building.

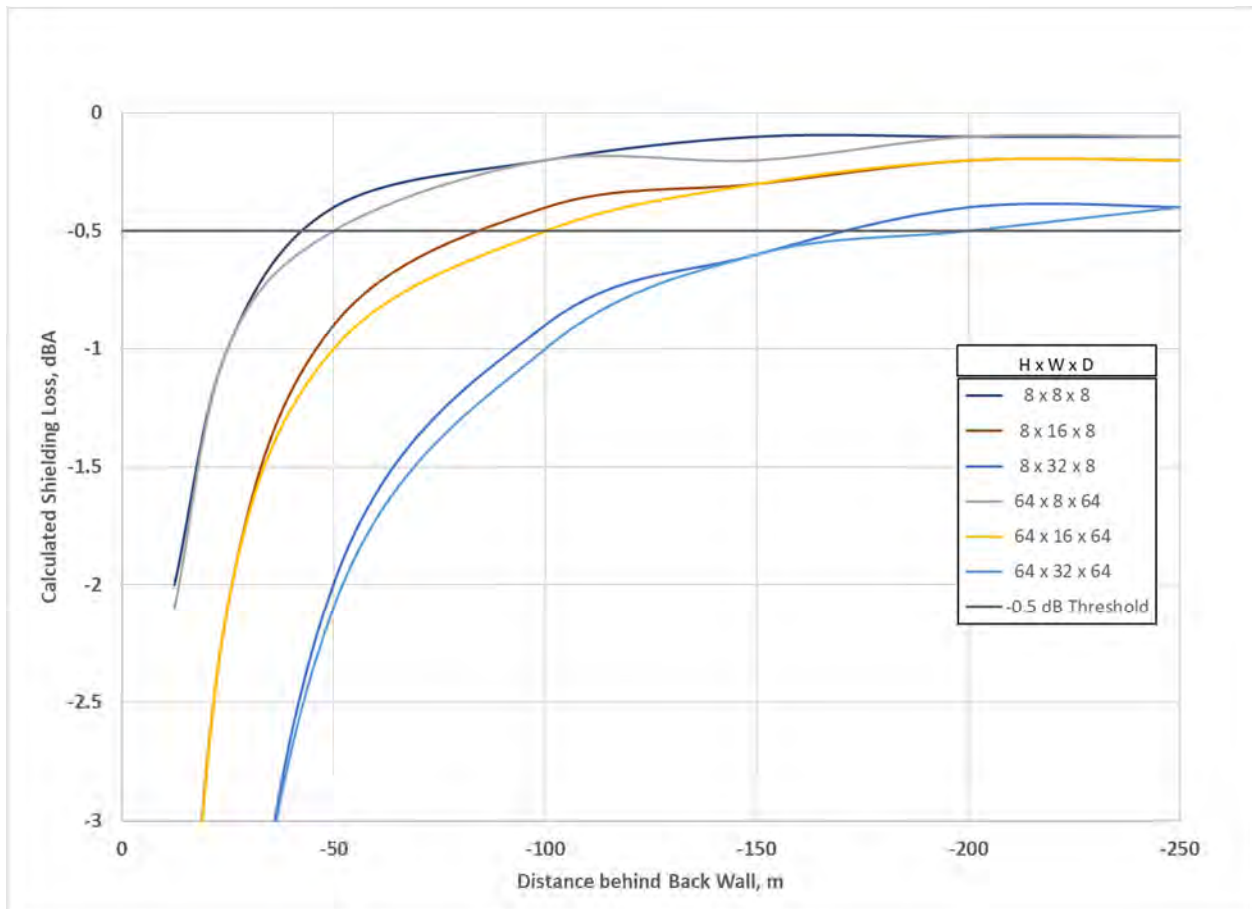


Figure 3-36. TNM insertion loss for a ground-based (0 m AGL) noise source at an offset distance of 2,000 m

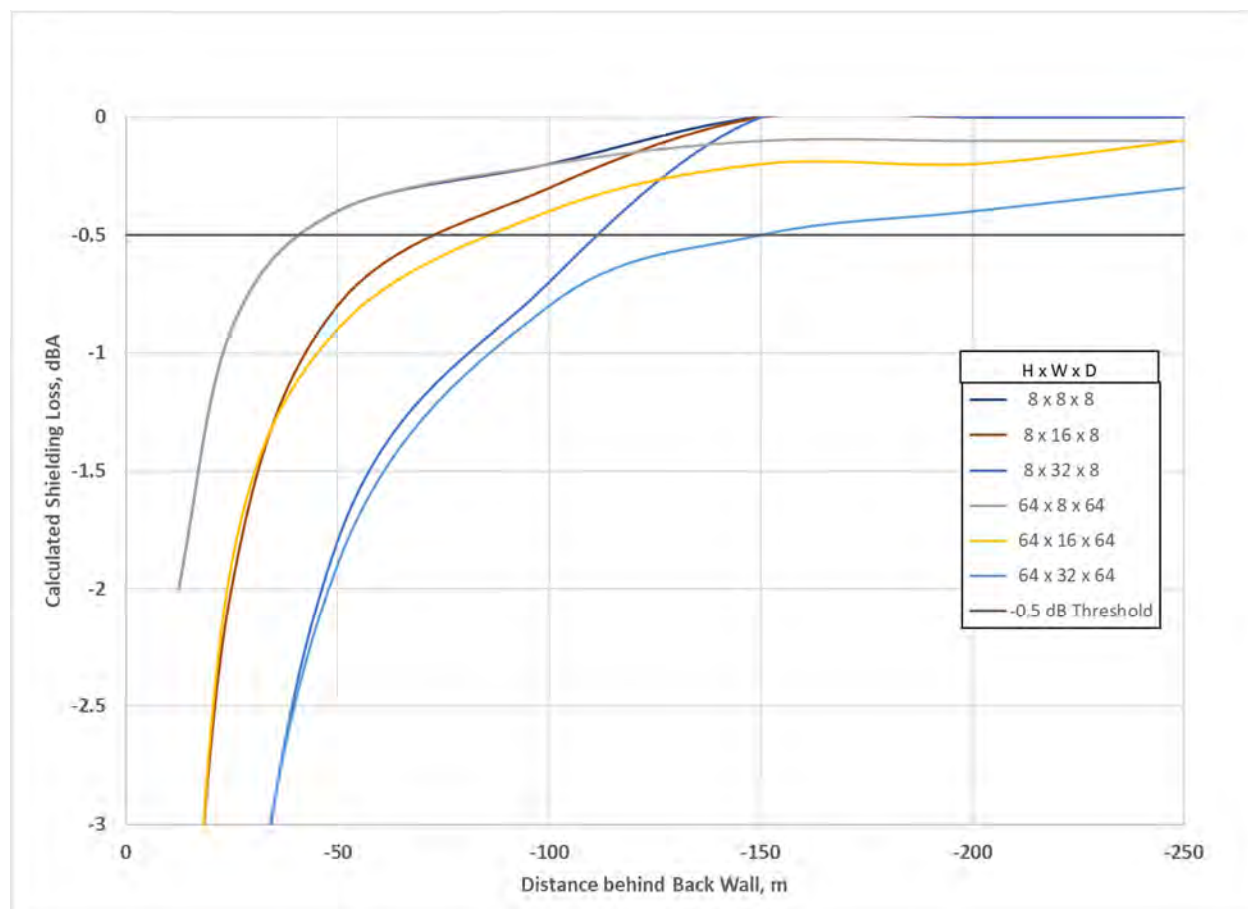


Figure 3-37. TNM insertion loss for a 100 m AGL noise source at an offset distance of 2,000 m

In addition to the insertion loss, Figure 3-38 shows the reflection gains for the ground-based line source at 2,000 m (6,562 ft). For these cases, the reflection gains are less than 0.5 dBA within a distance of 150 m (492 ft) in front of the building. Thus, at this distance from the runway, the reflection gain has a small area of influence compared to the shielding loss. It should be noted that these reflection results are independent of building height.

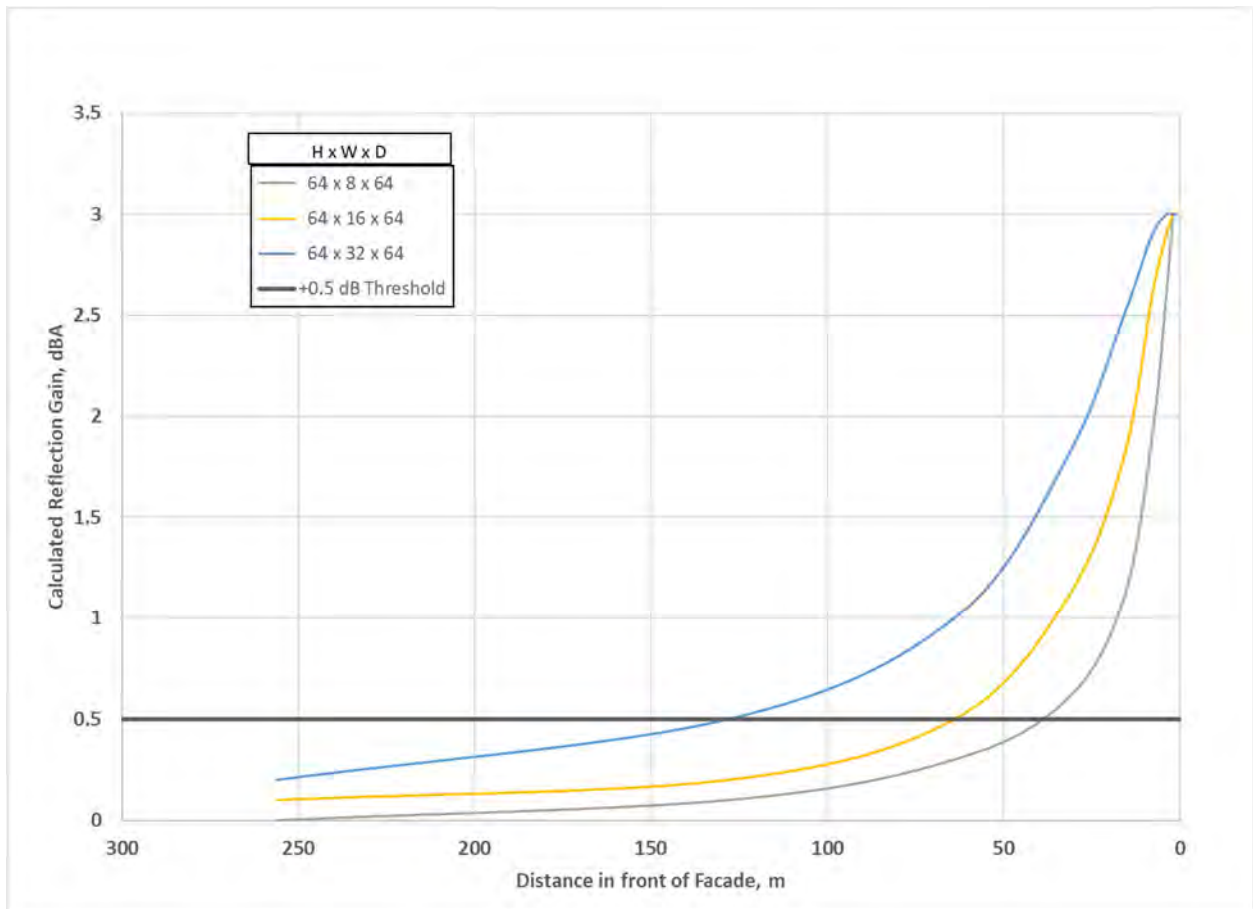


Figure 3-38. TNM reflection gain for a ground-based noise source at an offset distance of 2,000 m

Using a minimum shielding loss of 0.5 dBA, these results suggest dimensions of the standard region of application of the manmade structures. Along the runway, the region should extend to 2,621 m (8,600 ft) before the runway threshold. This distance is set based on an aircraft altitude of 152 m (500 ft) AGL on a 3° glide slope arrival. Lateral to the runway, the region should extend to 2,200 m (7,218 ft). At these dimensions, the effects of buildings should be less than 0.5 dBA except for areas very close to the building.

To provide a smooth transition in the predicted noise levels from the region of application to the rest of the computational domain, a transition region should be applied to minimize discontinuities in the noise grid. At a boundary distance of 2,200 m (7,218 ft) lateral to a line source, the overall noise levels decrease by 0.5 dBA due to spreading with an additional 268 m (881 ft) in lateral offset. Thus, the transition region is applied over a distance of 328 m (1,000 ft). Within the transition region the magnitude of the GL_{BM} values are linearly decreased with distance such that they are 0 at the boundary. Beyond the transition zone, the structure effects will be neglected, and the aircraft noise calculation only involves terrain effects. A conceptual example of these regions are shown in Figure 3-39 for an 8,000 ft runway, where the green area is the region of application for building effects, and the dark blue area represents the transition region.

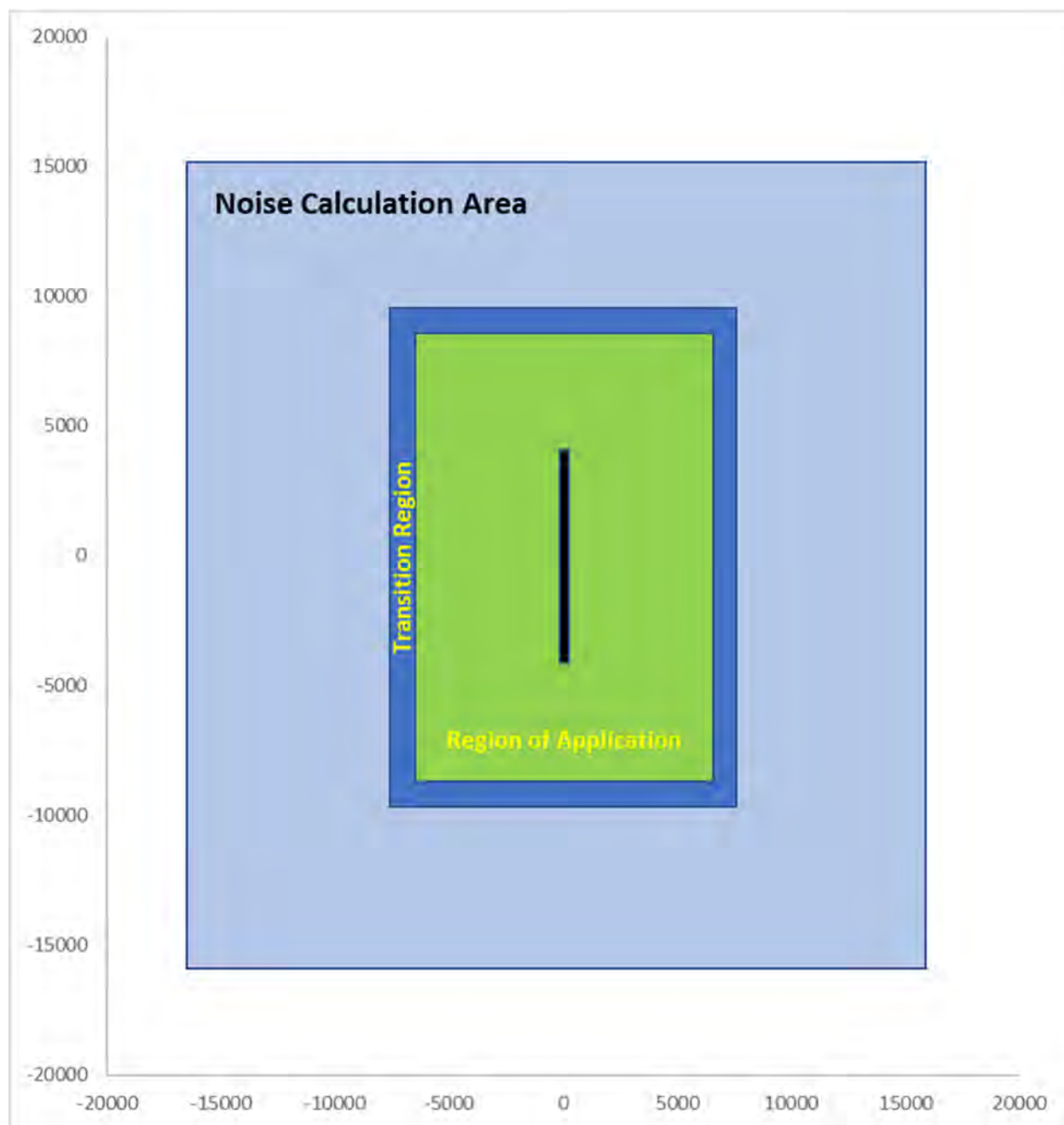


Figure 3-39. Illustration of regions of application and transition for the blended method building effects

3.3.4 Outside of Region

Outside of the defined region, the effects of buildings for both shielding and reflection is highly localized based on observations in the field and results from the computational benchmarking. However, for buildings close to but outside the lateral portion of the region of application, reflections can be estimated by the NCHRP Barrier Reflections Screening Tool. In this region, the aircraft altitude should be at or below 152 m (500 ft), which is within the validity of the tool. The tool's validity is greatly reduced for an elevated

noise source. Thus, this tool should not be used along the extended runway centerline outside of the defined region. Additionally, this tool can be used as an interim screening tool for potential reflection effects outside of the FAA AEDT as the blended method is being incorporated into AEDT as long as its application remains within the limits of valid application.

3.3.5 Blended Method Summary

For manmade structural effects, the boundaries have been defined over which the effects calculated by TNM are applied, and a transition region outside that boundary produces a smooth transition to the baseline AEDT noise contouring. The boundaries are set based on the benchmarking results and confirmed by observations within our measured data at LAX and LGB airports. The set boundaries are 2,621 m (8,600 ft) from the runway threshold along the runway centerline and laterally to 2200 m (7,218 ft). The transition region extends 328 m (1,000 ft) past the set boundaries. These standard areas capture the flight operations with altitudes at 152 m (500 ft) AGL and below. For a given airport, the region of application of manmade structural effects can be reduced if no major buildings are present within a localized area. Within the structural effect region, TNM calculations of the gain/loss factors include the effects of terrain, but the gain/loss factors only include the effect of manmade structures. This calculation is accomplished by running TNM with and without the manmade structures while all other modeling parameters remain constant. For terrain effects, AAM's terrain algorithms are applied to the entire area of calculation. Thus, the calculation of terrain effects is consistent both within and outside of the structure effects region.

3.3.6 AEDT Integration

Within AEDT, the Aircraft Acoustics Module contains the noise modeling formulation. Recommended changes to AEDT involve updates to this module. At present all model features are handled as adjustments to the baseline noise-power-distance propagation results. For example, lateral directivity is computed based on the geometry and applied as a correction. Similar corrections are handled for duration adjustments (due to speeds differing from the 160 kt reference NPD speed) and for directivity behind the start of takeoff roll. The mode of operation for AEDT for computation of supplemental metrics such as time audible, requires additional sub-segmentation due to the need to compute changes in line-of-sight blockage. The incorporation of improved propagation over natural terrain and manmade structures can be implemented in AEDT in a similar manner.

3.3.6.1 Computational AEDT Integration

3.3.6.1.1 Terrain Effects Integration

The inclusion of the terrain effects algorithms from AAM and NoiseMap require minimal modification other than translating the code from FORTRAN to the AEDT native C# software programming language.

Data Sources: AEDT currently allows the importing of elevation data, which are required for the inclusion of terrain effects within the noise prediction algorithms. The recommended resolution of 1/3 arc-second resolution is desired for the terrain calculation (FAA 2017). Thus, no additional data source importing functionality needs to be added to AEDT.

Algorithms: The terrain algorithms in AAM and NoiseMap are currently coded in FORTRAN. Thus, the first step in the integration is translating the code to C#. Once translated, the code is directly integrated into the noise exposure calculation computational flow in the AEDT Acoustics Module. The format of the internal evaluation data needs to be reconciled to ensure the AAM/NoiseMap algorithms are using the correct reference frame for the coordinates (Plotkin et al. 2013).

For the calculation of the terrain effects, the AAM/NoiseMap algorithms calculate a terrain cut between the source and receiver points. This calculation overlays five points along the terrain cut to classify the cut into six terrain models. Figure 3-40 provides these classifications (the “Wedge with flats” includes a single and dual flat plane). Once the cut is classified, the attenuation for that terrain model is calculated. For NoiseMap, the attenuation can be calculated on either an A-weighted or spectral basis. For AAM, the calculation is only performed on a spectral basis. For the integrated approach, NoiseMap calculates the attenuation for each segment. For line segments, the attenuation is calculated for each terrain cut for each end point and the closest point of approach, if it lies between the end points. For that segment, the maximum attenuation is applied to the noise exposure fraction. For turn segments, the attenuation is calculated for each end point only, and again the maximum attenuation is applied for that segment.

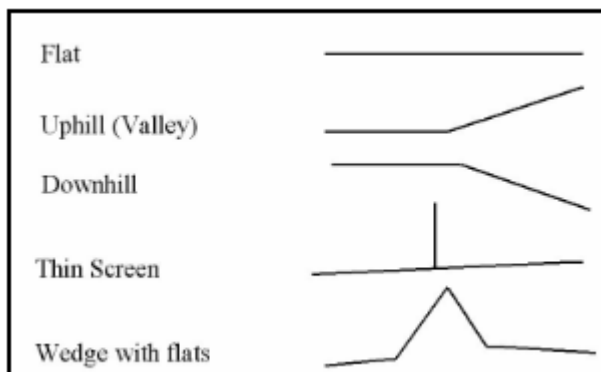


Figure 3-40. AAM geometric terrain models (Bradley et al. 2016)

Thus, the AEDT computational code would have to include the terrain cut and attenuation calculation. This inclusion should be simple since the loss factors are calculated in a serial linear flow. The existing AEDT Acoustics Module performs a line-of-sight calculation for computing audibility metrics. This portion of the code calculations could be leveraged for inclusion of terrain effects.

Interface Requirements: The inclusion of terrain effect within AEDT would require no changes to the AEDT interfaces.

3.3.6.1.2 Manmade Structural Effects Integration

The inclusion of the manmade structural effect algorithms in TNM 3.0 requires more effort for integration into AEDT. This integration requires the development of a new module within AEDT to import the required terrain and building data, define the area of application, transfer the operational modeling data (elevation data, spectral class, flight and taxi profiles, and tracks), perform the gain/loss calculation, and index the gain/loss grids.

Data Sources: The primary data requirement for this portion of the blended method is building data. For this project’s analysis, LiDAR data were obtained for both the Los Angeles International Airport and Long Beach Airport. However, LiDAR data are not universally available at all locations. A review of potential future building databases will be required at the time of actual integration since more datasets are being developed, and may be developed, such as Microsoft’s building footprint database for OpenStreetMap. When the database is selected, the data will require conversion to an appropriate format compatible for use with the TNM algorithms. The analysis conducted at LAX demonstrates the suitability of this approach.

Algorithms: Since this module is standalone in terms of the computational flow, the TNM 3.0 algorithms only need to be modified to convert the flight and taxi paths into “road” segments. With the inclusion of the building data and conversion of the modeled paths, TNM algorithms calculate an OTOB gain/loss grid for each modeled profile and convolve the grid with that specific profile’s spectral class data. Next, the transition region is applied to the gain/loss grid grid. Each convolved gain/loss grid is indexed to its individual profile for inclusion in the noise grid calculation.

Moreover, the implementation of the TNM algorithms within AEDT are inherently linked to the degree of geometric modeling fidelity in the manmade structural data and the chosen TNM objects to represent these objects. The following should be considered for the integration of TNM algorithms into AEDT:

- Barrier (wall) objects can be used for both shielding and reflections. The importation of the building data must select the most acoustically important façades to model, since a barrier cannot be a closed structure as it is currently implemented. Barriers are treated as solid objects (no transmission through the wall), and noise can diffract over the top and around the ends. For small structures such as a home, barriers can result in very localized shielding and reflection effects.
- Building row objects can be used for shielding and represent a row of buildings. The TNM user must specify the building percentage; if the gaps between buildings percentage is 20% or less, the user must use a barrier object instead. These objects calculate shielding as a barrier would then account for only a portion of that shielding, since some of the sound will pass between buildings. The sound attenuation due to a building row is calculated as the following:

$$\Delta_{attn} = \left\{ -10 \log_{10} \left(\text{Linear Gap Fraction} \times 10^{\text{Barrier Insertion Loss}/10} \right) \right\}_{MAX}^0$$

- It may be possible to apply a similar equation to reflections and use building rows to calculate reflected sound, where the effect would be reduced as the percent gap increases; this effect needs to be investigated for final integration.

In the benchmarking study and comparison with dedicated empirical measurements at LAX and LGB, two TNM object types: barriers (benchmarking and LAX/LGB) and building rows (only for LAX/LGB) were utilized and evaluated for the calculation of shielding and reflections. For the LAX and LGB cases, only barriers were used for reflections, and a combination of barriers and building rows were used for

shielding. Unless a specific geometry warranted additional rows, neighborhoods were typically modeled with three rows of homes in the vicinity of a particular microphone location. Rows were modeled with building row objects unless spaces between homes were small or homes were not linearly placed. The modeling was done to most accurately predict gain/loss factors at very specific locations (microphone locations). For AEDT applications, modeling should be done to calculate the most effective and reasonable noise contours, and whole neighborhoods/areas of buildings will need to be represented, not just in the vicinity of a particular backyard, for example. TNM will account only for the most acoustically important objects in a sound propagation path for each point on a contour grid.

Interface Requirements: The structural effects inclusion requires additional interfaces with AEDT. The first interface will allow a user to import building data for the appropriate area. Within this interface, AEDT should suggest an area of application, but users should have the opportunity to modify the area of application for each runway. Once a user confirms the area of application, the OTOB gain/loss grids can be processed.

3.3.6.2 Summary of Blended Method Integration

The blended method is composed of two computational paths. First, the effects of terrain are included in the normal noise exposure calculation flow. These effects are modeled using the algorithms contained in AAM using the implementation found in NoiseMap, and they are modeled throughout noise calculation area. Second, the effects of manmade structures are modeled in a separate module based on TNM 3.0 algorithms. This module calculates OTOB gain/loss grids for each profile and convolves the grid with the spectral class data for that operation. This convolved OTOB gain/loss grid is indexed and provided to the noise exposure calculation module. This second module only needs to be calculated once for each profile as long as buildings remain the same within the area of application.

FAA has provided a chart of AEDT Development Goals at a recent AEDT Development Meeting and Noise Operations Research Annual Review meeting June 2019. The results from this project are slated to be incorporated into AEDT 4x around the 2022 timeframe. This timeline is FAA's current goal, but timeline may change depending on agency and development needs. Additionally, once the decision is made to incorporate the model, our estimate on timelines is that it would be about a year to incorporate the changes into a release version of AEDT, which would include the required verification and validation testing. Volpe software development team typically develops a roadmap for code modifications including identifying the various sprint cycles to incorporate new algorithms. For this model, a major decision will be whether to rewrite existing algorithms, AAM terrain in FORTRAN, into native C# or develop a "wrapper" around the existing code. A two-phase effort to implement these modules could be utilized. The exact incorporation approach developed by FAA and Volpe will impact costs and timeline for this inclusion of the blended method.

As part of the integration of this research into AEDT 4x, specific guidance/document will be included in the AEDT 4x documentation. The exact documents and user guidance will depend on the AEDT implementation approach determined by FAA and Volpe. One item that is currently open is the importation of building data into AEDT. Current building databases are varied, but near future databases may have better resolution and consistency across the country.

The effect of ground surface types has been covered by ACRP 02-52 Noise Modeling of Mixed Ground Surfaces. The results from this research project will be integrated with the blend method within the AEDT 4x development. Additionally, as part of the AEDT4x goals, higher fidelity NPDs will also be implemented. The integration of this new feature with the blended method will have to be evaluated to understand how these NPDs can improve the blended method's calculations. The final guidance will depend on the actual implementation of the blended method along with other AEDT modeling additions.

4 Conclusions and Suggested Research

This research project has focused on improving AEDT modeling for aircraft noise reflection and diffraction from terrain and manmade structures. This focus has explored applying current noise models to capture the desired effects within AEDT. This task was accomplished through the evaluation of models with computational, empirical, and measured datasets. The evaluation of the blended method approach to terrain and manmade structures has resulted in the recommendation of algorithms from the following methods for incorporation into AEDT:

- Terrain effects: utilize the routines from AAM v2.0; and
- Manmade structural effects: utilize the routines from TNM v3.0.

For the inclusion of the blended method into AEDT, the effects and models are separated for computational efficiency and improved accuracy. First, the terrain effects algorithms can be integrated simply within AEDT's computational structure, and the effect can be easily modeled throughout the entire area of calculation.

Second, the manmade structural effects can be calculated separately outside of the main noise calculation module. This separation provides computational efficiency since the effect only needs to be calculated once for a given location if the buildings remain unchanged. Then, the gain/loss factors can be added to the noise calculation as a simple linear adjustment.

The region of influence of manmade structural effects is limited to locations surrounding the runway when the aircraft are at low altitudes. The fixed calculation area has been defined for application of TNM algorithms along with a simple transition region to the AEDT noise calculation. The defined boundaries are based on the benchmarking results and confirmed by observations within our measured data at LAX and LGB airports. The set boundaries are 2,621 m (8,600 ft) from the runway threshold along the runway centerline and laterally to 2200 m (7,218 ft). The transition region extends 328 m (1,000 ft) past the set boundaries. These standard areas capture the flight operations with altitudes at 152 m (500 ft) AGL and below. For a given airport, the region of application of manmade structural effects can be reduced or expanded to capture the major buildings within a localized area. Within the structural effect region, TNM calculations of the gain/loss factors include the effects of terrain, but the gain/loss factors only include the effect of manmade structures. This calculation is accomplished by running TNM with and without the manmade structures (while all other modeling parameters remain constant) and computing the difference. The gain/loss factors are calculated on a OTOB basis for application to a given flight operation's spectral class. For a modeled operation, the convolved results are included in the calculation of the overall noise metrics.

Additionally, during the field measurements, several interesting acoustic phenomena were observed. At the neighborhood of El Segundo, departing aircraft could be acoustically tracked although the aircraft could not be seen. This observation most likely arises from the reflection and scattering from the houses. At Playa del Oro neighborhood, in a backyard the reflections from multistory apartment building resulted in hearing two distinct aircraft flyovers. One from the actual aircraft and one from the reflected image in

the direction of the multistory building. The owner of this residence noted that the noise levels had significantly increased with the recent construction of the apartment building.

Suggested Future Research:

- Simple Reflection Tool
- Taxi Noise Modeling
- Ground Run-up Enclosures
- Urban Canyon Effects
- Blended Method Verification and Validation

Simple Reflection Tool: The updated NCHRP Barrier Reflections Screening Tool has been modified for airport planners to screen for potential reflection effects outside of the FAA AEDT. This tool has been modified for application to aircraft noise and can be used immediately to estimate reflection effects while the blended method recommendations are being incorporated into AEDT.

Taxi Noise Modeling: AEDT 3 does have the ability to model taxi operations in a limited fashion. The ACRP 02-27 project developed improved taxi NPD, spectral class and directivity data for AEDT and incorporation of improved taxi noise modeling is currently on the FAA roadmap for AEDT 4 (Page 2009; Page 2010; Page Hobbs 2012; Page 2013; Page 2014). The insertion losses from terrain and manmade structures is independent of the source noise level, so these future taxi improvements to AEDT will be compatible with the terrain and manmade structure recommendations made under this ACRP project.

Moreover, taxi operations were captured as part of the measurements at LGB. It is suggested that that data be used to test the use of TNM algorithms for calculating the gain/loss factors for these ground operations. Based on the test site layout, the reflection effect should be easily assessed. The shielding effect is more complicated due to nearby structures, and as such, additional data may be required to further test this effect. It is expected, however, that both reflection and shielding effects due to the nearby buildings can be properly calculated, since the ground operations are similar to TNM's intended purpose of calculating such effects for surface transportation.

Ground Run-up Enclosures: In addition to the tested application of TNM for the effects of buildings around airports, it may also be possible to apply the same algorithms to capture the noise-reducing effects of ground run-up enclosures. The modeling approach of the blended method can be combined with the ACRP 02-27 taxi noise project to model the stationary noise from a ground run-up enclosure. However, since these enclosures vary in configurations and sound absorption characteristics, it is recommended that the effect of these enclosures be evaluated by comparing the blended method results to data measured in the vicinity of enclosures. These comparisons will evaluate the validity of the blend method to these enclosures as well as refine the blended method for this application.

Urban Canyon Effects: Initial examination of TNM- and ISO 9613-2-calculated gain/loss factors for a complex urban environment (in this case, the hotel district at LAX), showed that both models were not

properly capturing related complex reflections. TNM 3.0 is designed to account for only one reflecting surface, a highway noise barrier, so it has no secondary or higher order reflections, and results from multiple building reflecting surfaces is limited (even with just single reflections). To improve TNM results in an urban environment, additional orders of reflection would need to be added, as well as the ability to incorporate effects from more surfaces than it currently allows. Without these modifications to the TNM reflection algorithms, the proposed method for applying reflection effects is applicable to many standard applications, but it is limited in application to complex building environments with multiple rows of high-rise buildings, which result in the urban canyon effect. However, algorithms for handling the shielding effects for complex urban environments are already implemented in TNM.

Blended Method Verification and Validation: Finally, the data measured as part of this project can be used to validate the results of the blended method when it has been integrated into AEDT. The complete measured airport noise dataset is archived for this potential application. The dataset includes the noise data (raw and analyzed), operational data, observed field notes, weather, terrain and building data, and AEDT modeling data. This archive will be held by the Volpe Center.

5 References

- Boeker, E., J. Rosenbaum, "Intelligent Switching Between Different Noise Propagation Algorithms: Analysis and Sensitivity," *Internoise 2012*, New York City, NY, August 2012.
- Boeker, E.R., E. Dinges, B. He, G. Fleming, C.J. Roof, P.J. Gerbi, A.S. Rapoza, J. Hemann, "Integrated Noise Model (INM) Version 7.0 Technical Manual," FAA-AEE-08-01, Office of Environment and Energy, Federal Aviation Administration, January 2008.
- Bowlby, W., R. Williamson, D. Reiter, C. Patton, G. Pratt, K. Kaliski, K. Washburn, J. Rochat, A. El-Aassar, H. Knauer, G. Sanchez, and D. Barrett. *NCHRP Web-Only Document 218: Field Evaluation of Reflected Noise from a Single Noise Barrier—Phase 1*. Transportation Research Board, Washington, D.C., 2016.
- Bradley, K.A., Hobbs, C., Wilmer, C., and Czech, J.J., "Advanced Acoustic Model Technical Reference and User Manual," Wyle Report No. WR 16-08, June 2016.
- Czech, J.J., and K.J. Plotkin, "NMAP 7.0 User's Manual," Wyle Laboratories Research Report No. WR 98-13, November 1998. <https://doi.org/10.21236/ADA406645>.
- Dinges, E. "Enhanced AEDT Modeling of Aircraft Arrival and Departure Profiles," ACRP 02-55. Active Project, 2017.
- Dinges, et al., "Integrated Noise Model (INM) Version 7.0 User's Guide," Report No. FAA-AEE-07-04, Washington D.C., Federal Aviation Administration, April 2007.
- Downing, M., J. Page, J. Rochat. *Improving AEDT Modeling for Aircraft Noise Reflection and Diffraction from Terrain and Manmade Structures: Selection of Transportation Noise Models*, ACRP 02-79 Interim Deliverable, November 2017.
- Eldred, Ken, "Approximating Aircraft Noise using a Model of a Moving Source with a 90o Dipole Radiation Pattern," KEE written communication, 1980.
- Eldred, Kenneth M. and Robert L. Miller, "Analysis of Selected Topics in the Methodology of the Integrated Noise Model," US-DOT-TSC-1782, also BBN Report No. 4413, Nov. 1980.
- Federal Aviation Administration, "Report to Congress on Nonmilitary Helicopter Urban Noise Study," December 2004.
- Federal Highway Administration TNM 3.0 Release Memo, https://www.fhwa.dot.gov/environment/noise/traffic_noise_model/tnm_v30/tnm3memo.cfm, 2017.
- Fleming, G.G., C.J. Roof, A.S. Rapoza, D.A. Senzig, "Reference Source Noise Data for GCNP Noise Model Validation Study" Letter Report DTS-34-FA065-LR2, May 2000.
- Hobbs, C. M., E. Boeker, A. Hasting, A. Rapoza, J. Page, and D. Senzig. *ACRP Web-Only Document 32: Improving AEDT Noise Modeling of Hard, Soft, Mixed Ground Surfaces*. Transportation Research Board, Washington, D.C., 2017. <https://doi.org/10.17226/24822>.
- Ikelheimer, B., M. Downing, and M. James, "Atmospheric Acoustic Propagation Prediction," SPAWAR SBIR, Final Report, January 2009.
- Ikelheimer, B., K. Plotkin, "Noise Model Simulation (NMSim) User's Manual," Wyle Report No. WR 0309, June 2005.

International Standards Institute, "Acoustics – Attenuation of sound during propagation outdoors – Part 2: General method of calculation", ISO 9613-2, December 1996.

Koopmann, et al., "Aviation Environmental Design Tool (AEDT) 2b User Guide," Report No. DOTVNTSC-FAA-15-07, Washington, D.C.: Federal Aviation Administration, November 2015.

Lee, R.A., Liasjo, K., Buetikofer, R., Svane, C., Plotkin, K.J., "Noise Measurements – Modeling for Topography," Noise-Con 96 Proceedings, 1996.

Menge, C., C. Rossano, G. Anderson, and C. Bajdek, FHWA Traffic Noise Model, Version 1.0 Technical Manual, Report No. FHWA-PD-96-010, U.S. Department of Transportation, February 1998 + 2004 TNM v2.5 update sheets.

Michalke, A., and U. Michel. Prediction of Jet Noise in Flight from Static Tests. *Journal of Sound and Vibration*, Vol. 67, No. 3, 1979, pp. 341–367.

Miller, N., G. Anderson, R. Horonjeff, C. Menge, J. Ross, M. Newmark, "Aircraft Noise Model Validation Study," HMMH Report No. 295860.29, January 2003.

Page, J. A., C. M. Hobbs, B. May, E. Boeker, H. Brouwer, and C. Morrow. *Guidance for Helicopter Community Noise Prediction*, Airport Cooperative Research (ACRP) Project No. 02-44, 2015. Available from <http://apps.trb.org/cmsfeed/TRBNetProjectDisplay.asp?ProjectID=3439>.

Page, J. A., and Boeker, E. "Ray Mode Development: AEDT-Ray SEL Implementation Plan", Technical Memorandum to FAA, 31 July 2015.

Page, J., 2014. "Turbofan and Propeller Aircraft Taxi Operating State Noise Power Distance and Spectral Class Database Development Process for AEDT," *SciTech*, AIAA-2014-0366, January 2014. <https://doi.org/10.2514/6.2014-0366>.

Page, J., K. Bassarab, C. Hobbs, D. Robinson, T. Schultz, B. Sharp, S. Usdrowski, and P. Lucic. *ACRP Web-Only Document 9: Enhanced Modeling of Aircraft Taxiway Noise, Volume 1: Scoping*. Transportation Research Board of the National Academies, Washington, D.C., 2009.

Page, J., C. M. Hobbs. "Modeling of Noise from Aircraft Taxiing Operations," NOISE-CON 2010, Joint 159th Meeting of the ASA / NOISE-CON 2010, Baltimore, Maryland, *J. Acoust. Soc. Am.*, 127(3) 2, 1834, 2010 <https://doi.org/10.1121/1.3384279>.

Page, J., C. Hobbs, P. Gliebe. *ACRP Web-Only Document 9: Enhanced Modeling of Aircraft Taxiway Noise, Volume 2: Aircraft Taxi Noise Database and Development Process*. Transportation Research Board of the National Academies, Washington, D.C., 2013. Available from: <https://doi.org/10.17226/22606>.

Page, J., C. Hobbs, and P. Gliebe. *Aircraft Taxi Noise Database and Development Process*. Wyle Research Report WR 12-24, Contract No. ACRP 02-27, Submitted to ACRP, November 2012.

Plotkin, K. J., T. Schultz, and J.A. Page, "Aircraft Noise Simulation Modeling for Propagation and Impact Prediction", NATO Paper RTO-MP-AVT-158-14, AVT Specialists Meeting: Environmental Issues Associated with Gas Turbine Powered Military Vehicles, Montreal, Canada, 13 - 16 October 2008.

Plovsing, B., "Aircraft Sound Propagation over Non-Flat Terrain; Development of Prediction Algorithms," The Danish Acoustical Institute, January 1994.

Rasmussen, K.B., "On the Effect of Terrain Profile on Sound Propagation Outdoors," *Journal of Sound and Vibrations*, 98(1), pp35-44, 1985. B. Reichman et al, "Comparison of Noise from High-Performance Military Aircraft for Ground Run-up and Flyover Operations," 2018 AIAA/CEAS Aeroacoustics Conference, June, 2018.

Rochat, J. and G. Fleming, Validation of FHWA's Traffic Noise Model (TNM), Report Number FHWA-EP-02-031, U.S. Department of Transportation, August 2002 + July 2004 TNM V2.5 addendum.

Rosenbaum J., E. Boeker, A. Buer, P. Gerbi, C. Lee, C. Roof, G. Fleming, "Assessment of the Hybrid Propagation Model: Volume 1: Analysis of Noise Propagation Effects," DOT-VNTSC-FAA-12-05.I, Final Report, August 2012.

Wyle Laboratories, Volpe National Transportation Systems Center, Netherlands Aerospace Centre, and KB Environmental Sciences. *ACRP Research Results Digest 24: Recommended Community Noise Model Enhancements to Improve Prediction of Helicopter Activity Impacts*. Transportation Research Board, Washington, D.C., 2016. Available from: <http://www.trb.org/main/blurbs/173719.aspx>.

US DoT Volpe Center, FAA, ATAC Corp, CSSI, Inc., and Metron Aviation, "Aviation Environmental Design Tool (AEDT) Technical Manual, Version 2d," DOT-VNTSC-FAA-17-16, September 2017.

Wei, W., T. Van Renterghem, and D. Botteldooren. Simplified Analytical Model for Sound Level Prediction at Shielded Urban Locations Involving Multiple Diffraction and Reflections. *Journal of the Acoustical Society of America*, Vol. 138, No. 5, Nov. 2015, pp. pp2744–pp2758.

Appendix A: Review Summaries of Individual Models

This appendix reviews AEDT and each method as identified in the literature review process considered for further evaluation. The following models are reviewed:

1. FAA Aviation Environmental Design Tool (AEDT)
2. NoiseMap 7.3
3. FHWA Traffic Noise Model (TNM)
4. Advanced Acoustic Model (AAM)
5. NoiseMap Simulation Model (NMSim)
6. FHWA Roadway Construction Noise Model (RCNM)
7. FTA Method
8. NCHRP Barrier Reflections Screening Tool
9. HARMONOISE/IMAGINE
10. CandaA
11. NORD2000
12. SoundPLAN
13. ISO 9613-2
14. Wei et al. Urban Diffraction and Reflection Method

For each model, the following information is reviewed:

- Model overview (main purpose, source type, calculation method, method summary).
- Noise source (data source, spectra, directivity, additional comments).
- Propagation algorithm (atmospheric absorption, atmospheric refraction, ground impedance, terrain, barriers, manmade structures, reflections).
- Source code (access, language, whether or not it has been acquired).

Model Overview: Aviation Environmental Design Tool (AEDT)			
Main Purpose:	AEDT is a software system that models aircraft performance in space and time to estimate fuel consumption, emissions, noise, and air quality consequences. AEDT is a comprehensive tool that provides information to FAA stakeholders on each of these specific environmental impacts. AEDT facilitates environmental review activities required under the National Environmental Policy Act by consolidating the modeling of these environmental impacts in a single tool.		
Source Type:	Fixed-Wing and Helicopter Integrated Noise-Power-Distance and Spectral Class (OTOB) data. Limited directivity for certain modeling circumstances	Calculation Method:	Integrated
Method Summary:	AEDT is designed to model individual studies ranging in scope from a single flight at an airport to scenarios at the regional, national, and global levels. AEDT leverages geographic information system (GIS) and relational database technology to achieve this scalability and offers rich opportunities for exploring and presenting results. Versions of AEDT are actively used by the US government for domestic aviation system planning as well as domestic and international aviation environmental policy analysis.		
Noise Source			
Data Source:	Measured / Manufacturer Provided / FAR-36 certification adapted data	Spectra:	OTOB data >50 Hz to 10 kHz
Directivity:	2D		
Additional Comments:	Limited directivity. Fixed-wing have generalized lateral directivity (wing vs. tail mounted engines). Generalized fixed-wing 2D curves for behind takeoff roll. Lateral directivity for rotorcraft in hover and vertical flight modes. <i>Generalized: single geometric relationship for the entire fixed-wing fleet.</i>		
Propagation Algorithm			
Atmospheric Absorption:	Society of Automotive Engineers (SAE) Aerospace Recommended Practice (ARP) 866A, SAE Aerospace Information Report (AIR) 1845 and SAE ARP 5534	Atmospheric Refraction:	None
Ground Impedance:	Soft Ground		
Terrain:	Line-of-sight blockage for calculation of time above metrics. Slant range offset due to varying ground altitude from terrain. Soft ground in the model. For propeller, one can “turn off” the soft ground to mimic hard ground, although it is not a physics-based hard ground capability.		
Barriers:	None		
Manmade Structures:	None		
Reflections:	None		
Source Code			
Access:	Controlled	Language:	C#
		Acquired:	<input checked="" type="checkbox"/>

Model Overview: NoiseMap 7.3			
Main Purpose:	The primary purpose of the DoD Airfield Noise Model is the calculation of differential nonlinearity (DNL) noise contours around military airfields based on user-developed operational inputs for both flight and ground operations of fixed-wing and rotorcraft aircraft. A secondary purpose is the calculation of supplemental noise metrics for the same scenario as the DNL contour to provide better context of the current or potential future operations at an airfield.		
Source Type:	NoiseFile, Integrated metrics SEL, SEL _t , EPNL, PNL, PNLT, L _{max} , L _{max,t} . Most data based on actual measurements (flight and ground run-up). Few aircraft have estimated data which are based on other aircraft measurements. NoiseFile is maintained by Air Force Research Laboratory, but they are not funded for this task.	Calculation Method:	Integrated: 1) Flat earth, Omega10 & 11 2) Topography Effects: A-wt Berger algorithms (NATO CCMS sponsored development)
Method Summary:	NoiseMap utilizes user-developed operational data to calculate cumulative and single event aircraft noise on an integrated basis. Topography Effects routines are transportable to AEDT.		
Noise Source			
Data Source:	NoiseFile database, which is separated into flight and ground run-up noise. Noise data are obtained from dedicated field measurements. Some reference noise data is estimated based on similar surrogate aircraft/engine combinations.	Spectra:	Flight: OTOB spectra at maximum noisiness for each engine power condition referenced to 1,000 ft. Ground Run-up: OTOB data at 250 ft at 10 deg increments from 0 to 180 deg.
Directivity:	2D		
Additional Comments:	Directivity is for Ground Run-up data and modeling only. Flight data and modeling does not include source directivity. Empirical excess ground attenuation curve.		
Propagation Algorithm			
Atmospheric Absorption:	SAE Aerospace Recommended Practice (ARP) 866A	Atmospheric Refraction:	None
Ground Impedance:	Flat earth mode assumes industrial grass. Topographical mode includes a binary mix of hard and soft surface separated at 1,000 rays.		
Terrain:	Topographical mode has three basic terrain cuts: Flat, Uphill, and Downhill. All three include impedance changes between hard and soft.		
Barriers:	None		
Manmade Structures:	None		
Reflections:	None		
Source Code			
Access:	FOUO	Language:	FORTRAN, C++
		Acquired:	<input checked="" type="checkbox"/>

Model Overview: Traffic Noise Model (TNM)			
Main Purpose:	Predict highway traffic noise at nearby receivers and aid in design of highway noise barriers.		
Source Type:	Road vehicles: automobiles, medium trucks, heavy trucks (cruise and full throttle), buses, motorcycles	Calculation Method:	Step-wise triangles
Method Summary:	TNM computes a predicted sound level with a series of adjustments to a reference level, where adjustments from the source level for each vehicle type are made for traffic parameters, distance, and shielding and ground effects. TNM is based on a 3D coordinate system, and computes the following metrics L_{Aeq1h} , L_{dn} , L_{den} , and OTOB L_v .		
Noise Source			
Data Source:	Measured	Spectra:	OTOB data, 50 Hz to 10 kHz
Directivity:	None		
Additional Comments:	Five vehicle types measured at various speeds, cruise and full throttle conditions, and traveling on different pavements. Each vehicle type has two representative sub-sources (2 heights). Assumes full streams of traffic for calculations, not individual vehicles.		
Propagation Algorithm			
Atmospheric Absorption:	ISO 9613-1, 1993. User can specify temperature and relative humidity. Standard atmospheric pressure is applied (one atmosphere at sea level).	Atmospheric Refraction:	None
Ground Impedance:	Variable effective flow resistivity (EFR). Choices within model: pavement, water, hard soil, gravel/loose soil, lawn, field grass, granular snow, powder snow. Can also enter a custom EFR value in cgs rays. The EFR values, along with angle of incidence, are used to compute the coefficient of reflection.		
Terrain:	Varying terrain based on user input of terrain lines and other TNM objects that define the ground elevation. Where terrain protrudes into propagation path, applicable reflection and diffraction equations are applied.		
Barriers:	Barriers are included as walls or earth berms. Parameters are user-defined; these include: coordinates (x, y, z; every two points defines a barrier segment), which define barrier length; height; perturbation parameters; noise reduction coefficient; for berms, slope and top width. Double-barrier diffraction is included. The net effect of diffraction from the most effective pair of barriers, berms, or terrain that blocks the line-of-sight is computed.		
Manmade Structures:	One of TNM's input objects is building rows, with user-definable height and percentage of area blocked by the buildings relative to the source roadway(s). Calculations include diffraction and reduction in insertion loss due to gaps. Users can alternatively use wall barriers to define building façades; barrier calculations apply to this method.		
Reflections:	For all versions, a parallel barrier module allows for multiple reflections between barriers, in two dimensions; a ray tracing procedure is applied. For TNM version 3.0, propagation paths are added based on barrier coordinates and dimensions, and TNM acoustics calculations apply to those paths, with inclusion of absorptive barrier surface effects, where applicable.		
Source Code			
Access:	Controlled	Language:	C/C++/C#
		Acquired:	<input checked="" type="checkbox"/>

Model Overview: Advanced Acoustic Model (AAM)			
Main Purpose:	A suite of computer programs that predicts far-field noise from fixed-wing or rotary-wing aircraft, using time-varying noise levels for each step in a user-defined flight trajectory. AAM is based on 3D spectral noise source modeling defined as compact sources (multiple sources can be used per vehicle) with OTOB, narrowband or pure tone and phase. Sound propagation accounts for geometric spreading, air absorption and finite ground impedance, and varying ground terrain or atmospheric gradient effects. Non-linear propagation effects associated with high noise levels are computed.		
Source Type:	Sound spheres obtained from flight tests, wind tunnel measurements, or theoretical predictions. Vehicle source characteristics may be described in any combination of broadband (OTOB levels), narrowband, or as pure tone data (in the form of specific frequency sound pressure level and phase).	Calculation Method:	Simulation
Method Summary:	Calculates the noise levels in the time domain and a variety of integrated metrics at receiver positions on or above the ground at points of interest and over a uniform grid. Vehicle operations are defined in either single event (e.g. flight track) or multiple events mode (e.g. an airfield). Vehicle source characteristics are prescribed as a function of vehicle operating state along a defined flight trajectory. This acoustic source characteristic database lookup procedure allows the code to be utilized for numerous flight vehicles such as conventional fixed-wing aircraft, thrust-vectorized fixed-wing aircraft, rotorcraft, and tilt-rotor vehicles. It can also be used for ground-based vehicles.		
Noise Source			
Data Source:	Measured (standard), hybrid empirical/analytical or modeling	Spectra:	OTOB and/or Narrowband and/or pure tone/phase from 10 Hz to 10 kHz
Directivity:	3D		
Additional Comments:	Empirical dataset for rotary-wing and some DoD fixed-wing aircraft. Procedures exist for development of polar sources from AEDT NPD and NoiseMap NOISEFILE data using assumed directivity.		
Propagation Algorithm			
Atmospheric Absorption:	ANSI S1.26 (R2004). Applies absorption to a layered atmosphere	Atmospheric Refraction:	Ray Refraction
Ground Impedance:	The ground surface is characterized by a complex acoustic impedance based on the work by Chien and Soroka (1975), and by Chessell (1977) with the corrections by Daigle (1979). The algorithm uses the Doppler-shifted frequencies based on the speed of the vehicle and its direction relative to the receiver.		
Terrain:	Topographic attenuation, caused by the reflections and absorption from barriers formed by the terrain located between the source and the receiver, is modeled using the algorithms developed by Rasmussen (1985). In the limit as the terrain approaches a flat plate divided by a thin screen, Rasmussen's algorithms asymptote to Maekawa's (1968) thin screen theory. The topography propagation module combines the ground reflection and attenuation, and topographic attenuation.		
Barriers:	Ideal barriers (with pure vertical surfaces) are not treated. In the limit, with dense gridding, barriers can be analyzed using the Terrain algorithms described above.		
Manmade Structures:	Manmade Structures (with pure vertical surfaces) are not treated. In the limit, with dense gridding, manmade structures can be analyzed using the Terrain algorithms described above.		
Reflections:	Not handled.		
Source Code			
Access:	Controlled	Language:	FORTRAN
		Acquired:	<input checked="" type="checkbox"/>

Model Overview: NoiseMap Simulation Model (NMSim)			
Main Purpose:	Simulation Model for user-defined sound sources and operations. Single events analysis, or a small number of simultaneous events. Best suited for analyzing effects of terrain and changing ground impedance on propagation.		
Source Type:	2D axisymmetric OTOB spectra from measurements or estimated	Calculation Method:	Simulation
Method Summary:	Uses the full Rasmussen propagation algorithm		
Noise Source			
Data Source:	Includes measured, empirical, and user-defined source data.	Spectra:	Sources are based on axisymmetric 2D source. Data are stored in each frequency desired, but OTOB are recommended.
Directivity:	2D		
Additional Comments:	NMSim was developed while the topographical routines were being developed for NoiseMap 7 by Dr. Ken Plotkin. After initial DoD effort, NPS updated the model to include a graphical user interface. Routines have been developed to incorporate NORD2000 atmospheric propagation, Acoustic detection, etc. Topography Effects routine are directly transportable to AEDT. Model can be used to benchmark current and blended method.		
Propagation Algorithm			
Atmospheric Absorption:	ANSI S1.26	Atmospheric Refraction:	Ray Refraction
Ground Impedance:	Varying impedance is modeled		
Terrain:	Terrain cuts are classified as Flat, Uphill, Downhill, Hill, and Barrier		
Barriers:	Yes		
Manmade Structures:	Manmade structures may be modeled as barriers		
Reflections:	None		
Source Code			
Access:	Open Source	Language:	FORTRAN
		Acquired:	<input checked="" type="checkbox"/>

Model Overview: Roadway Construction Noise Model (RCNM)			
Main Purpose:	Predict roadway construction noise		
Source Type:	Point sources, over 50 types of construction equipment	Calculation Method:	Point
Method Summary:	RCNM uses the primary equation described in the CA/T Construction Noise Control Specification 721.560 [Construction Noise Control Specification 721.560, Central Artery/Tunnel Project, Massachusetts Turnpike Authority, Boston, MA, 2002] for construction noise calculations.		
Noise Source			
Data Source:	Two options: measured or from CA/T specifications	Spectra:	Version 1: Overall (broadband) level New version expected to be OTOB
Directivity:	None		
Additional Comments:	Most are measured L_{max} at 50 ft for more than 50 types of construction equipment. Some use Spec 721.560 published L_{max} at 50 ft. Each equipment type has an associated usage factor. User-defined equipment/usage factors can be entered.		
Propagation Algorithm			
Atmospheric Absorption:	None	Atmospheric Refraction:	None
Ground Impedance:	Does not account for different ground types.		
Terrain:	<p>User-defined shielding. Appendix A of the RCNM User's Guide provides guidance for estimating shielding (based on experience from Boston CA/T construction):</p> <ol style="list-style-type: none"> 1. If a noise barrier or other obstruction (like a dirt mound) just barely breaks the line-of-sight between the noise source and the receptor, use 3 dBA. 2. If the noise source is completely enclosed or completely shielded with a solid barrier located close to the source, use 8 dBA. If the enclosure and/or barrier has some gaps in it, reduce the effectiveness to 5 dBA. 3. If the noise source is completely enclosed and completely shielded with a solid barrier located close to the source, use 10 dBA. 4. If a building stands between the noise source and receptor and completely shields the noise source, use 15 dBA. 5. If a noise source is enclosed or shielded with heavy vinyl noise curtain material (e.g., SoundSeal BBC-13-2" or equivalent), use 5 dBA. 6. If dilapidated windows are replaced with new acoustical windows, or quality internal or exterior storm sashes, use an incremental improvement of 10 dB for an overall Outside-to-Inside Noise Reduction of 35 dBA. <p>If work is occurring deep inside a tunnel using the "top-down" construction method, use 12 dBA.</p>		
Barriers:	<i>See note immediately below.</i>		
Manmade Structures:	User-defined shielding. See estimated shielding from Appendix A of RCNM User's Guide above (Terrain).		
Reflections:	Does not account for reflections.		
Source Code			
Access:	Controlled	Language:	Visual Basic
		Acquired:	<input checked="" type="checkbox"/>

Model Overview: FTA Method

Main Purpose:	Predict and assess noise and vibration impacts of proposed mass transit projects		
Source Type:	Trains and ancillary sources	Calculation Method:	Point and line source
Method Summary:	There are three levels of analysis that can be applied to mass transit projects: screening procedure, general assessment, and detailed assessment. The detailed assessment allows for simplified implementation of sound propagation elements beyond geometrical divergence. The two metrics computed are $L_{eq,1hr}$ and L_{dn} .		
Noise Source			
Data Source:	Measured	Spectra:	Overall (broadband) level only
Directivity:	None		
Additional Comments:	Noise sources for both trains and ancillary equipment can be extracted from the FTA Guidance or measured as L_{max} or SEL and used in the predictions. Noise sources considered include rail cars and locomotives, horns, bells, traction power substations, maintenance facilities, park & ride facilities, and many others.		
Propagation Algorithm			
Atmospheric Absorption:	None	Atmospheric Refraction:	None
Ground Impedance:	There are two general ground categories: hard and soft. For hard ground, no adjustments are made to reference sound levels. For soft ground, adjustments are made based on propagation path proximity to the ground, the effective path height, for which calculations are provided.		
Terrain:	A simplified method is applied for shielding effects for terrain protruding into the propagation path. The method is the same as for barriers (see below).		
Barriers:	A simplified method is applied. Barrier insertion loss is calculated based on the barrier parameter and change in soft ground effects. The barrier parameter is the difference in path length of the diffracted sound path and direct path. The amount of shielding is limited. Absorptive barriers within 5 feet of the tracks provide an additional 3 dB reduction behind the barrier		
Manmade Structures:	A simplified method is applied. Attenuation due to shielding from rows of buildings is based on the number of rows and the percent gap between buildings in the row(s).		
Reflections:	None		
Source Code			
Access:	Open Source	Language:	Excel
		Acquired:	<input checked="" type="checkbox"/>

Model Overview: NCHRP Barrier Reflections Screening Tool			
Main Purpose:	Estimate effect of barrier reflections		
Source Type:	No source sound levels included	Calculation Method:	Line source divergence
Method Summary:	The tool provides a quick estimate of the expected increase in traffic noise due to reflections from a barrier on the opposite side of the road. User enters XYZ coordinates for source and receptor along with the distance from the source to the noise barrier. Calculations for the barrier reflection effect are based strictly on direct and reflected path lengths, which appears to be the controlling factor in highway noise reflections. The tool validates well when comparing to measured barrier effects as part of the NCHRP 25-44 project.		
Noise Source			
Data Source:	NA	Spectra:	None
Directivity:	None		
Additional Comments:	A noise source is not required, since only increases in sound level are being calculated, and it's based strictly on distances.		
Propagation Algorithm			
Atmospheric Absorption:	None	Atmospheric Refraction:	None
Ground Impedance:	None		
Terrain:	None		
Barriers:	Assumes a barrier is encountered either at the closest point of approach or up- or downstream.		
Manmade Structures:	None		
Reflections:	Calculations for determining the barrier reflection effect are made simply by accounting for cylindrical divergence for both direct and reflected sound paths, and comparing results. The method allows for applying user-defined shielding to either the direct or reflected sound paths.		
Source Code			
Access:	Controlled	Language:	Excel Acquired: <input checked="" type="checkbox"/>

Model Overview: HARMONOISE/IMAGINE			
Main Purpose:	Predict environmental noise for use in noise assessment and noise mapping		
Source Type:	Highway, rail, aircraft, industrial	Calculation Method:	Integrated
Method Summary:	The European model HARMONOISE was developed to help generate consistent, comparable noise assessments and noise maps. The model includes road traffic noise and rail traffic noise. IMAGINE extended the HARMONOISE source databases and added aircraft noise and industry noise predictions.		
Noise Source			
Data Source:	Measured/predicted	Spectra:	OTOB: 25 Hz to 10 kHz
Directivity:	3D		
Additional Comments:	For aircraft, source is characterized by its spectral and angular distribution of emitted sound power, independently from the environment in which this source is placed. IMAGINE can create source data by measurement or by reverse engineering of NPD data. For highway, there are three categories with two representative sub-sources (2 heights).		
Propagation Algorithm			
Atmospheric Absorption:	ISO 9613-1. User can specify ambient temperature, ambient pressure, and relative humidity.	Atmospheric Refraction:	Ray Refraction: Ground-curving
Ground Impedance:	Impedance classes. Use of EFR and Attenborough and Delany & Bazley equations mentioned – maybe others can be applied as well. The ground effects are part of the excess attenuation.		
Terrain:	Ground is defined, and protrusions in a propagation path apply diffraction using the Deygout formula, which applies the Fresnel number. The effect is combined with the ground effect to determine the excess attenuation.		
Barriers:	Barriers are defined, and they are included as points in the propagation path. Diffraction (Deygout and Fresnel number) and ground effects around the barrier are included in the excess attenuation calculations.		
Manmade Structures:	Buildings – includes height and roof shapes. Buildings are included in the propagation path, and diffraction and ground effects around buildings are applied in the excess attenuation.		
Reflections:	In a propagation path, the noise level appears to be corrected using an effective energy reflection coefficient, which is based on the size of the reflecting surface relative to the Fresnel zone.		
Source Code			
Access:	Proprietary	Language:	Implementation-dependent
		Acquired:	<input type="checkbox"/>

Model Overview: CadnaA			
Main Purpose:	Calculation and prediction of industrial, road, rail, and aircraft noise exposure. Air pollution can also be calculated.		
Source Type:	Point, line, horizontal and vertical area sources, roads, railways, and air routes	Calculation Method:	Simulation
Method Summary:	CadnaA determines a predicted noise level using a ray tracing (default) or angle scan method, both methods use a straight ray approximation. In the ray tracing method, ray paths between sources and receivers are constructed deterministically, and extended sources are subdivided dynamically using a projection process. In the angle scan method, the level is calculated by emanating rays in equal angle steps from the receiver, then sources inside a sector are virtually projected onto the calculation ray. A variety of equivalent noise metrics can be specified and calculated.		
Noise Source			
Data Source:	User Defined	Spectra:	Octave band data, 31.5 Hz to 8 kHz
Directivity:	3D		
Additional Comments:	A large variety of national and international standards can be implemented. Noise from aircraft can be determined from INM 7.0, CNOSSOS-EU and others. Noise from roads can utilize TNM. Railway noise can be determined from FTA/FRA, Schall03, CNOSSOS-EU and others. Levels due to industrial sources conform to ISO 9613-2.		
Propagation Algorithm			
Atmospheric Absorption:	Conforms to ISO 9613-2. Can specify temperature and relative humidity. Corrections to account for effects of wind speed, wind direction and atmospheric stability can be made with CONCAWE or HARMONOISE.	Atmospheric Refraction:	Ray Refraction
Ground Impedance:	Two methods to compute absorption according to ISO 9613-2, spectral (section 7.3.1) and non-spectral (section 7.3.2). The spectral method uses a Ground Factor G, that ranges from 0 (hard ground) to 1 (porous ground). See section 3.8 of CadnaA Reference Manual v3.8.		
Terrain:	3D Digital Terrain Models can be imported, as well as GIS based contour elevation files. Screening effects of the topology are accounted for; foliage can be included as an obstacle.		
Barriers:	Barriers are defined by length and height. They can be specified as non-reflecting or reflecting with separate left-right reflection loss (dB), and absorption coefficients. The barrier can be floating, where rays passing underneath the barrier are not attenuated. Diffraction around the bottom edge is not included. Double diffraction is accounted for where appropriate.		
Manmade Structures:	3D buildings, bridges and other structures can be imported directly or drawn by hand. Buildings and artificial barriers are specified by height (relative or absolute), reflection loss or absorption coefficient, and percent acoustical transparency. Three-point diffraction is used for each source-receiver pair that is separated by an arbitrary number of screening structures.		
Reflections:	All objects can be defined as reflective. An absorption coefficient can be assigned to their surface as a single number or as a spectrum. The reflection calculation is carried out according to the image source method. For densely packed structures corrections for multiple reflections can be implemented.		
Source Code			
Access:	Proprietary	Language:	Acquired: <input checked="" type="checkbox"/>

Model Overview: NORD2000

Main Purpose:	Predict ground noise sources for a variety of weather conditions and complex terrain		
Source Type:	Various ground vehicles at multiple heights. Also allows user-defined point sources.	Calculation Method:	Simulation
Method Summary:	Rigorous collection of propagation algorithms for complex acoustic propagation conditions. Primary focus is one ground vehicle traffic and rail noise.		
Noise Source			
Data Source:	Measured and user-defined	Spectra:	OTOB
Directivity:	3D		
Additional Comments:	The model was used for benchmarking the current selected algorithms and the blended method developed in this project.		
Propagation Algorithm			
Atmospheric Absorption:	ISO 9613-1	Atmospheric Refraction:	Ray Refraction
Ground Impedance:	Complex		
Terrain:	Segments variation in terrain cuts into 10 to 15 segments		
Barriers:	Includes up to two finite length barriers. For multiple barriers, it selects the two most efficient barriers. The contribution from diffraction around vertical edges is included. Also includes the effects of wind and temperature gradients to calculate barrier insertion loss.		
Manmade Structures:	Includes the effects of manmade structures as “scattering zones.”		
Reflections:	Includes reflections from vertical obstacles by calculating a reflected ray path from source to receiver. Allows adjustment in the efficiency of the reflection and assumes incoherent with direct sound at the receiver.		
Source Code			
Access:	Proprietary	Language:	MATLAB
		Acquired:	<input checked="" type="checkbox"/>

Model Overview: SoundPLAN			
Main Purpose:	Calculation and prediction of industrial, road, rail, and aircraft noise exposure, as well as air pollution		
Source Type:	Point, line, and area sources at user-defined locations	Calculation Method:	Simulation
Method Summary:	SoundPLAN uses ray tracing with a straight ray approximation to determine propagation over varied terrain and barriers with a variety of meteorological conditions. Propagation paths are considered for each source-receiver combination and obstacles are calculated according to user-selected standards.		
Noise Source			
Data Source:	User Defined	Spectra:	Octave band, OTOB (1 Hz – 20 kHz)
Directivity:	3D		
Additional Comments:	SoundPLAN has implemented a wide array of national and international standards for computation. Users can select standards for road, rail, industry, parking lot, and wind turbine noise. Examples for industry and road noise include TNM 2.5, NORD2000, FHWA, and ISO 9613-2. Aircraft noise can be calculated, as well.		
Propagation Algorithm			
Atmospheric Absorption:	ISO-9613-1. Users can select temperature, relative humidity, and atmospheric pressure. NORD2000 calculations allow input for temperature and temperature gradient, humidity, pressure, wind speed and direction, turbulence, and roughness.	Atmospheric Refraction:	Ray Refraction
Ground Impedance:	Complies with ISO 9613-2 and NORD2000. For computations under ISO 9613-2, users can specify a value between 0 and 1 for percentage of soft ground over study area. For NORD2000 calculations, users must specify the flow resistivity of the ground.		
Terrain:	Terrain may be imported from a variety of CAD formats and converted into spot heights and elevation lines. SoundPLAN supports interpolation to decrease the overall size of the digital ground model. Foliage and berms can also be included as separate elements.		
Barriers:	Barriers are specified by their geometry and frequency-dependent acoustic absorption characteristics. Diffraction along both the top and bottom edges is considered.		
Manmade Structures:	Building footprint and height may be input directly or imported using various GIS and CAD formats. Building faces are flat by default, but SoundPLAN includes methods to account for more detailed façades. Roads, bridges, and parking lots can also be defined.		
Reflections:	Buildings, terrain, and barrier reflections are considered in all calculation modes. Users can select a specific number of reflections to consider before terminating the computation for a given ray.		
Source Code			
Access:	Proprietary	Language:	Acquired: <input checked="" type="checkbox"/>

Model Overview: ISO 9613-2			
Main Purpose:	To enable noise levels in the community to be predicted from sources of known sound emission. Methods are general in that they may be applied to a wide variety of noise sources, and cover most of the major mechanisms of attenuation.		
Source Type:	Point sources	Calculation Method:	Point-to-Point
Method Summary:	Standard for basic community noise calculation. The model was used for benchmarking the current selected algorithms and the blended method developed in this project.		
Noise Source			
Data Source:	User Defined	Spectra:	Primarily for octave bands: 63 Hz to 8 kHz
Directivity:	None		
Additional Comments:	Developed algorithms can use this Standard as a basis of technical support.		
Propagation Algorithm			
Atmospheric Absorption:	ISO 9613-1	Atmospheric Refraction:	Simple
Ground Impedance:	Empirical Hard, Porous, and Mixed		
Terrain:	Blocked line-of-sight		
Barriers:	Thin-walled, thick-walled (Buildings), and double thin-walled		
Manmade Structures:	As barriers and reflections		
Reflections:	Empirical equations		
Source Code			
Access:	Open Source	Language:	Text
		Acquired:	<input checked="" type="checkbox"/>

Method Overview: Wei et al. Urban Diffraction and Reflection Method			
Main Purpose:	Simplified analytical model for sound level prediction at shielded urban locations involving multiple diffractions and reflections		
Source Type:	Generic	Calculation Method:	Point-to-point
Method Summary:	Presents simplified diffraction formulas, multiple edge diffraction formulas, and multiple reflection formulas updated for an urban environment. The most important steps are the introduction of an approximation for the Fresnel Integral, the assumption that the effect of multiple diffraction can be approximated by including only the shortest path connecting all rooftops, and by compacting the sum over all image sources.		
Noise Source			
Data Source:	NA	Spectra:	Calculations are frequency-based
Directivity:	None		
Additional Comments:			
Propagation Algorithm			
Atmospheric Absorption:	NA	Atmospheric Refraction:	None
Ground Impedance:	NA		
Terrain:	Protruding terrain could be applied with diffraction equations.		
Barriers:	Barriers could be applied with diffraction and reflection equations, <i>discussed more below</i> .		
Manmade Structures:	Includes multi-edge diffraction over successive buildings. Based on Pierce's diffraction theory, where the Fresnel Integral is approximated by trigonometric functions for efficient evaluation, and parameterized for urban environments.		
Reflections:	Includes multiple reflections between parallel façades. Compared to explicitly summing up the image source contributions, the Hurwitz-Lerch transcendent is more efficient if the number of image sources is greater than three.		
Source Code			
Access:	Open Source	Language:	Article Equations Acquired: <input checked="" type="checkbox"/>

Appendix B: Measurement Site Photographs

This appendix shows photographs for each of the positions in the general measurement locations for both LAX and LGB:

1. LAX, El Segundo neighborhood, positions A00-A09
2. LAX, Kittyhawk Ave neighborhood, positions B00-B03
3. LAX, hotel district, positions C00-C06
4. LAX, LAWA administration building, positions D00-D11
5. LAX, Playa Del Oro neighborhood, positions E00-E06
6. LGB, Long Beach, positions G00-G11

A00



A01



A02



A03



LAX, El Segundo neighborhood, positions A00-A03

A04



A05



A06



A07



LAX, El Segundo neighborhood, positions A04-A07

A08



LAX, El Segundo neighborhood, positions A08-A09

A09



B00



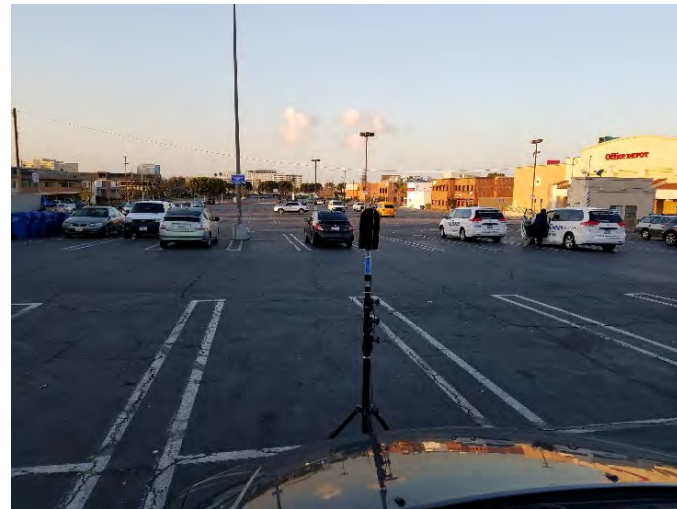
B01



B02



B03



LAX, Kittyhawk Ave neighborhood, positions B00-B03

E00



E01 NA – canceled position

E02



E03



LAX, Playa Del Oro neighborhood, positions E00-E03

E04



E05



E06



LAX, Playa Del Oro neighborhood, positions E04-E06

G00



G01



G02



G03

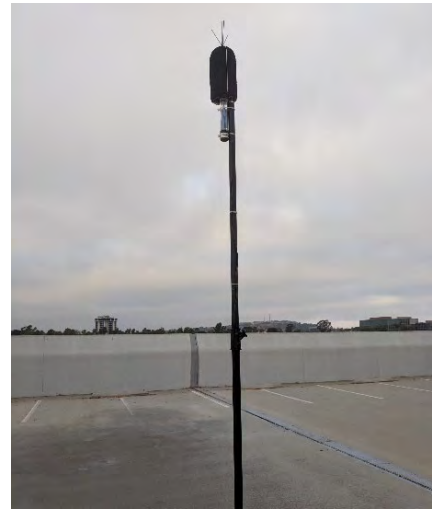


LGB, Long Beach, positions G00-G03

G04



G05



G06



G07



LGB, Long Beach, positions G04-G07

G08



G09



G10



G11



LGB, Long Beach, positions G08-G11

Appendix C: Additional Airport Noise Measurement Locations

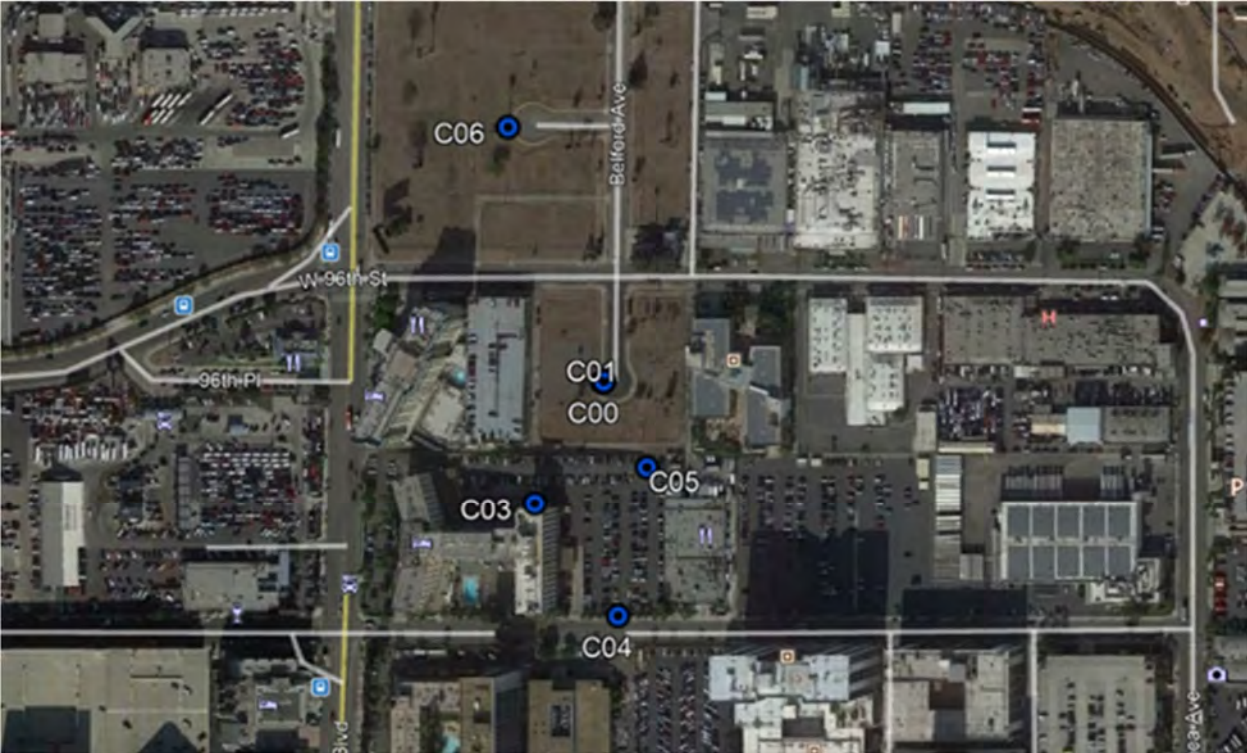
The airport noise measurements described in Section 3.2.3 were conducted as part of the effort to define and validate a blended method for incorporation into AEDT. This appendix describes two locations – hotel district and Administration Building – that were not used in the present analysis. Analysis of these locations was deemed redundant since the results gathered from the other four locations establish the essential trends for the blended method. Furthermore, the four selected locations offer a range of distinct community characteristics that are not expanded with the inclusion of either of the two remaining locations. The two additional airport noise measurement locations are documented here to allow for potential future analysis or validation.

Hotel District

Table C-1 lists each of the positions at which sound was measured and associated site attributes.

Table C-5-1. LAX, hotel district measurement positions and site descriptions

Position	Site	Potential Effects	
		Diffraction/Shielding	Reflection Effect
C01/C00	Sidewalk, open area	None for closest point of approach; otherwise 10+-story building to W and 2-story building to E	9+-story buildings to W and S, 2-story building to E
C02	[canceled]		
C03	Parking lot, raised	None for closest point of approach; otherwise 10+-story building to W and 2-story building to E	
C04	Parking lot	None for closest point of approach; otherwise 9+-story buildings to W and 2-story building to NE	
C05	Parking lot	None for closest point of approach; otherwise 10+-story building to W and 2-story building to E	
C06	Sidewalk, open area	None	Possibly distant 9+-story buildings to south

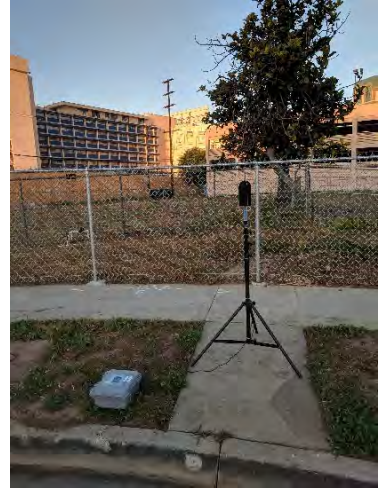


LAX, hotel district, overview

C00



C01



C02 NA – canceled position

C03



LAX, hotel district, positions C00-C03

C04



C05



C06



LAX, hotel district, positions C04-C06

LAWA Administration Building

Table C-2 lists each of the positions at which sound was measured and associated site attributes.

Table C-1-2. LAX, LAWA administration building area measurement positions and site descriptions

Position	Site	Potential Effects	
		Diffraction/Shielding	Reflection Effect
D01	N side of building, close	Hangar (N runways) 10-story building (S runways)	10-story building (N runways)
D02/D00	Parking lot	Hangar to W (N runways) 10-story and lower buildings (S runways)	2-10-story and buildings (N runways)
D03			
D04			
D05			
D06	S side of building, close	10-story building (N runways) 2-story building (S runways)	10-story building (S runways)
D07	S side of LAWA building, along road	10-story building (N runways) 2-3 story buildings (S runways)	2-10-story and buildings (S runways)
D08			
D09			
D10	Parking lot	2-10-story buildings (N runways) 2-3 story buildings (S runways)	
D11			



LAX, LAWA administration building, overview

D00



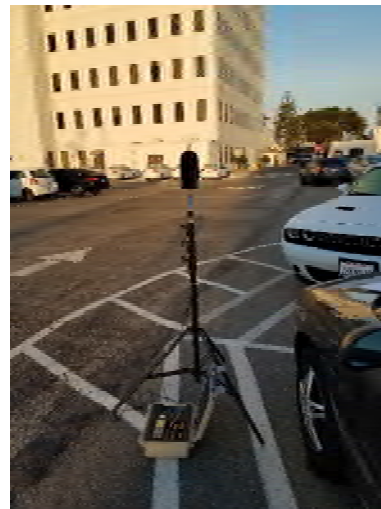
D01



D02



D03



LAX, LAWA administration building, positions D00-D03

D04



D05



D06



D07



LAX, LAWA administration building, positions D04-D07

D08



D09



D10



D11



LAX, LAWA administration building, positions D08-D11

Appendix D: Comparison of Blended Method Approaches

The key task in this research is to develop a blended method for inclusion into AEDT based on the selected models. Following the completion of the evaluation of selected methods, our research team has arrived at three potential approaches for the blended method for manmade structures:

- Direct calculation within AEDT source-based integrated framework,
- Independent calculation of the gain and loss from manmade structures, or
- Full simulation.

Direct Calculation Within AEDT Framework

The first potential approach leverages the existing segmentation within AEDT's integrated framework. Currently, AEDT approximates the aircraft flight track as a line source and segments the source according to aircraft operational parameters.

Performing a direct calculation based on the existing segmentation would leverage the current framework and preserve the integrated modeling of AEDT. However, the current segmentation is determined solely based on source characteristics and would not provide the consistent resolution required to capture the important effects of nearby manmade structures.

Figure D-1 provides a conceptual illustration of the potential segmentations needed to approximate the received noise exposure for a single point between two simple manmade structures. This illustration demonstrates that the source-based segmentation (black dashed lines) may not properly account for the effect of the two buildings. The red dashed lines mark the closest point of approach segmentation that would provide the noise exposure at the receiver point with an unblocked line-of-sight. However, such a segmentation would omit the portion of the flight path observed by the receiver via the reflected path, as shown by the green line segmentation. Moreover, adjusting the segmentation for each receiver point would be outside of the current segmentation framework of AEDT. In addition to this conceptual segmentation, Figure D-2 provides an actual AEDT segmentation for a departure from LGB relative to one of our measured locations. The initial segmentations provide short segments to capture the effect of the nearby manmade structures. However, segments four and five have a mix of inclusion of manmade effects that miss the point where the receiver location has a clear line-of-sight to the aircraft.

To address this issue, segment lengths could be defined by receiver properties such as distance to the flight track and manmade structures. A drawback to this approach is that densely packed urban environments would dramatically increase computational cost. Some computational burden may be reduced using empirical relationships based on building density and height, yet building effects at specific receivers would need to be balanced with overall effects.

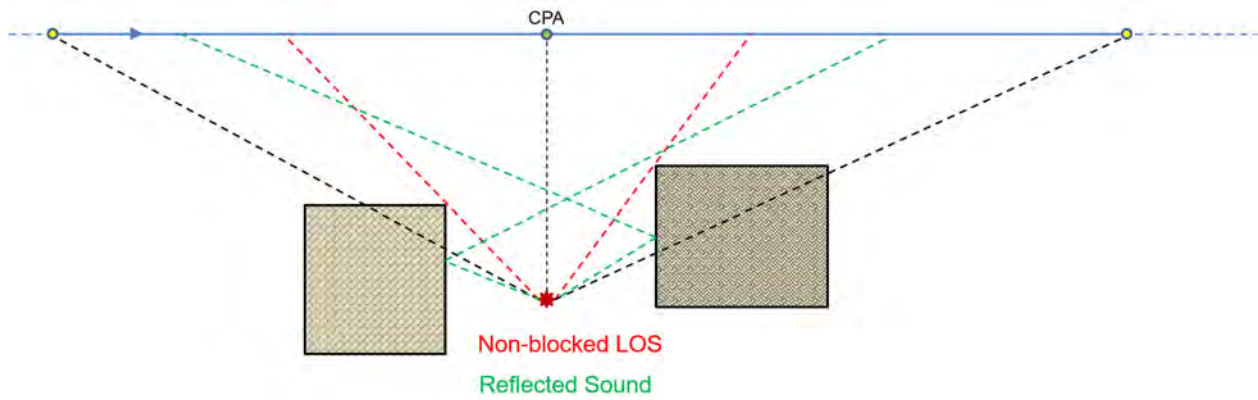


Figure D-1. Conceptual schematic of segmentation and manmade structures

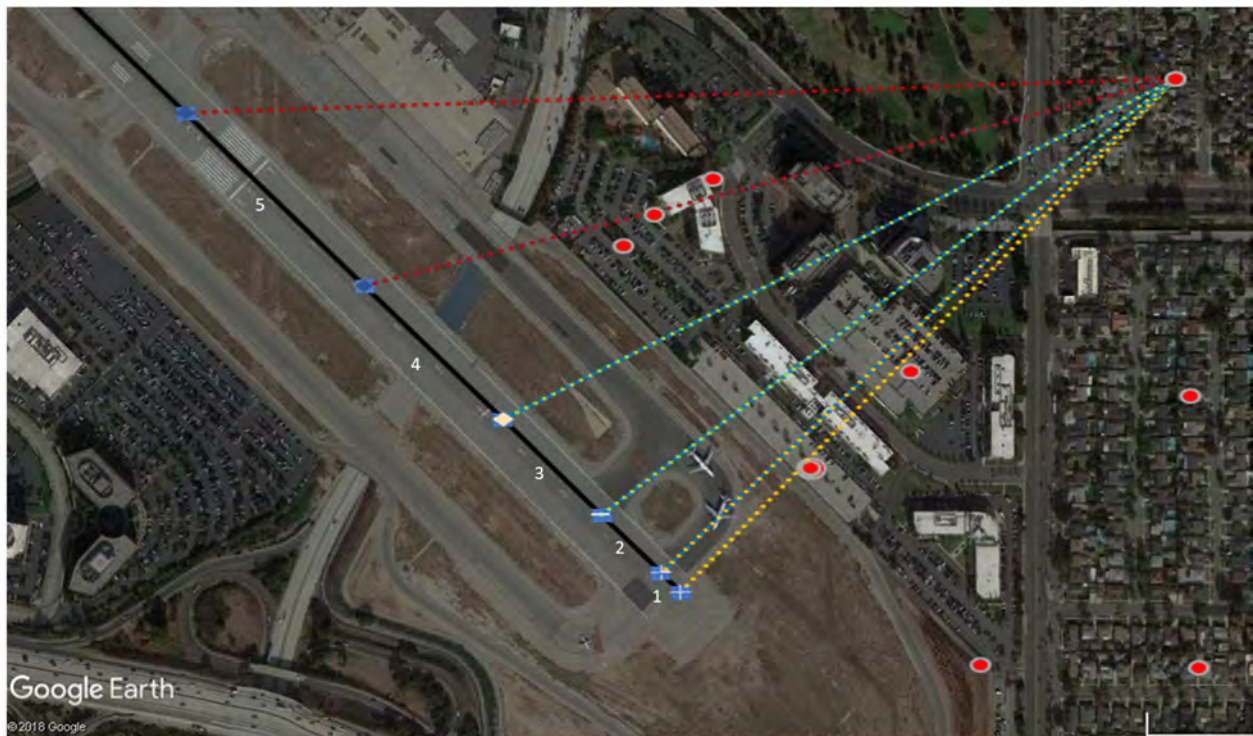


Figure D-2. AEDT schematic for a departure at LGB relative to a community receiver location

In addition to increased computational cost, short segments introduce additional uncertainty to the noise fraction calculations. Figure D-3 compares the uncertainty due to a 10,000 ft flight track that has been segmented into 100 and 1,000 ft lengths for two grid sizes.

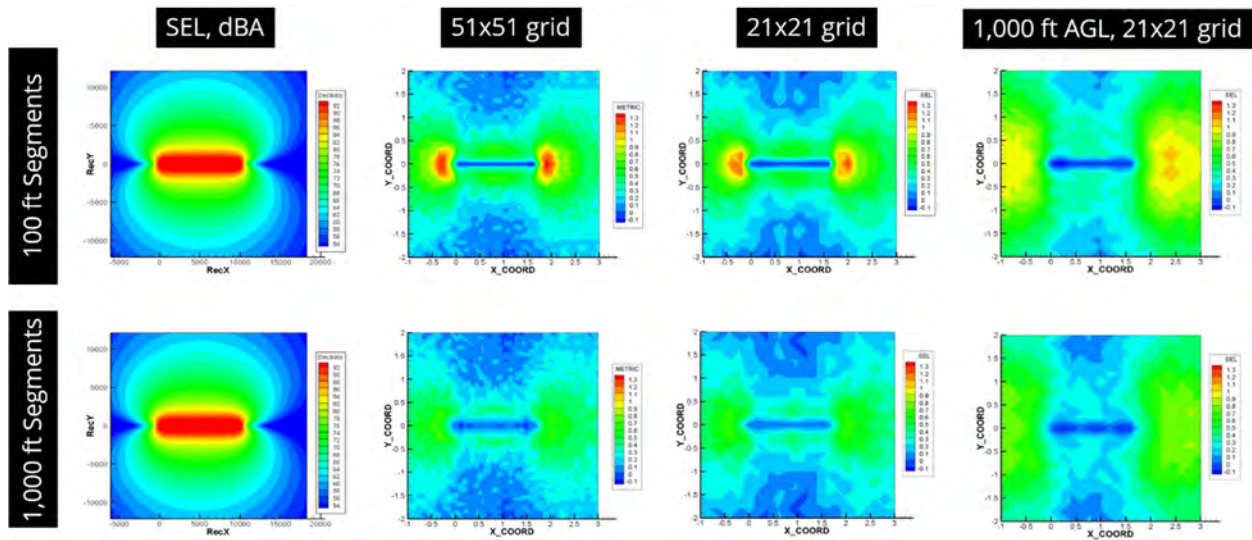


Figure D-3. Uncertainty introduced in noise fraction calculations due to reduced segment length

Due to the increased segmentation required to capture building geometry and the uncertainty associated with shorter segments, our research team does not recommend pursuing this approach.

Independent Calculation for Manmade Structures

The next approach leverages key results from the models considered in this research to independently calculate regions of influence near manmade structures and terrain features. As our team evaluated the various methods and models, we found that we could utilize the direct noise calculation of the aircraft noise with the calculation of various effects such as building reflections to compare with measured field results.

Utilizing linear acoustics, the predictions would be obtained in the existing AEDT integrated framework without manmade structures. Then, the acoustic effect of all manmade structures would be considered based on the regions of influence due to elevation angle and propagation distance. The acoustic effect would be calculated using transition relationships between each of the selected methods. The AEDT calculations and the effect due to manmade structures and terrain features would then be combined to produce a final result. This hybrid method has the advantage of using high fidelity prediction methods for nearby buildings to calculate the effects of reflection gains and insertion loss. Effects of manmade structures are considered separately and can be toggled on and off. In addition, this approach reduces overall computational cost as it can be calculated once and updated only when the physical environment changes.

An example of this process is provided in Figure D-4 through Figure D-6. Figure D-4 provides the SEL footprint of an arrival to LGB focused on our measurement area. Figure D-5 provides the gain/loss predicted by ISO 9613-2. These two calculations can simply be combined because of linear acoustics to provide an estimate of the actual SEL with the inclusion of the effects of manmade structures.

The recommended process for the inclusion of manmade structures is the following:

- Perform an independent calculation of the effect of manmade structures using high-fidelity implementation of the selected models.
- Compute aircraft noise using the current AEDT noise calculation.
- Combine the independent calculation of the effect of manmade structures with the AEDT noise calculation to obtain the overall result.

As stated above, calculation of manmade structure gain/loss will use higher fidelity methods compared to direct implementation in AEDT's integrated source-based calculation. Our team will investigate the variation of aircraft noise spectra on the resulting gain/loss calculations to better refine the hybrid calculation approach.

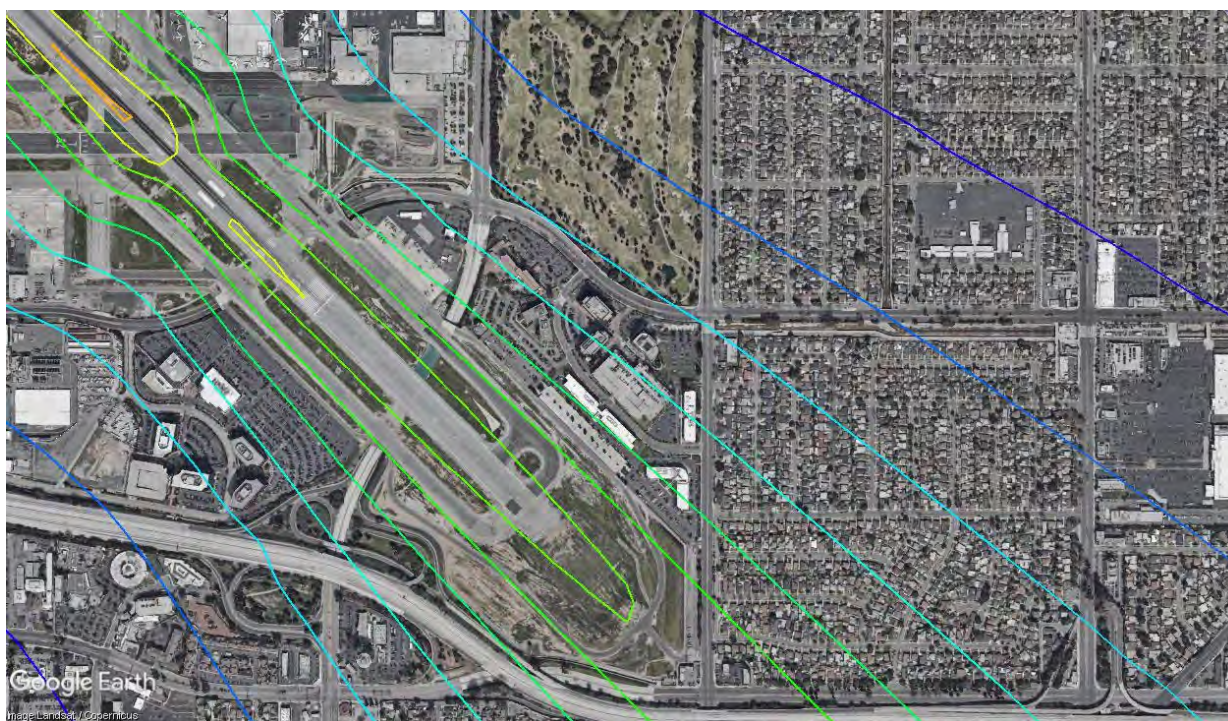


Figure D-4. Results at LGB computed using existing AEDT calculations



Figure D-5. Acoustic effect associated with manmade structures at LGB according to ISO 9613-2

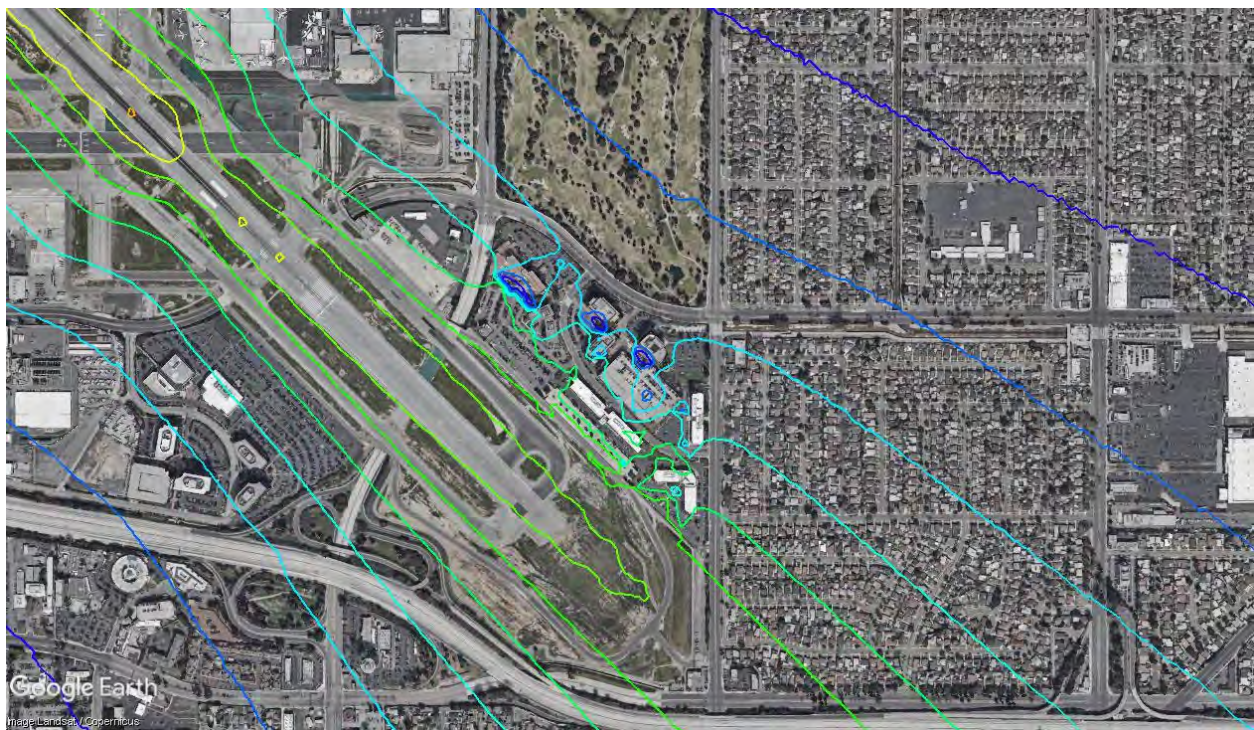


Figure D-6. Combination of existing AEDT calculations and acoustic effect from manmade structures

Full Simulation

The final potential approach for characterizing the many paths that exist from source to receiver introduced by manmade structures would be to implement a full simulation approach. In a simulation framework, such as AAM, sources are considered during small time steps and propagation for multiple paths is considered. The proprietary benchmarking software used in this research, SoundPLAN and CadnaA, implement various methods in a simulation environment.

Although a simulation approach would allow additional details to be captured when compared with the first approach, the current AEDT framework is an integrated model and thus incompatible with a simulation model approach.